DYNAMIC DESERTS:
THE SYNERGISTIC EFFECTS OF FUNGI, SUNLIGHT, AND NON-RAINFALL MOISTURE ON PLANT LITTER DECOMPOSITION IN DRYLANDS

By

James Robert Logan V

A DISSERTATION

Submitted to
Michigan State University
in partial fulfillment of the requirements
for the degree of

Integrative Biology – Doctor of Philosophy
Ecology, Evolutionary Biology, and Behavior – Dual Major

2021

ABSTRACT

DYNAMIC DESERTS: THE SYNERGISTIC EFFECTS OF FUNGI, SUNLIGHT, AND NON-RAINFALL MOISTURE ON PLANT LITTER DECOMPOSITION IN DRYLANDS

By

James Robert Logan V

Drylands cover well over one third of the Earth's land and are an important part of the global carbon cycle. Despite this, most models underestimate carbon turnover in arid and semi-arid systems, limiting our ability to predict how they will respond to changing climates. This is partly because many models are driven by rainfall, assuming little to no decay between precipitation events. Unlike in many wetter systems though, plant litter decomposition in drylands is largely controlled by non-rainfall processes including photodegradation and biotic decomposition supported by non-rainfall moisture (fog, dew, and water vapor; "NRM"). Despite their importance however, few studies have examined how these drivers interact with one another and with fungal communities to influence carbon turnover.

In this dissertation, I demonstrate how photodegradation, NRM, and fungal decomposers interact to accelerate carbon turnover in drylands. To do this, I leveraged a natural gradient of NRM frequency in the Namib Desert that receives intense solar radiation. In one study, I used a reciprocal transplant design to show that moisture regime exerts a strong influence on litter-associated fungal communities and show that

the relationship between NRM and litter decay rates depends on the composition of the decomposer community. In another study, I manipulated solar radiation for three years and found that photodegradation of the plant cuticle allows litter to absorb more water during NRM events, accelerating biotic decomposition. By examining litter-associated fungal communities under these same radiation treatments, I also show that fungi are largely insensitive to radiation stress and that photodegradation mainly affects decomposition rates in this system through photochemical changes in litter that increase subsequent biotic decomposition. Finally, to quantify the relationship between NRM and carbon turnover on multi-year timescales, I measured mass loss for 30 months along a moisture gradient spanning an order of magnitude of NRM frequency. By coupling these data with continuous meteorological measurements over the same period, I show that accounting for NRM and temperature sensitivity substantially improves the performance of a simple exponential litter decay model.

These findings build on previous work demonstrating the importance of solar radiation and NRM as crucial drivers of litter decomposition and point a way forward for future studies to examine how these two processes may interact under future climate scenarios. Drylands are undergoing significant changes from anthropogenic climate change and understanding the drivers of litter decomposition allows us to better predict how these ecosystems are responding to global change.

This dissertation is dedicated to my Papaw, John Cromer, who instilled in me a deep love and respect for the outdoors. He spent his career teaching and serving others and his personal life loving his family and playing in nature. I can think of no better way to go through life.

Also to Professor Jackie Brown, who taught me that ecology has as much to do with beauty, curiosity, and wonder as it does with quadrats, experimental design, and linear models. However, he didn't let me forget that the exciting discoveries only come through hard work, telling my classmates and me on our second day of college "a lot of people think that ecology's just going out and grooving in the forest; and it is, if you think that grooving is taking data and doing t-tests." Thanks for showing me how to groove.

Finally, I would like to dedicate this dissertation to the friends, family members, teachers, and mentors who have encouraged my curiosity from a young age. Nothing is better preparation for a PhD than a childhood full of questions and wonder of the natural world.

The most elementary and valuable statement in science, the beginning of wisdom, is, "I do not know." –LCDR Data

That may be the most important thing to understand about humans. It is the unknown that defines our existence. We are constantly searching, not just for answers to our questions, but for new questions. We are explorers. We explore our lives day by day, and we explore the galaxy, trying to expand the boundaries of our knowledge. And that is why I am here. Not to conquer you with weapons, or with ideas. But to coexist and learn. –CDR Benjamin Sisko

ACKNOWLEDGEMENTS

No one completes a dissertation on their own and I am no exception. First, I would like to thank my friend and advisor, Sarah Evans, for her amazing support and guidance over the last several years. Sarah has always challenged me to push myself farther than I would have on my own and always helped me keep my focus on the "big picture." Whether we were collecting samples in the rain at 3:00am in Namibia, brainstorming research ideas on walks through the Michigan woods, or grabbing drinks in the evening to talk about anything *but* science for a change, she helped make getting a PhD one of the most fun experiences I could have asked for. I would also like to thank my committee members, Kathy Jacobson, Steve Hamilton, and Ashley Shade, for their support and input into my dissertation. Many of the ideas in here came from conversations with them and this dissertation would not be anything close to what it is today without all of their input.

Kathy Jacobson and Peter Jacobson in particular have been invaluable colleagues, close friends, and sometimes quirky mentors, without whom, I would never have fallen in love with the Namib. They have not only been a central part of my professional career since college, they have also been a big part of my life in general, there to celebrate the highs and push through the lows. I cannot count the number of times we would distract each other from work by bouncing around exciting new ideas for

projects or the thousands of times they would be there when I just wanted to vent about some frustrating part of grad school while I was on the other side of the world doing fieldwork and nothing seemed to be working. They were always there to help.

Thank you to my friend and dune adventuring partner Mary Seely who always thought my work was exciting but still asked me "so what?!" more times than anyone else, just to keep me on my toes. She has always pushed me to expand how I think about the social benefits and consequences of my research and showed me that the most exciting science often needs little more than an interesting question, a good set of eyes, and the patience to just look at what surrounds you.

To my co-authors and collaborators including Roland Vogt, Kathe Todd-Brown, and Paul Barnes, thank you so much for your feedback and help on my chapters. They helped me connect my research to the broader literature so that my ideas would contribute to others' work. Without them, this work would have been a lot less applicable to the broader world.

I would like to thank the Namibian Ministry of Environment and Tourism, the National Commission on Research, Science, and Technology, the National Botanical Research Institute, and the Gobabeb Namib Research Institute for their permission and support over the years as I worked throughout the Namib. Special thanks to all the staff and interns at Gobabeb who have helped me, in ways big and small, including Gillian Maggs-Kölling, Elna Irish, Leena Kapulwa, Martin Handjaba, Angela Curtis,

Ritha Kapitango, Doris Kinyaga, Cassie Miller, Hannah Lieberman, Monja Gerber, Petra Mutota, Roland Mushi, Oliver Hasley, Paulina Schmid, Eugene Marais, Bryn Morgan, the GTRIP 2017 participants, and many others. I would especially like to thank Martin Handjaba and Ritha Kapitango for their support and maintenance of my massive UV experiment over many years. No matter how many times I worried that a stray donkey, an unusually strong east wind, or some overly eager tourist would knock over the experimental shelters, Martin and Ritha were always there to make sure things went smoothly. I'd also like to recognize my Namib lab/office-mate Angela Curtis for her enthusiasm whenever I would find something cool and for fun conversations when I was caught in the lab late at night. Thanks also to Gillian Maggs-Kölling, without whom I may never have been able to navigate all the bureaucratic and political hurdles that come with doing an international PhD. Thank you to my friends Nerson Tjelos, Elise Nghalipo, Nick Jacobson, Mary Jacobson, and Sarah Fitzpatrick who made my many frequent field trips to Namibia fun and exciting adventures.

Thank you to current and former Evans Lab members including Jennifer Jones, Heather Kittredge, Tayler Ulbrich, Corinn Rutkoski, Emily Burgess, Holly Vander Stel, Lukas Bell-Dereske, Rémy Van Geersdaële, Steve Gougherty, Quinn Carvey, Kevin Dogherty, Will West, Sharon Carpenter, and Esbeiry Cordova-Ortiz. Grad school is hard and y'all helped me out in so many ways I can't begin to count! I am particularly thankful for Corinn Rutkoski and her encouragement and excitement as I'd hit

milestones in my dissertation over the last few years. Whether I was stressing out about work tasks late at night or we were celebrating some small victory, she made some of the lows of dissertation writing a little better and the highs even higher.

Extra thanks to the KBS Writing Group including Isabela Borges, Meaghan Clark, Brendan Reid, Ravi Ranjan, Sara Garnett, Ava Garrison, Jennifer Jones, Carmella Vizza, Samantha Mosier, Kyle Jaynes, Kara Haas, Hsunyi Hsieh, Yahn-Jauh Su, and Meredith Zettlemoyer. They provided intense feedback over the years, from helping me refine "shitty first drafts" of grant proposals so I could fund my fieldwork to brainstorming dissertation titles as I wrapped things up. They've probably read more of my writing than anyone else over the last three years and I have become a better writer as a result.

Enormous thanks to Jenny Smith and Sarah Reimer for their hours upon hours helping me navigate the financial and logistical challenges of conducting an international PhD. No one likes writing expense reports, organizing receipts, and tracking plane flights, yet they helped me with all of these more times than I can count. Without their help, I wouldn't have been able to manage getting any actual science done. They always shared my excitement about my field trips and I always looked forward to hanging out with them when I'd return from the field.

The fog chamber I used in Chapter Two was constructed and loaned by Kyle Jaynes at the W. K. Kellogg Biological Station. Thanks to Tyler Scifres, who spent

Christmas Eve 2017 with me in the Lightwire studio in New Orleans, building litter racks just days before I flew off to Namibia for fieldwork.

Thank you to all of my friends at KBS, who are too numerous to mention right here, but who made living in Michigan so much fun over the last six years. Northern winters can be hard on this southern extrovert, but between the movie nights, Lake Michigan hikes, backpacking trips, backyard bonfires, hot chocolate parties, KBS retreats, pot lucks, scavenger hunts, canvassing shifts, paddle trips, afterwork drinks, backroad runs, LTER walks, and more ice cream breaks than I thought were possible, you helped me build a community and make a home here in Michigan that I will miss dearly.

My dissertation work has been funded by many people and groups including the National Science Foundation's Graduate Research Fellowship Program; Michigan State University's Ecology, Evolution, and Behavior program, Department of Integrative Biology, Graduate School, and College of Natural Science; the International Association for Plant UV Research; the Michigan Space Grant Consortium; the National Science Foundation's Improvements to Biological Field Stations and Marine Laboratories program; the MSU African Studies Center; the MSU International Studies & Programs Office's Dr. Charles and Marjorie Gliozzo Dissertation Research Scholarship; the MSU Council of Graduate Students; the W. K. Kellogg Biological Station through its T. Wayne and Kathryn Porter Graduate Fellowship and the George H. Lauff Scholarship;

and the taxpayers of the United States and Michigan. Grinnell College also provided funding for one of my field trips as well as substantial instrumentation in the field for which I am very grateful.

Finally, thank you to my family for their love and support over the last three decades. Doing a PhD is a pretty big undertaking and while y'all didn't always understand exactly what I was doing, you were always excited about it, proud of me, and willing to learn more. I want to specifically thank my mom who has always encouraged my insatiable curiosity and excitement for the natural world and who, at 4:51am CDT on August 27, 2003, sat with me on the roof of our house so I could look at Mars when it was at its closest approach to Earth in 60,000 years. She told me she would wake me up for it on the condition that, years in the future, when I was recognized for a big scientific achievement, I would remember what she did and thank her for all the times she helped feed my curiosity. Well here I am, finishing the biggest scientific achievement of my life so far, saying thank you for all of it!

TABLE OF CONTENTS

LIST OF TABLES

LIST OF FIGURES

INTRODUCTION

To the layman a desert is merely a hot, dry area of the earth's surface where the vegetation is usually stunted, often bizarre in form and either absent or patchily distributed. This concept could serve us quite well, but an examination of the some of the contradictions is also justified.

Gideon Louw and Mary Seely
Ecology of Desert Organisms (1982)

In the desert you rediscover, every time you go back, the cleanness that exists in spite of the dust, the complexity that underlies the apparent openness, and the intricate web of life that stretches over the apparent barrenness; but above all you rediscover the echoing silence that you had thought you would never forget.

Colin Fletcher
The Complete Walker IV (2002)

Arid and semi-arid systems cover roughly 45% of Earth's land surface, making drylands the most extensive terrestrial biome on the planet (Schimel, 2010). Although they support lower primary productivity than mesic systems, they nevertheless play a crucial role in the global carbon cycle. For example, plant productivity and litter decomposition in drylands are highly sensitive to water availability and as a result, drylands account for a substantial proportion of inter-annual variability in global carbon storage (Poulter et al., 2014; Zhang et al., 2016). Despite their importance however, our understanding of carbon turnover in arid and semi-arid systems lags behind that of other, more mesic systems. Ecosystem models have long underestimated litter decay rates in drylands, suggesting that previously unaccounted for decomposition mechanisms play a role (Whitford et al., 1981; Parton et al., 2007;

Adair et al., 2008). Without understanding and incorporating these mechanisms into modeling frameworks, our ability to predict how global carbon storage will change in the face of changing climates will be limited. Effectively managing dryland systems and forecasting changes in global carbon stores requires a strong understanding of the mechanisms and drivers of carbon turnover in water-limited systems.

Historically, decomposition in deserts was viewed as a relatively simple process, controlled by rainfall and macrodetritivore activity (Noy-Meir, 1974). Early culture-based microbiological studies concluded that deserts did not harbor large or particularly diverse microbial communities (le Roux, 1970). Litter bag studies found that, unlike in forested systems where a background level of soil moisture can promote slow litter decomposition over time, belowground decomposition in deserts is often restricted to periods following large rain events (Louw and Seely, 1982; Jacobson and Jacobson, 1998). This led to the development of a pulse-reserve paradigm that viewed most biological activities and biogeochemical cycles in drylands as restricted to periods following infrequent rain events, with relatively inactive "reserves" left over in the intervening periods (Noy-Meir, 1973). While rain pulses are important in arid and semi-arid systems however, they do not fully describe many of the spatio-temporal nuances of dryland dynamics and this often results in an underestimation of many dryland processes (Collins et al., 2014).

Fortunately, our understanding of the complexity of carbon turnover in drylands has grown considerably in the past few decades. Next-generation sequencing technology and improvements in culturing techniques have shown that a diverse group of bacteria and fungi occupy deserts (Evans et al., 2019; Logan et al., 2021). Beginning in the 1980s, researchers studying the effects of ozone depletion discovered that photodegradation by solar radiation can accelerate litter decay during dry periods and prime litter to decompose faster once water becomes available (King et al., 2012; Lin and King, 2014). Also important has been the recognition that biological decomposition is not as tightly linked to large rainfalls as was previously thought (Whitford et al., 1981; Austin, 2011). Rain events as little as 1 mm can stimulate biological activity and carbon fluxes from drylands (Huxman et al., 2004) and non-rainfall moisture (fog, dew, and water vapor; collectively "NRM") can support substantial litter decomposition even in the absence of rain (Dirks et al., 2010; Gliksman et al., 2017; Wang et al., 2017a). In some arid systems, NRM is even responsible for more annual mass loss than rainfall (Evans et al., 2020). These discoveries have required us to update our conceptual and predictive models of dryland systems to better reflect these non-rainfall-based drivers (Collins et al., 2014; Chen et al., 2016), but more work is needed to understand how these different drivers function and interact with one another in natural systems.

In this dissertation, I studied three processes that play important yet under-described roles in dryland carbon cycling: (1) photodegradation by solar radiation (2) NRM-driven microbial litter decomposition and (3) fungal decomposers' response to different climatic regimes. By examining how these three processes interact with one another, my dissertation expands on previous work that has largely (though not exclusively; see Wang et al., 2015) focused on these processes individually. My work was based in the Namib Desert in western Namibia. The Namib is a useful natural laboratory for studying these processes because it receives scant rainfall but abundant solar radiation and frequent NRM (Eckardt et al., 2013). Litter decay dynamics in the Namib are not well captured in current coupled carbon-climate models and working in the range where models break down is an excellent way to evaluate their limits. By developing a stronger mechanistic understanding of these processes, we can incorporate them into ecosystem models and expand our understanding of arid and semi-arid lands.

In Chapter One, I use a reciprocal transplant design to see whether fungal communities on senesced grass litter differ between NRM-dominated or rain-dominated regions. Changing rainfall patterns can cause microbial communities to shift in functionally significant ways (Glassman et al., 2018), but we do not yet know whether changes in NRM have similar effects. Anthropogenic climate change is altering both NRM and rainfall patterns in drylands, so if fungal communities under

these two moisture regimes differ, then current relationships between climate and litter decay rates may not hold in a warmer world.

In Chapter Two, I use a 36-month manipulation of solar radiation in the field to test a novel mechanism of photodegradation. Plant cuticles minimize evaporative water loss when plants are alive but can also prevent litter from absorbing water once the plant senesces. By examining how physical properties of grass tillers change over time when exposed to different levels of solar radiation, I describe how photodegradation interacts with NRM and plant traits to accelerate decomposition in the early-stages of decay. Understanding how the relationship between these two decomposition processes is mediated by plant litter properties can help us better predict how litter decay rates will respond as ecosystems (both their climate and plant communities) change.

In Chapter Three, I use next-generation sequencing to determine how litter-associated fungal communities respond to radiation stress. While solar radiation often accelerates decomposition rates by aiding in the breakdown of plant litter constituents, it can also reduce or alter decomposer communities in ways that slow decay rates, through a process known as photoinhibition. The net effect of radiation on decomposition therefore depends in part on how well decomposer communities tolerate radiation stress. Understanding how fungi in a hyperarid desert respond to the

physiological stress of solar radiation can help us better understand how the dual processes of photodegradation and photoinhibition interact to influence litter decay.

Finally, in Chapter Four, I develop and evaluate multiple methods for explicitly incorporating NRM into litter decay models. I conducted a multi-year litter mass loss study at six sites spanning an order of magnitude of NRM frequency, creating the largest multi-site comparison of NRM-driven litter decay rates in a dryland system to date. By combining mass loss data with continuous meteorological measurements and explicitly incorporating NRM sensitivity and temperature dependence into a simple exponential decay model, I demonstrate how current earth system models may improve their ability to describe carbon cycling in arid and semi-arid systems by accounting for this currently under-represented driver.

CHAPTER ONE:

FUNGAL COMMUNITIES ON STANDING LITTER ARE STRUCTURED BY MOISTURE TYPE AND CONSTRAIN DECOMPOSITION IN A HYPERARID GRASSLAND

What did you go out into the desert to see? A reed swayed by the wind?

Luke 7:24

Yes.

Robert Logan (2021)

INTRODUCTION

Decomposition of organic matter is a major source of greenhouse gas emissions in terrestrial systems and plays an essential role in ecosystem carbon and nutrient cycling (Kravchenko et al., 2017; Cavicchioli et al., 2019). Biotic decomposition rates are influenced by abiotic factors including moisture and temperature, and because bacteria and fungi are the actual agents of decomposition, their response to environmental conditions often mediates the relationship between environmental drivers and decomposition rates (Bradford et al., 2017). Since microbial decomposers differ widely both in their responses to environmental conditions and their ability to decompose plant litter (Treseder and Lennon, 2015), litter decay rates can sometimes depend on how specific decomposers respond to environmental conditions (Allison et al., 2013; Glassman et al., 2018). As climate change alters temperature and moisture regimes, litter decomposition rates and subsequent CO_2 efflux may be controlled by

the size and composition of existing decomposer communities as well as how they respond to changing abiotic conditions. Understanding when and how microbial communities are driven by different climate variables and when compositional shifts have functional consequences will help us better predict how carbon cycling will change under changing climate conditions.

One of the most important climatic factors determining microbial community structure and decomposition rates is moisture availability (Adair et al., 2008). While rainfall is a particularly important driver of litter decomposition rates (Jacobson and Jacobson, 1998; Allison et al., 2013), surface litter and soil decomposition rates are often more sensitive to the frequency and timing of precipitation than to the total amount of rainfall (Yu et al., 2019). Altered drying-rewetting cycles can stress soil microorganisms, inducing changes in both microbial physiology (Treseder and Lennon, 2015) and community structure (Evans and Wallenstein, 2012; Allison et al., 2013; Matulich et al., 2015). Community responses to drying-rewetting cycles are important in water-limited systems, such as in drylands, where organisms already face significant desiccation stress. In many arid and semi-arid systems, organisms cope with water limitation by using non-rainfall moisture (fog, dew, and atmospheric water vapor; hereafter "NRM") as a supplemental water source (Dirks et al., 2010; Jacobson et al., 2015; Gliksman et al., 2017; Wang et al., 2017a). In some grasslands, dew can occur as frequently as 95% of nights (Ritter et al., 2019) and recent work has demonstrated that

NRM is an important driver of decomposition in both arid and mesic grasslands alike (Evans et al., 2020). NRM can be a particularly important moisture source for standing litter (senesced litter that has not fallen to the ground surface yet), where frequent wetting and subsequent microbial growth can "prime" litter for decomposition once it reaches the soil surface (Wang et al., 2017a). Since standing litter can make up the majority of total plant litter in grasslands (Zhou et al., 2009), NRM is an important driver of carbon cycling across these systems. To date though, we do not know whether microbial communities respond differently to NRM and rain or if communities are insensitive to differences between these two moisture types. Since the frequency and intensity of rainfall and NRM are changing (Johnstone and Dawson, 2010; Niu et al., 2010; Haensler et al., 2011; Dai, 2013; Akimoto and Kusaka, 2015; Kutty et al., 2019; Hůnová et al., 2020), understanding how microbial communities respond to these different moisture sources will help us predict how arid- and semi-arid systems respond to changing climate regimes.

There are several reasons why microbial communities could differ in NRM- and rain-dominated environments. First, in many systems fog and dew occur more regularly than rainfall (Eckardt et al., 2013), so organisms that rely on NRM may not face such prolonged dry periods as those relying solely on rain, and may therefore be more sensitive to desiccation (Jacobson et al., 2015). Second, since NRM typically forms at night and in the early morning when temperatures are low, the ability to

remain active at colder temperatures may be more important for organisms relying on NRM as a primary moisture source than those that are solely rainfall-dependent (Evans et al., 2020). Finally, fog can transport microbial communities that differ from those dispersing through rain and clear air (Evans et al., 2019). Distinct airborne communities in fog-dominated systems could lead to distinct communities on senesced litter compared to in non-NRM affected systems. Whether or not these factors actually lead to differences in microbial communities under NRM- versus rain-dominated conditions is currently unknown, limiting our understanding of microbial community assembly and our ability to predict how decomposition rates are responding to changing climates.

We provide the first assessment of how fungal communities are differentially influenced by NRM and rainfall. Specifically, we addressed the following research questions:

(1) How does moisture regime (NRM- versus rain-dominated) drive fungal community composition?

(2) Do changes in fungal community composition driven by moisture regime influence rates of litter decomposition?

We hypothesized that differences in the air-derived fungal communities (fungi that colonized pre-sterilized tillers) as well as selection for different moisture regimes would lead to different fungal communities under the two regimes. We further

hypothesized that some fungi would specialize in a particular environment. Finally, we hypothesized that these differences in community structure would affect decomposition rates, with fungi decomposing litter faster under their native moisture regime than in non-native conditions.

METHODS

Site descriptions and climatic data collection

We conducted our study in the Namib Sand Sea, a fog-affected coastal dune system in western Namibia. The Namib is ideal for studying the influence of moisture regime on microbial function because it is pristine (a sand dune system with no permanent human settlements) and has two very different moisture regimes in close proximity to one another: the western region is dominated by fog and dew and receives scant rainfall while the inland eastern areas receive more rainfall but very little non-rainfall moisture (Figure 1.1A). Work was conducted at the Gobabeb Namib Research Institute (NRM Site) (23°33.6'S 15°02.46'E) and at the Far East Dune (Rain Site) (23°47.04'S 15°46.86'E), approximately 75 km apart (Figure 1.1A). To assess differences in the abiotic environment that fungi experienced, we monitored air temperature, relative humidity, rainfall, and wetness (presence of liquid water, i.e. dew/fog) at each site. Leaf wetness sensors allowed us to determine the number of hours with liquid water on tillers. Meteorological measurements were made at each

site, from weather stations situated <50 m from where the tillers were deployed. Weather data for the NRM Site were taken from the Gobabeb Met station, part of the SASSCAL FogNet array (www.sasscalweathernet.org) maintained by the Gobabeb Namib Research Institute (www.gobabeb.org). At the Rain Site, we used a HOBO data logger (H21-002, Onset Computer Corporation, USA) and sensors to record temperature and relative humidity (S-THB-M002), rain (Davis S-RGD M002), and leaf wetness (S-LWA-M003). Measurements were recorded once per minute and converted into hourly averages. The weather station at the Rain Site failed two months before the end of the experiment, so we used data from a nearby weather station (Dieprivier Namib Desert Lodge, also on the SASSCAL weather network, 40 km south). An analysis comparing weather data from the two eastern stations (Dieprivier and the Rain Site) for ten months before the failure showed that the two sites had comparable weather regimes. Since solar radiation can accelerate litter decomposition by photodegradation (King et al., 2012) and alter litter-associated decomposer communities (Pancotto et al., 2005), we estimated solar irradiance at the two sites. Since the weather stations we used did not measure solar irradiance, we used collected these data from two nearby proxy stations, both part of the SASSCAL weather network. The Rain Site's proxy station (Dieprivier) was about 30 km SSE of the Rain Site and used a Young Model 70092 Solar Radiation sensor (R.M. Young Company, Traverse City, USA) and the NRM Site's proxy station (Coastal Met) was 70 km NW of

that site and used an NR-LITE net radiometer (Kipp & Zonen, The Netherlands). In both cases the stations are farther into their respective climatic zones, providing an upper estimate of differences in solar irradiance. Plant diversity data came from previously published work (Yeaton, 1988).

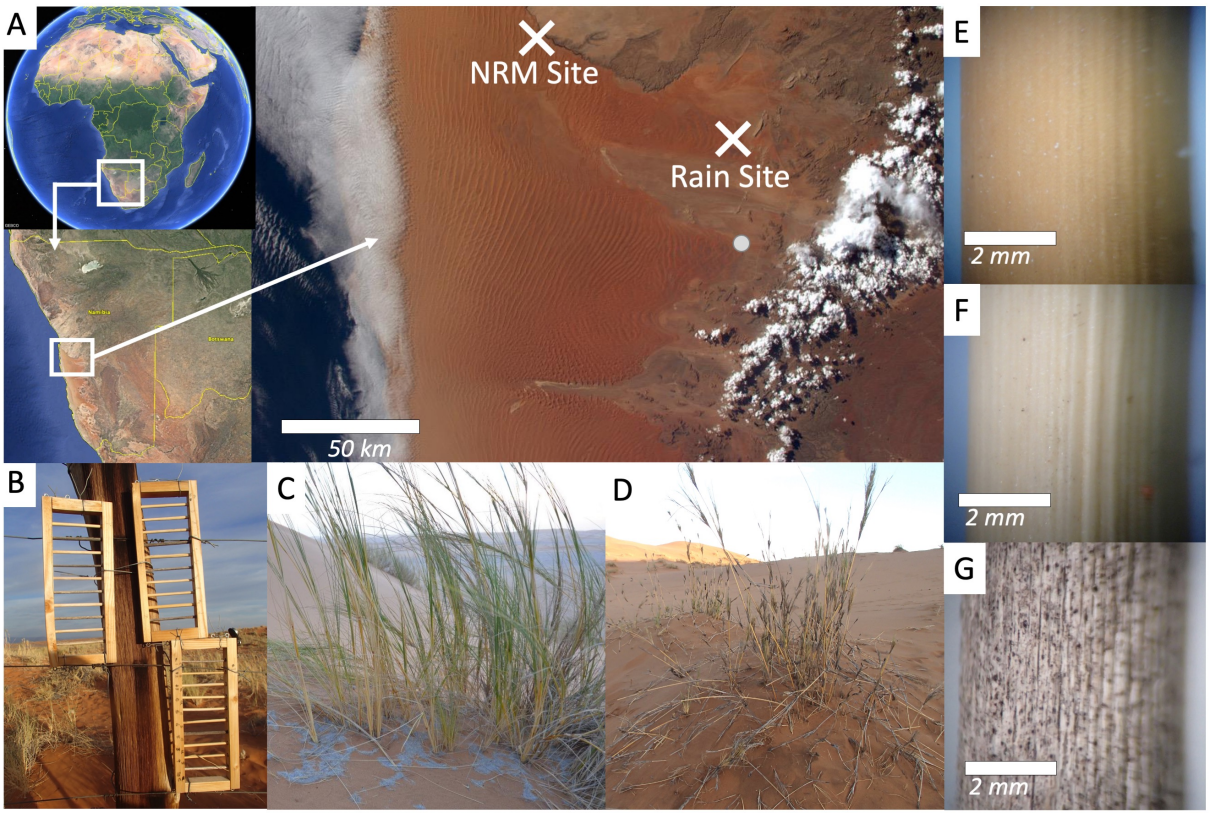

Figure 1.1. (A) Location of field sites in the Namib Sand Sea, with visible coastal fog in the west and rain clouds in the east (https://twitter.com/astroterry/status/590929048596951040), the grey dot shows the location of the Dieprivier weather station that served as a proxy weather station for the Rain Site for two months; (B) litter racks to minimize microclimate effects and ensure that tillers were fully exposed to sunlight and ambient moisture conditions at both locations; (C) living *S. sabulicola* hummock in the dunes; (D) standing dead *S. sabulicola* tillers will persist for years; (E-G) as tillers decompose, the outer cuticle is degraded and dark pigmented fungi colonize the surface.

Reciprocal transplant design

To see whether fungal communities functioned similarly under NRM- versus rain-dominated conditions, we reciprocally transplanted litter between the two sites (Reed and Martiny, 2007). Hereafter, we refer to "native" tillers as those deployed at the location from which they were collected (i.e. not transplanted). At the end of one year we measured mass loss, a proxy of fungal biomass, and fungal community composition of transplanted and native litter at both sites. We focused on fungi because they are considerably more abundant than bacteria on litter in this system and previous work found that fungi are important surface-litter decomposers here (Jacobson et al., 2015). We sought to identify differences in litter-associated fungal communities at the two sites, and determine what caused any differences. Specifically, we compared the importance of three potential factors that could influence litter-associated fungal communities: the species pool available as air-derived inoculum could differ between the sites, litter quality (lignin content, C:N ratios, etc.) could differ between the sites, and each site could be dominated by fungi that are particularly well suited to the meteorological conditions at that site (i.e. climatic variables could drive desiccation, thermal, and UV tolerance).

We examined native, transplanted, and autoclaved tillers of *Stipagrostis sabulicola* at the two sites. *S. sabulicola* is the dominant grass in the Namib Sand Sea and grows in hummocks on unstable dune faces (Figure 1.1C). Hummocks can be several meters

across and persist for decades though individual tillers will senesce and fall after several years (Figure 1.1D). We avoided the microclimate effects associated with litter bags by deploying standing dead tillers (>2 mm diameter) in "litter racks," wooden frames designed to hold 9-cm long tiller pieces (mean initial mass 0.77 g ± 0.27 S.D) while exposing them to ambient moisture and solar radiation (Figure 1.1B). Each rack had 0.5 cm deep indentations cut into the interior so that the tillers would fit snuggly between the longest wooden pieces of the frame without having to be glued in place. Racks were covered with a dewaxed shellac to waterproof them and minimize any fungal growth on the frames themselves and placed 80–125 cm above the ground surface to mimic standing grass in a hummock. We collected tillers from various hummocks at each site covering an area of roughly 1 km^2, within 2 km of the weather stations. Sample sizes are reported in Table S1.1. After one year (June 2015–June 2016), we collected tillers, air dried them, and weighed them on an analytical balance to determine mass loss before processing them for DNA sequencing.

Despite the fact that this study was conducted in a sand dune system, sandblasting and aeolian-driven mass loss were not substantial mass loss drivers in this study. First, we used only coarse tillers, leaving no attached leafy material that would be shredded or easily removed, even during very high winds (Figure 1.1B). Secondly, tillers were suspended high enough above the ground (80–125 cm) that they were removed from prolonged sandblasting they would encounter if they were at the sand

surface. Finally, visual observations of *S. sabulicola* tillers suspended in identical racks in other experiments we have conducted in the Namib Desert showed no signs of abrasion from sandblasting or aeolian mass loss, even after three years in the field (data not shown). We confirmed this in the present study by visually examining tillers for evidence of sand blasting after collection.

We used tillers at two different stages of decay to see whether moisture regime structured communities differently as tillers decomposed. Early-stage tillers were harvested from recently senesced stems that still had inflorescences attached (<2 months post-senescence), were yellow, had no visible fungal growth, and had a visibly intact cuticle. Late-stage tillers were harvested from upright stems that had been standing for at least one year. These were characterized by coverings of light and dark-pigmented fungi and a cracked cuticle that was considerably more permeable to water (Jacobson et al., 2015) (Figure 1.1E-G). The primary difference between the litter stages was that late-stage tillers had 72–444x greater fungal biomass than early-stage tillers. Since our study was confined to standing dead grass litter that had not fallen over yet, our terminology of "early" and "late" does not reflect the entire decomposition process but is meant to highlight relative successional differences between the litter types based on time since senescence and how well developed their associated fungal communities were.

To assess how colonization from air-derived fungi affected litter community assembly, we deployed "bait tillers," which were autoclaved early-stage tillers collected from the NRM Site. We included bait tillers from only one site because space limitations in our litter racks prevented us from including bait tillers from both sites. Sterilization was confirmed by plating tillers on culture media. Autoclaving is an imperfect means of sterilization because it can alter associated chemistry but since our goal was to identify air-derived fungi, this deployment of standardized bait tillers allowed us to estimate the contribution of air-derived fungal sources (i.e. spores) since the only fungi present on autoclaved tillers after one year would have been deposited from the air. Importantly, any confounding effects of autoclaving on litter properties would have been the same for litter deployed at both sites, allowing us to use a standardized litter type to compare air-derived fungal communities at the two sites.

Litter physical and chemical analysis

We measured C:N ratios in litter on a Thermo Finnigan Flash-1112EA microanalyzer (Thermo Fisher Scientific, Waltham, MA, USA). We used an ANKOM 200 Fiber Analyzer and Daisy Incubator (ANKOM Technology, Macedon, NY, USA) to measure acid detergent lignin, cellulose, and hemicellulose of live tillers and a subset of early- and late-stage tillers to determine initial litter chemistry at the start of the study. To determine whether mass loss was driven solely by differences in leaching

from tillers at the two sites, we measured leaching on a subset of recently senesced tillers collected from the two sites that were identical to those used in our decomposition study. We sealed the cut ends of each tiller with glue, submerged them in ultrapure water at 4°C for 24 hours, dried them, and weighed them to quantify mass loss due to leaching.

Molecular methods

Fungal communities were analyzed using molecular methods. We extracted DNA from tillers using a MoBio PowerSoil DNA extraction kit supplemented with 10 minutes of sonication prior to mechanical lysis. We sequenced the ITS region (ITS1-F: CTTGGTCATTTAGAGGAAGTAA; ITS2: GCTGCGTTCTTCATCGATGC) using 250-bp paired-end sequencing on the MiSeq Illumina (V2) platform at Michigan State University's Research Technology Support Facility Genomics Core. We used the same clustering and filtering pipeline used for Namib fungal (ITS) sequences in described elsewhere (Evans et al., 2019). All sequences are available on NCBI's Sequence Read Archive under BioProject number PRJNA685174.

Fungal contigs were created using default settings in fastq_mergepairs implemented in the USEARCHv8.1 pipeline (http://drive5.com/usearch/). Merged sequences were quality filtered to an expected error threshold of 1.0 fastq_filter (Edgar and Flyvbjerg, 2015). Sequences were then truncated to 380 bp with shorter

sequences padded to reach the 380 bp because ITS region length is highly variable (Nilsson et al., 2008). Combined reads were dereplicated and OTUs were picked at the 97% identity level using UPARSE (Edgar, 2013) then chimera checked using reference based UCHIME2 (Edgar, 2016) against the UNITE 7.1 ITS1 chimera database (Kõljalg et al., 2013) within the USEARCHv9.1 pipeline.

Reads per sample ranged from 1,805 to 52,926 averaging 22,425. We used multiple extraction blanks to check for contamination, eventually removing three OTUs from the dataset. After OTU clustering, we removed any taxa that fit all three of the following criteria: it had more than 100 reads when summed across three blanks, had never been found in any previous sequencing datasets from working in the Namib Desert, and had never been cultured from the Namib in previous studies (e.g. Jacobson et al. 2015). This left us with two potential contaminants, one of which (an unknown ascomycete) was only present in a single blank but was also present in several real samples that had been processed immediately before that blank leading us to believe this was likely a crossover contaminant from a real sample so kept it in the dataset. This left only one potential contaminant that we removed from our dataset (OTU258 *Trametes versicolor* a basidiomycete found in forests). We also removed two OTUs that were identified as *S. sabulicola*, the host plant.

Since fungal reference databases have considerable errors in taxonomic identifications (Hofstetter et al., 2019), anytime we identify a specific taxon by name,

we first manually verified its identity by using the NCBI's Basic Local Alignment Search Tool, using a conservative cutoff of ≥97% similarity and ≥80% coverage (Raja et al., 2017), using only type species as references (Ko et al., 2011). Whenever possible, we verified identity by comparing our sequences of the ITS 1-2 region (250-300 bp) to those of known fungi that we had isolated from *S. sabulicola* tillers in previous studies in the Namib, which had been identified with the longer ITS 1-4 region (~600 bp) (Jacobson et al., 2015).

As a proxy of fungal biomass, we used quantitative PCR to count the number of ITS gene copies per sample and normalized it to the tiller's dry biomass (Song et al., 2014). While this proxy did not allow us to directly quantify fungal biomass, we were able to compare relative differences among treatment groups. For qPCR, one subset of DNA that was submitted for sequencing from each sample was diluted ten-fold and then amplified using ITS1-F/ITS2 primers and SYBR Green Supermix (BIO-RAD, USA) on the following thermocycle program: 95°C for 15 min, 40 cycles of 95°C for 30 sec then 50°C for 30 sec then 72°C for 30 sec, and finally 95°C for 15 sec, 60°C for 15 sec, and ramp from 60–95° for 20 min to obtain a melting curve. We used DNA extracted from *Saccharomyces cerevisiae* as a standard to quantify ITS gene copies and normalized this to the dry mass of litter used for the extraction to produce a proxy of fungal biomass reported as $\log_{10}$ ITS copies $gram^{-1}$.

Statistical Analysis

We analyzed mass loss and fungal biomass data in R (R Core Team, 2020) using 't.test' and 'lm' functions and analyzed the reciprocal transplant experiment with Type III ANOVAs using the 'Anova' function in the *car* package. PERMANOVAs and NMDS ordinations were generated using Bray-Curtis distances calculated using the distance function in the *phyloseq* package (McMurdie and Holmes, 2013). We calculated PERMANOVAs and ordinations using relative abundance data for each taxon. We calculated Shannon-Weiner diversity and evenness using the 'diversity' function in *vegan* (Oksanen et al., 2019). Correlations between taxa abundances were calculated using the 'cor.test' function.

While dominance at a particular site suggests that the taxon is well-suited for that environment, high abundance could also be driven by stochastic processes or historical contingencies. To determine whether taxa that were more abundant on litter at a particular site were also those that were more common in the air at that site, we used a simple linear regression to see if the magnitude of a taxon's greater abundance at one site over the other was correlated with its relative abundance in air-derived communities on bait tillers. For taxa with non-zero abundances at both sites, we calculated site preference as:

$$Site\ Preference = log_{10}(\frac{A_{NRM}}{A_{RAIN}}) \quad \text{(Equation 1.1)}$$

where A_{NRM} and A_{RAIN} are average relative abundances in each community based on sequence reads. A site preference value of zero means that a taxon had the same abundance at both sites while each unit above or below zero indicates a 10-fold greater relative abundance at one site. A positive site preference denotes greater abundance at the NRM Site and negative denotes greater abundance at the Rain Site.

RESULTS

Site and litter characterization

We observed marked meteorological differences between the Rain and NRM Sites. During the one-year study, the NRM Site had 4.8x more hours of wetness and 10.7x more hours of high humidity (Table 1.1). Although both sites are hyperarid, the Rain Site received 5.4x more rain (56 vs. 10.3 mm yr^{-1}) and more frequent rain events than the NRM Site. The average time between wet events (either rain or NRM events) was 33 hours at the NRM Site and 90 hours at the Rain Site ($p = 0.001$). Dry periods lasting for more than 100 hours were not uncommon at the Rain Site (Figure S1.1). Previous work has shown that wet events are longer at the NRM Site (Evans et al., 2020); for example, at the NRM Site, only 5% of wet events lasted two hours or less while at the Rain Site 22% of wet events were this short. Mean temperature during wet events was only slightly lower at the NRM Site, which had a narrower temperature range (range 1.6–26.9°C) than did the Rain Site (range -0.7–39.1°C).

Table 1.1. Site differences during the one-year study period. NRM events and duration included times when leaf wetness sensors were wet but there was no recorded rain. Solar irradiance values are estimates based on data from nearby proxy locations. Plant diversity and biomass values come from Yeaton (1988). The last two months of weather data for the Rain Site came from a nearby site because of equipment failure.

Value	Units	NRM Zone	Rain Zone	P
Time deployed	days	352	344	—
Rainfall	mm	10.3	56	—
Rain events ≥2 mm	Events	1	5	—
Rain events <2 mm	Events	1	11	—
Rain duration	Hours	10	42	—
NRM duration	Hrs of leaf wetness	1495	311	—
Time between wet events	Hours	33	90	0.001
Time >90% rel. humidity	Hours	779	73	—
Temp when wet (range)	°C	13.0 (range 1.6–26.9)	14.8 (range -0.7–39.1)	<0.001
Temp when dry (range)	°C	22.7 (range 3.3–42.3)	23.6 (range 0.2–42.6)	<0.001
Mean daily temp	°C	19.7	23.2	0.008
Mean daily max	°C	29.9	32.3	<0.001
Mean daily min	°C	13.2	14.4	0.004
Time ≥40°C	Hours	4	23	—
Avg Daily Solar Irradiance	MJ m^{-2}	21.7	23.7	<0.001
Perennial Grass richness	Species	1	4	—
Perennial Grass Biomass (n=14)	g m^{-2}	14.9 (SE 5.8)	448.9 (SE 64.6)	—

Perennial grass biomass and richness are lower at the NRM Site than at the Rain Site (Table 1.1). Average daily solar radiation (MJ m^{-2}) during the study period was 9% greater in the vicinity of the Rain Site than the NRM Site, though these were based on estimates from proxy sites and likely overestimate differences between our sites. Both sites had similar bidirectional NW and E wind regimes with seasonal variation in wind direction, suggesting similar source regions of air-derived fungi, though the Rain

Site had a stronger southern component (Figure S1.2). Windspeed was greater at the NRM Site than at the Rain Site (Figure S1.3), though we saw no evidence of physical damage (flaking, abrasion marks) that would indicate differences in wind damage between the two sites. Overall, the Rain Site was characterized by more frequent and longer dry periods, shorter wet periods, higher temperatures, more variable temperatures when wet, and slightly greater solar irradiance compared to the NRM Site.

Litter chemistry varied between sites and litter stages (Table 1.2). In live tillers, acid detergent lignin was higher and cellulose and hemicellulose concentrations were lower at the Rain Site than at the NRM Site. In both early and late senescent tillers, like those we used in the study, we did not observe significant differences in C:N, lignin:N, or percent N (Table 1.2). In our lab-based leaching test, early-stage tillers from the NRM Site lost more mass due to leaching than did those from the Rain Site, likely driven by increased water absorption by senescent tillers from the NRM Site (Figure S1.4).

Table 1.2. Fungal biomass, fungal:bacterial ratios, and litter chemistry values for live *S. sabulicola* tillers and standing dead litter at both sites. Significant differences ($P < 0.05$) from t-tests are in bold. ND = Not Determined. Reported values are means ± S.E.M. N = 5 for each group.

Value	Units	Live Tillers		Early-Stage Senesced		Late-Stage Senesced	
		NRM	Rain	NRM	Rain	NRM	Rain
Fungal Biomass	Log_{10}(ITS copies $gram^{-1}$)	ND	ND	4.8±0.3	4.0±0.2	7.1±0.1	6.7±0.1
Fungi:Bacteria	ITS copies : 16S copies	ND	ND	**9.5±1.5**	**0.02±0.01**	10.6±2.4	8.2±2.8
Acid Detergent Lignin	% m/m	**18.1±0.6**	**23.3±1.4**	21.0±2.3	23.4±5.0	10.6±1.5	19.1±6.5
Cellulose	% m/m	**44.0±1.0**	**39.6±0.9**	37.2±2.0	33.6±3.6	45.4±1.1	44.1±5.4
Hemicellulose	% m/m	**22.7±5.3**	**19.2±3.6**	**23.7±0.5**	**20.3±0.9**	**27.0±0.5**	**20.7±0.4**
Percent N	% m/m	ND	ND	0.19±0.06	0.51±0.23	0.29±0.07	0.30±0.08
C:N Ratio	Ratio m/m	ND	ND	325 ± 106	148 ± 37	191 ± 39	382 ± 254
Lignin:N Ratio	Ratio m/m	ND	ND	151 ± 53	69 ± 19	48 ± 16	331 ± 294

Drivers of fungal community composition

Fungal community richness, diversity, and evenness on native early- and late-stage litter were not significantly different between the sites, though fungal biomass was greater at the NRM Site for both litter stages (Table 1.3). Forty-two percent of taxa were core taxa found on native litter at both sites (Figure S1.5), and these taxa make up the majority of reads (96.0% of native NRM Site reads and 88.0% of native Rain Site reads).

Fungal communities on native tillers differed between the sites (Figure 1.2A). Site explained more variation in community composition on native tillers than did litter stage ($R^2_{site} = 0.31$, $R^2_{stage} = 0.06$, Figure 1.2A). The most dominant taxa on native tillers also differed between the two sites (Figure 1.3). For example, at the NRM Site the three most abundant fungi on early- and late-stage litter (*Neophaeothecoidea* species (OTU4), *Neostagonospora caricis* (OTU8), and *Phaeococcomyces mexicanus* (OTU30)) together accounted for more than 53.0% of reads, but less than 1.4% at the Rain Site (Figure 1.3). Likewise, the top three taxa at the Rain Site (*Aureobasidium melanogenum* (OTU3), *Phaeococcomyces* sp. (OTU17), *Alternaria alternata* (OTU1)) accounted for 50.8% of Rain Site reads but only 9.2% of NRM Site reads.

Although the sites had statistically different air-derived fungal communities ($R^2 = 0.23$, $P = 0.008$) (Figure 1.2A), they also shared a group of core taxa (Figure S1.5); the 73 taxa that were present in the air-derived community at both sites made up

96.4% of reads at the NRM Site and 83.2% at the Rain Site. Taxa that were more common on bait tillers at each site also tended to be more common on early-stage and late-stage native litter at that site (Figure 1.4), suggesting that air is an important source of inoculum for tillers. Bait tillers at the NRM and Rain Sites had similar total richness, richness per tiller, and fungal biomass, though Shannon Diversity of the air-derived community was greater at the Rain Site, driven by a more even community structure (Table 1.3; Figure S1.6).

Table 1.3. Comparisons of air-derived and litter-associated fungal communities at each site. Values are only for native (i.e. non-transplanted) tillers. Values are reported as means ± 1 S.E. Bolded text denotes significant differences. Sample sizes are reported in Table S1.1.

Litter Type	Site	Total OTU Richness	Richness Tiller^{-1}	Shannon Diversity Tiller^{-1}	Evenness Tiller^{-1}	Log^{10} ITS Copies g^{-1}
Bait Tillers	NRM	177	59 ± 11.0	**2.02 ± 0.22**	**0.51 ± 0.06**	4.9 ± 0.8
	Rain	172	58.4 ± 13.5	**2.68 ± 0.16**	**0.67 ± 0.03**	3.2 ± 0.3
	P		0.97	**0.04**	**0.046**	0.15
Early-Stage	NRM	218	63.6 ± 5.2	1.91 ± 0.16	0.46 ± 0.04	**4.8 ± 0.3**
	Rain	159	54.6 ± 3.8	2.43 ± 0.28	0.61 ± 0.07	**4.0 ± 0.2**
	P		0.19	0.16	0.11	**0.04**
Late-Stage	NRM	143	53.5 ± 3.9	1.87 ± 0.19	0.47 ± 0.05	**7.1 ± 0.1**
	Rain	174	61.4 ± 12.9	1.82 ± 0.29	0.44 ± 0.05	**6.7 ± 0.1**
	P		0.59	0.90	0.67	**0.03**

The three most abundant air-derived taxa at the Rain Site (*Aureobasidium melanogenum* (OTU3), unknown Pleosporales (OTU104), and *Alternaria alternata* (OTU1)) made up 31.0% of the Rain Site air-derived reads and 25.8% of the NRM Site

air-derived reads. The top three air-derived taxa at the NRM Site (*Cladosporium cladosporioides* complex (OTU2), *Alternaria alternata* (OTU1), and *Selenophoma linicola* (OTU33)) made up 43.7% of NRM Site air-derived reads and 10.2% of Rain Site air-derived reads (Figure 1.3). Some taxa, (e.g. *Alternaria alternata* (OTU1) and *Aureobasidium melanogenum* (OTU3)) were highly abundant on both bait tillers and native tillers at both sites.

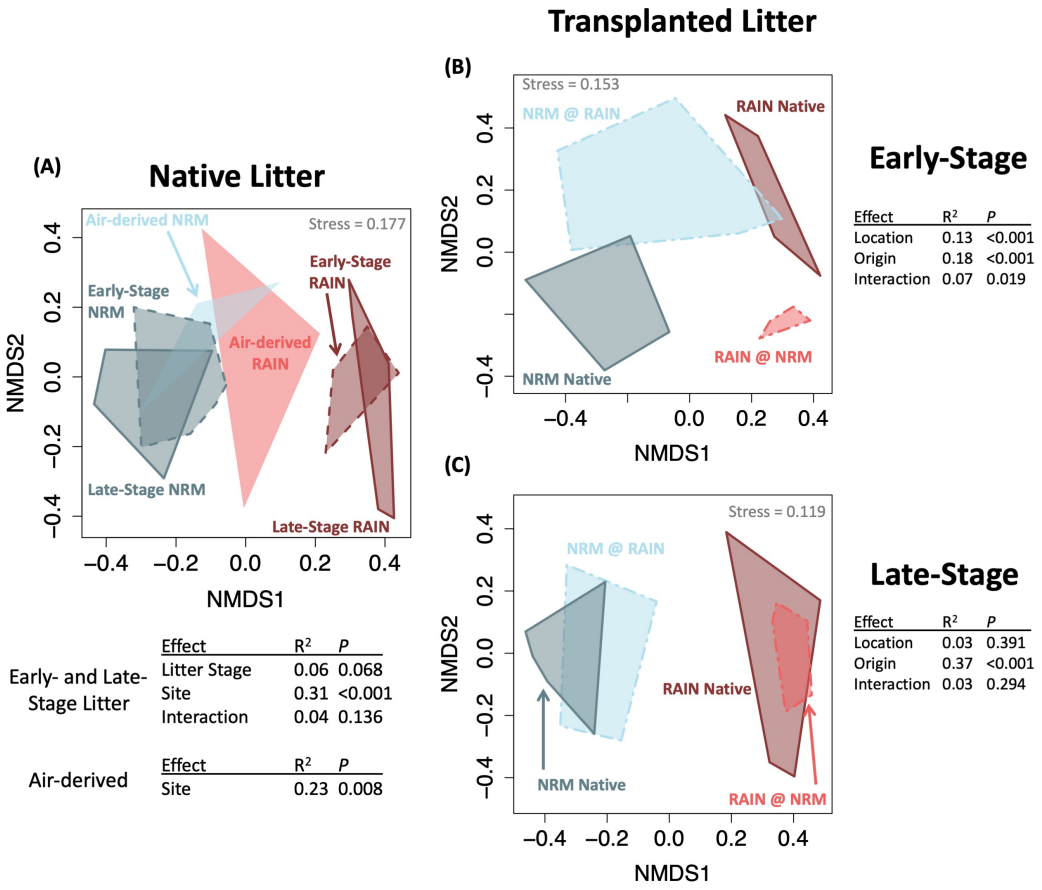

Early- and Late-Stage Litter	Effect	R^2	*P*
	Litter Stage	0.06	0.068
	Site	0.31	<0.001
	Interaction	0.04	0.136

Air-derived	Effect	R^2	*P*
	Site	0.23	0.008

Early-Stage	Effect	R^2	*P*
	Location	0.13	<0.001
	Origin	0.18	<0.001
	Interaction	0.07	0.019

Late-Stage	Effect	R^2	*P*
	Location	0.03	0.391
	Origin	0.37	<0.001
	Interaction	0.03	0.294

Figure 1.2. NMDS ordinations (Bray-Curtis distance) of fungal communities with groups connected by convex hulls. (A) Native litter and air-derived fungal communities at both sites, top table shows the PERMANOVA just for litter communities and bottom table shows results for just air-derived communities (B) Transplanted early-stage litter with PERMANOVA results (C) Transplanted late-stage litter with PERMANOVA results.

OTU	Native NRM	Native Rain	Air-derived NRM	Air-derived Rain	Species
OTU3	4.9%	22.2%	10.9%	13.8%	*Aureobasidium melanogenum*
OTU4	25.9%	0.5%	10.7%	2.9%	*Neophaeothecoidea species*
OTU1	3.1%	14.6%	14.9%	7.3%	*Alternaria alternata*
OTU2	7.0%	0.7%	17.8%	2.2%	*Cladosporium cladosporioides complex*
OTU8	15.9%	0.8%	7.4%	4.1%	*Neostagonospora caricis*
OTU17	0.9%	14.0%	0.2%	5.3%	*Phaeococcomyces species*
OTU2456	1.2%	5.0%	0.5%	1.0%	*Phaeococcomyces species*
OTU24	1.3%	2.3%	6.1%	5.7%	*Didymella microchlamydospora*
OTU30	11.6%	0.1%	2.7%	0.3%	*Phaeococcomyces mexicanus*
OTU33	6.7%	0.2%	11.0%	0.7%	*Selenophoma linicola*
OTU72	0.0%	4.0%	0.0%	0.2%	Unknown (Teratosphaeriaceae) species
OTU40	4.9%	0.2%	4.2%	4.5%	*Filobasidium species*
OTU15	0.0%	3.5%	0.3%	6.0%	*Pseudopithomyces species*
OTU83	0.0%	4.3%	0.0%	0.1%	*Cyanodermella oleoligni*
OTU104	0.0%	0.0%	0.0%	9.9%	*Pleosporales species*
OTU238	0.0%	4.6%	0.0%	0.0%	*Bartalinia species*

Figure 1.3. Identities of taxa that constitute the top 80% of reads across all tillers (native, transplanted, and bait tillers) and their average read abundance in native and air-derived (bait tiller) communities. Percentages for "Native" category represent the average read abundance for that OTU across both early- and late-stage tillers.

When we transplanted early-stage tillers, community composition changed to resemble native tillers at their new site, while transplanted late-stage tillers retained their native fungal communities (Figure 1.2B-C; PERMANOVA $P_{origin*location} = 0.019$ for early-stage, $P_{origin*location} = 0.294$ for late-stage). Early-stage tillers moved to the NRM Site had higher fungal biomass than those that remained at the Rain Site (Figure 1.5B). When late-stage tillers were moved to the Rain Site, fungal biomass was lower than for those that remained at the NRM Site (Figure 1.5C).

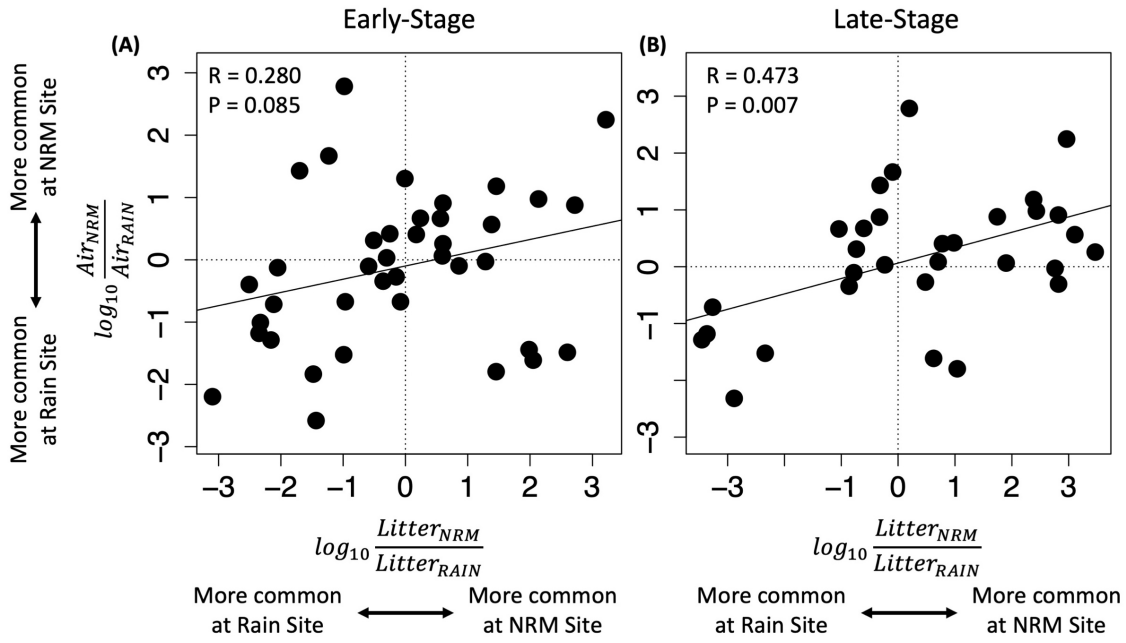

Figure 1.4. The degree of site preference on bait tillers versus site preference on native litter for taxa with non-zero abundances at both sites. Note that taxa that are abundant on native litter at one site (x-axis) are also more abundant on bait tillers colonized by air-derived fungi at that site (y-axis). This pattern is stronger for late-stage than for early-stage tillers. Each point represents one OTU and each unit above or below zero corresponds to a 10-fold greater relative abundance at a particular site with positive values indicating a greater relative abundance at the NRM site and negative values indicating a greater relative abundance at the Rain site. Regression lines and statistics are for simple linear regression.

Consistent with our hypothesis that fungi were specialized to particular environments, fungi that were more common on native litter at each site increased when litter was moved to that site and decreased when litter was moved away from that site (Figure 1.4), though this pattern was much stronger for early-stage tillers than for late-stage tillers. We identified 38 taxa that consistently showed greater abundance at the NRM Site (i.e. they were more abundant on NRM native litter, increased when

transplanted to the NRM Site, and decreased when moved away from the NRM Site) which together made up 61.2% and 77.0% of reads on early- and late-stage native litter at the NRM Site (Table S1.2). Fifty-five taxa showed similar preferences for the Rain Site, making up 50.2% and 60.9% of reads on early- and late-stage native litter at the Rain Site (Table S1.2).

Functional significance of decomposer communities

Fungal biomass of bait tillers tended to be higher at the NRM Site than at the Rain Site, though not significantly so ($P = 0.104$; Figure 1.5A) and bait tiller mass loss was 4.8x greater at the NRM Site ($P = 0.065$; Figure 1.5D). Fungal biomass at the end of the study was positively correlated with mass loss on both early- and late-stage tillers (Figure S1.7). A visual inspection of tillers showed no evidence of sandblasting on the tillers upon collection. Mass loss showed a significant interaction between litter origin and deployment location for late-stage litter but not early-stage litter (Figure 1.5E-F). Late-stage NRM Site tillers decomposed 2.7x faster at their home (NRM) location compared to the Rain Site, but decomposition of late-stage Rain Site tillers was not significantly different between locations (Figure 1.5F). Early-stage litter did not decompose differently when deployed at the two sites, though we did see a marginally significant effect of origin with early-stage litter from the Rain Site moved to the NRM Site, showing greater mass loss than similarly aged litter from the NRM

Site (Figure 1.5E). Mass loss patterns for late-stage tillers mirrored those for fungal biomass in that tillers from the Rain Site did not differ significantly whether they were transplanted or not, while NRM tillers decomposed considerably less and had significantly lower fungal biomass when they were moved to the Rain Site (Figure 1.5C,F).

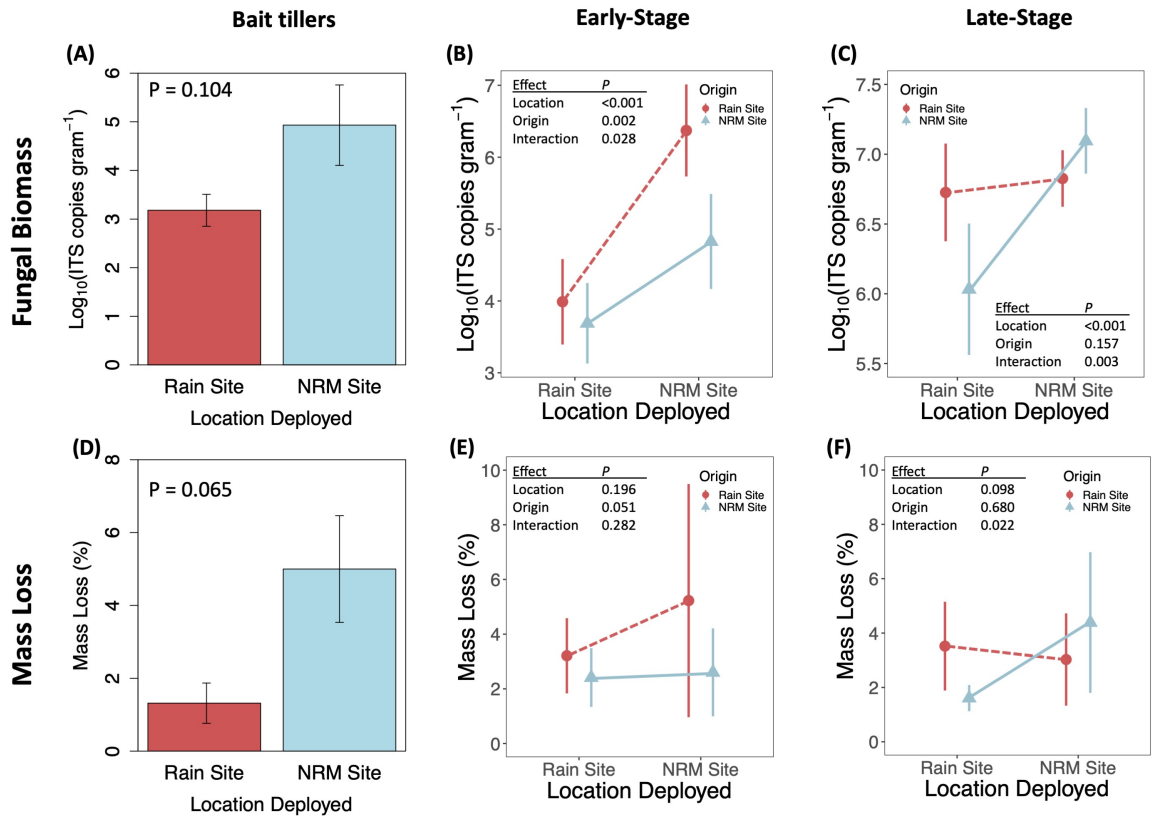

Figure 1.5. Fungal biomass as indicated by Log_{10} ITS copies $gram^{-1}$ (top row) and mass loss after one year (bottom row) for bait tillers, early-stage tillers, and late-stage tillers. P-values are for t-tests for bait tillers and two-way ANOVAs for early- and late-stage tillers; full ANOVA results are reported in Supplementary Tables 1.3, 1.4, 1.5, and 1.6. Fungal biomass statistics were run on log10 transformed data. Error bars show 95% CI. Sample sizes are included in Table S1.1.

DISCUSSION

Understanding how microbial communities mediate the relationship between environmental drivers and ecosystem functions can help us predict how ecosystems will respond to changing climates. Many factors influence the composition of litter-associated microbial communities including the availability of inoculum, biotic interactions among saprotrophs, the environment, and substrate quality. We have shown that, in the Namib Sand Sea, climatic differences between the NRM and Rain Sites explain differences in fungal community composition and that decomposition rates depend in part on the composition of the extant fungal community.

Throughout litter decomposition, decomposer communities typically shift in predictable ways as rapidly-growing early colonizers give way to slower specialists that degrade more recalcitrant compounds (Voříšková and Baldrian, 2013; Gołębiewski et al., 2019). While litter moisture content influences fungal communities (Dix and Webster, 1995), in grasslands, litter age can be a more important determinant of decomposer communities than environmental drivers (Matulich et al., 2015). We found that regional climatic differences influenced community composition far more than litter stage. While litter-associated communities were only marginally different between early- and late-stage litter within each site, communities differed substantially between the sites (Figure 1.2A). Furthermore, tillers from the same site that differed in their time since senescence by roughly two years had highly variable litter quality

but had communities that were more similar to each other than same-aged tillers at different sites. This demonstrates the importance of NRM and rain as climatic drivers of fungal communities in this system.

Fog alters the microbiology of air and factors like proximity to the ocean can affect airborne microbial community composition in coastal fog systems (Evans et al., 2019). In our study, the correlation between air-derived and litter-associated taxa abundances (Figure 1.4) could be driven by two factors. First, spores that are more abundant in the air may provide more inoculum for litter, making the litter communities resemble those in the air. Alternatively, abundant litter-associated fungi may produce more spores that disperse through the air, making the airborne communities resemble those on litter. Likely, both of these processes happen simultaneously, but we suspect the latter may be more important. If the former were the most important, we would expect early-stage tillers, which have more open niche space for colonization, to be more similar to air-derived communities than would late-stage tillers that are already well established. Instead, air-derived community abundances were more strongly correlated with late-stage tillers than early-stage tillers (Figure 1.4), suggesting that this relationship may be mainly driven by the production and release of airborne spores by abundant litter fungi across the landscape.

Two fungi stand out as abundant and widespread across all litter types at both sites. *Alternaria alternata* (OTU1) and *Aureobasidium melanogenum* (OTU3) each

represented over 10% of read abundances on native or bait tillers at both sites (Figure 1.3) and are both globally ubiquitous species with high stress tolerances. *Alternaria alternata* is saprotrophic and pathogenic to a diverse range of agricultural crops worldwide (Adachi et al., 1993; Aradhya et al., 2001; Kgatle et al., 2019) and *Aureobasidium* is a polyextremophilic genus isolated from environments as wide ranging as hypersaline water, glacial ice, aviation fuel tanks, and in epiphytic and endophytic lifestyles worldwide (Gostinčar et al., 2014). Both of these taxa are capable of producing dark pigments, an important strategy for coping with high solar radiation and desiccation stress (Cordero and Casadevall, 2019). That these were among the most abundant taxa isolated from native and bait tillers at both sites is perhaps unsurprising given their widespread distributions and tolerance of many environmental stressors including desiccation and UV irradiation.

Other fungi however showed strong discrimination between the sites. Four taxa were highly abundant on native and bait tillers at the NRM Site but not at the Rain Site (Figure 1.3): *Cladosporium cladosporioides complex* (OTU2), *Neophaeothecoidea spp.* (OTU4), *Phaeococcomyces mexicanus* (OTU30), and *Selenophoma linicola* (OTU33). Despite their low abundance at the warmer, drier Rain Site, most of these taxa are closely related to organisms known for their desiccation and thermal tolerance. *Neophaeothecoidea* is a monotypic genus first isolated from protea plants in South Africa and, while its ecology has not yet been described in detail, it's confamiliars in Teratosphaeriaceae occupy a

wide range of habitats including highly acidic soils (Hujslová et al., 2013) and rock surfaces in Antarctic and alpine desert environments, where they grow in highly melanized forms (Ruibal et al., 2009). *Phaeococcomyces mexicanus* has been found as an epiphyte on desert shrubs (Moreno-Rico et al., 2014), a leaf endophyte (Ricks and Koide, 2019), and in Antarctic snow (de Menezes et al., 2019) and is related the black yeasts, which are notoriously tolerant of environmental stressors associated with low water activity (Gostinčar et al., 2010). *Cladosporium cladosporioides complex* is a cosmopolitan group found on decaying plant litter in aquatic habitats (Freitas, 2018), in air samples (Bensch et al., 2010), and associated with leaf litter and living leaves of dozens of plant species (Freitas, 2018). Despite its widespread distribution, *Cladosporium* may be sensitive to prolonged exposure to extreme desiccation and heat; *Cladosporium* airborne spore abundance was substantially higher in the cooler, humid winter months than during the hot, dry summer in Riyadh, Saudi Arabia (Al-Suwaine et al., 1999), though it is still present in the desert year round. *Selenophoma linicola* is a member of the Dothideales, which contain extremotolerant rock-inhabiting fungi (Ruibal et al., 2009), though most *Selenophoma spp*. have been isolated from less extreme environments such as agricultural grasses and plant litter (Vanterpool, 1947; Brokenshire and Cooke, 1975; Crous et al., 1995; Sutton and Sankaran, 1995).

Two fungi showed much greater abundances at the Rain Site than the NRM Site: *Pseudopithomyces species* (OTU15) and *Phaeococcomyces species* (OTU17). *Pseudopithomyces*

is often found on dead plant litter and as a pathogen of some plants (Ariyawansa et al., 2015) including in nearby Angola (Crous and Groenewald, 2018). The closely related genus *Pithomyces* is globally distributed throughout warm climates but is particularly common in humid coastal regions (Dingley, 1962). Interestingly, the other taxon that exhibited a strong preference for the Rain Site, *Phaeococcomyces species* (OTU17), is a congeneric of a fungus with a strong preference for the NRM Site (*Phaeococcomyces mexicanus* OTU30), suggesting that the traits responsible for thriving under the NRM-dominated versus rain-dominated environment may not be so clearly delineated along taxonomic lines.

Overall, we did not find clear differences in desiccation tolerance or general stress tolerance among the fungi that preferred the NRM Site versus the Rain Site based on our literature searches. While culture-based follow-up studies may provide more information about the desiccation and thermal tolerances of these organisms, biotic interactions may also play a role in determining which taxa dominate at each site. For instance, while some NRM Site fungi may be fully capable of surviving the abiotic conditions of the warmer, drier Rain Site, they may simply be outcompeted by others with even slightly greater drought resistance. Similarly, Rain Site fungi appear fully capable of utilizing NRM when given the opportunity (Figure 1.5C,F), but over extended periods, they may be outcompeted by fungi better able to take full advantage of NRM at the low temperatures associated with that environment. Future studies

examining how these fungal communities assemble over time may be able to identify how competitive dynamics and successional changes interact with climatic tolerances to structure decomposer communities.

The fact that both of these sites harbored diverse fungi associated with such wide ranging niches was surprising, since we might have expected that only specialized fungi could tolerate the radiation and desiccation stressors of the hyperarid Namib Desert. Instead, several of the most abundant taxa were found worldwide in mesic and arid environments. This could be partially explained by considering the traits that support wide distributions. In bacteria, some of the traits that permit growth in an arid, sunny environment (such as pigmentation) correlate with large geographic ranges (Choudoir et al., 2018), since they aid in dispersal and permit individuals to grow in a wider range of environments. That many of the dominant fungi in this hyperarid landscape were globally cosmopolitan species suggests that this may be the case for some fungi as well.

By using bait tillers, instead of direct air sampling, to assess the air-derived fungal community, we focused on those fungi that were capable of colonizing senesced grass tillers. These results show that the airborne and litter-associated fungal communities appear to interact with one another, representing a shared pool of dominant fungi. Although we were unable to determine whether air-derived communities at these two sites differed primarily due to differences in local plant

diversity at the two sites, long-distance dispersal from wind, or other factors, we did find that the two sites contained a large pool of shared taxa. Cosmopolitan taxa (those that were present at both sites) make up the vast majority of reads on bait tillers at both locations, suggesting that similar air-derived species pools are available to colonize litter at both sites. Overall, litter-associated communities differed between the sites much more than air-derived communities did, suggesting that post-colonization processes play a role in structuring fungal communities differently at the two sites.

Fungal communities on some transplanted tillers changed, as would be expected if some fungi performed better in one environment than the other. Fungal communities on early-stage tillers shifted while well-established late-stage tillers retained their initial communities (Figure 1.2 B-C). That we did not see a similar shift in community composition for transplanted late-stage tillers is likely because they had such well-developed communities by the time they were moved that there was little available space for other fungi to grow. Others have shown that litter decomposition is influenced by microbial adaptation to historical moisture regimes (Allison et al., 2013; Frossard et al., 2015; Martiny et al., 2017; Glassman et al., 2018), but these studies usually only examine responses to rainfall amount. If the decrease in mass loss when late-stage NRM tillers were moved were driven solely by the reduction in water availability and not a community-specific response to the new conditions, then these

tillers would have decomposed at a similar rate as native Rain Site tillers. Instead, litter decomposition rates depended on the origin of fungi (Figure 1.5C,F), demonstrating that the existing fungal community influences how litter decomposes under different moisture regimes.

We found that fungi responded strongly to transplantation between two sites with radically different moisture regimes. Since our study used only two sites, we cannot definitively identify moisture type (rain vs. NRM) as the sole driver of fungal community differences that we observed, though it was likely the dominant factor. We collected standing dead litter from a sand dune system and suspended it aboveground so any differences in soil type would not be a factor. NRM duration differed by a factor of five to ten between the sites while minimum and maximum temperatures were far more comparable (Table 1.1). The Rain Site also experienced slightly more hours above 40°C during the study (Table 1.1), which could have altered communities by differentially stressing certain fungi. Although small changes in mean temperature can have outsized effects on decomposer activity (Salah and Scholes, 2011), others studies in the Namib Desert have found that NRM-driven moisture content describes the majority of variation in biological CO_2 respiration (Jacobson et al., 2015) and litter mass loss (Evans et al., 2020), even without explicitly including temperature in their models. Furthermore, another study (Jacobson et al., 2015) found that fungi cultured from litter at the NRM Site were able to grow in the lab under a diel temperature cycle

that included five hours at 50°C, substantially higher than the maximum temperatures we observed at either site during our study period (42.3°C at the NRM Site and 42.6°C at the Rain Site). Finally, disentangling the effects of temperature and moisture type is complicated by the fact that fog and dew will only form once temperatures drop below the dew point (Ritter et al., 2019), so we would expect some degree of temperature difference between the sites, at least during wet conditions. Indeed we found that while the range of temperatures while dry were very similar at the two sites, maximum temperatures when wet were considerably lower at the NRM Site (Table 1.1). Future studies examining fungal responses to NRM across sites could explicitly examine the role of temperature extremes to understand how fungal communities will respond in the face of both warming temperatures and altered moisture regimes.

Although we did not attempt to identify specific traits that drove differentiation in fungal communities at the two sites, our results suggest that the ability to tolerate the harsher conditions of the warmer, drier rain-dominated environment is an important driver of fungal differentiation across this gradient. The NRM-to-Rain transition may be difficult because the Rain Site is warmer, experiences less frequent wetting, greater solar irradiance, longer dry periods, and shorter NRM events (Evans et al., 2020) (Table 1.1, Figure S1.1), conditions that may challenge organisms requiring long wet, cool periods for metabolic activity and growth. Conversely, Rain Site fungi were able to grow and decompose litter equally effectively at both, suggesting that

most litter-associated fungi in this system have the capacity to use NRM. Jacobson et al. (Jacobson et al., 2015) proposed that certain physiological traits may be important for NRM-adapted fungi including a cool to mesic thermal optima for growth, rapid activation in response to wetting, and efficient desiccation processes that facilitate repeated diel on-off cycling. A follow up study (Evans et al., 2020) measuring respiration from *S. sabulicola* tillers at these same locations, found that the relationship between litter gravimetric moisture content and CO_2–C flux did not differ between the two sites, demonstrating that fungi from both sites respire similarly under NRM . Our results showing that Rain Site fungi moved to the NRM Site decompose litter at the same rate as native NRM Site fungi would seem to corroborate this. Taken as a whole, this suggests that optimization for fog and dew by NRM specialists may not reflect any particular ability to utilize NRM so much as their inability to cope with the harsher (warmer, drier) conditions associated with the Rain Site.

Microbial biomass strongly regulates decomposition at regional scales and can predict how decomposition rates respond to changing climatic conditions (Bradford et al., 2017). Fungal biomass was correlated with mass loss (Figure S1.7) and with fungal biomass at the end of our experiment, mirroring the pattern we observed for mass loss (Figure 1.5). While fungal biomass may be a proximate control of litter decomposition rates, fungal abundance is itself ultimately controlled by how well fungi are able to tolerate local climatic conditions. Previous work has suggested that

microbes that must invest more energy in stress tolerance may decompose organic matter less efficiently as they divert resources away from growth and resource acquisition (Schimel et al., 2007). Since non-rainfall moisture is a common (Ritter et al., 2019) and important driver of litter decomposition in water-limited ecosystems (Evans et al., 2020), saprotroph desiccation tolerance and specialization to use NRM may be important to terrestrial carbon cycling.

Plant litter decomposition is influenced by many factors, including photodegradation (Austin et al., 2016), litter quality (Adair et al., 2008), decomposer communities (Glassman et al., 2018), and moisture availability (Jacobson and Jacobson, 1998; Evans et al., 2020). We showed that on standing dead litter in a hyperarid landscape, the relative availability of water from NRM vs. rain structures microbial communities with important consequences for litter decomposition rates. Litter communities were affected by succession and dispersal, though most divergence in community structure was driven by specialization to specific climatic regimes. Even though most of the dominant taxa were cosmopolitan extremophiles, many fungi preferred one moisture environment over the other, suggesting that general stress tolerance traits may not fully predict how microbial communities respond to changing moisture environments. As rainfall and NRM regimes change worldwide, (Forthun et al., 2006; Johnstone and Dawson, 2010; Niu et al., 2010; Haensler et al., 2011; Dai, 2013; Akimoto and Kusaka, 2015; Kutty et al., 2019; Hůnová et al., 2020), decomposer

communities may respond to climatic shifts in unique ways, altering decomposition rates differently in environments with different predominant moisture regimes.

APPENDIX

Table S1.1. Sample sizes for each treatment group in the study.

Litter Stage/Type	**Origin**	**Location Deployed**	**N**
"bait" tillers	NRM Site	NRM Site	5
"bait" tillers	NRM Site	Rain Site	5
early-stage	NRM Site	NRM Site	8
early-stage	NRM Site	Rain Site	8
early-stage	Rain Site	NRM Site	5
early-stage	Rain Site	Rain Site	5
late-stage	NRM Site	NRM Site	6
late-stage	NRM Site	Rain Site	7
late-stage	Rain Site	NRM Site	5
late-stage	Rain Site	Rain Site	5

Table S1.2. Subset of taxa that showed consistent preferences for one site by fitting three criteria: (1) higher relative abundance on native litter at that site (2) decreased in abundance when moved away from that site and (3) increased in abundance when moved to that site. This list is a subset that only includes OTUs that had an average relative abundance above 0.5% across the six groups (in total, there were 38 OTUs with consistent NRM Site preferences and 55 with consistent Rain Site preferences).

Site	OTU	Early-Stage Litter		Late-Stage Litter		Airborne	
Preference		NRM	RAIN	NRM	RAIN	NRM	RAIN
NRM	OTU4	23.65%	0.98%	28.06%	0.02%	10.69%	2.90%
NRM	OTU33	10.33%	0.36%	3.13%	0.01%	10.97%	0.72%
NRM	OTU40	8.67%	0.45%	1.06%	<0.01%	4.19%	4.48%
NRM	OTU8	6.56%	1.64%	25.21%	0.01%	7.35%	4.06%
NRM	OTU2	5.21%	1.30%	8.75%	0.01%	17.84%	2.19%
NRM	OTU88	2.01%	0.00%	1.46%	<0.01%	1.81%	0.01%
NRM	OTU166	0.75%	0.10%	4.20%	0.00%	1.23%	1.53%
RAIN	OTU17	1.73%	16.94%	0.05%	11.13%	0.16%	5.32%
RAIN	OTU1	2.13%	6.86%	4.13%	22.36%	14.86%	7.26%
RAIN	OTU15	0.04%	5.21%	<0.01%	1.85%	0.31%	5.95%
RAIN	OTU2456	1.61%	3.67%	0.87%	6.33%	0.47%	1.03%
RAIN	OTU72	0.01%	1.17%	<0.01%	6.83%	0.04%	0.20%
RAIN	OTU201	<0.01%	0.75%	<0.01%	0.00%	0.00%	5.03%
RAIN	OTU382	0.00%	0.58%	0.00%	<0.01%	<0.01%	4.40%
RAIN	OTU335	<0.01%	0.12%	2.14%	0.00%	<0.01%	0.00%
RAIN	OTU238	<0.01%	0.09%	0.00%	9.10%	0.00%	<0.01%

Table S1.3. Type III ANOVA table for early-stage tillers in Figure 1.5B. Calculated using the 'Anova' function in *car* package in R.
Formula: Log_{10} (ITS copies $gram^{-1}$) ~ Location * Origin

	SS	Df	F	P
Intercept	548.33	1	1269	<0.001
Location	19.08	1	44.18	<0.001
Origin	5.23	1	12.107	0.002
Location * Origin	2.38	1	5.516	0.028
Residuals	9.50	22		

Table S1.4. Type III ANOVA table for late-stage tillers in Figure 1.5C. Calculated using the 'Anova' function in *car* package in R.
Formula: Log_{10} (ITS copies $gram^{-1}$) ~ Location * Origin

	SS	Df	F	P
Intercept	1003.28	1	8545	<0.001
Location	1.91	1	16.24	0.007
Origin	0.25	1	2.170	0.157
Location * Origin	1.31	1	11.15	0.003
Residuals	2.23	19		

Table S1.5. Type III ANOVA table for early-stage tillers in Figure 1.5E. Calculated using the 'Anova' function in *car* package in R.

Formula: Percent Mass Loss ~ Location * Origin

	SS	Df	F	P
Intercept	270.9	1	66.1	<0.001
Location	7.307	1	1.78	0.196
Origin	17.56	1	4.28	0.051
Location * Origin	4.998	1	1.22	0.282
Residuals	86.1	21		

Table S1.6. Type III ANOVA table for late-stage tillers in Figure 1.5F. Calculated using the 'Anova' function in *car* package in R.

Formula: Percent Mass Loss ~ Location * Origin

	SS	Df	F	P
Intercept	221.8	1	90.7	<0.001
Location	7.386	1	3.02	0.098
Origin	0.420	1	0.176	0.680
Location * Origin	15.10	1	6.177	0.022
Residuals	46.4	19		

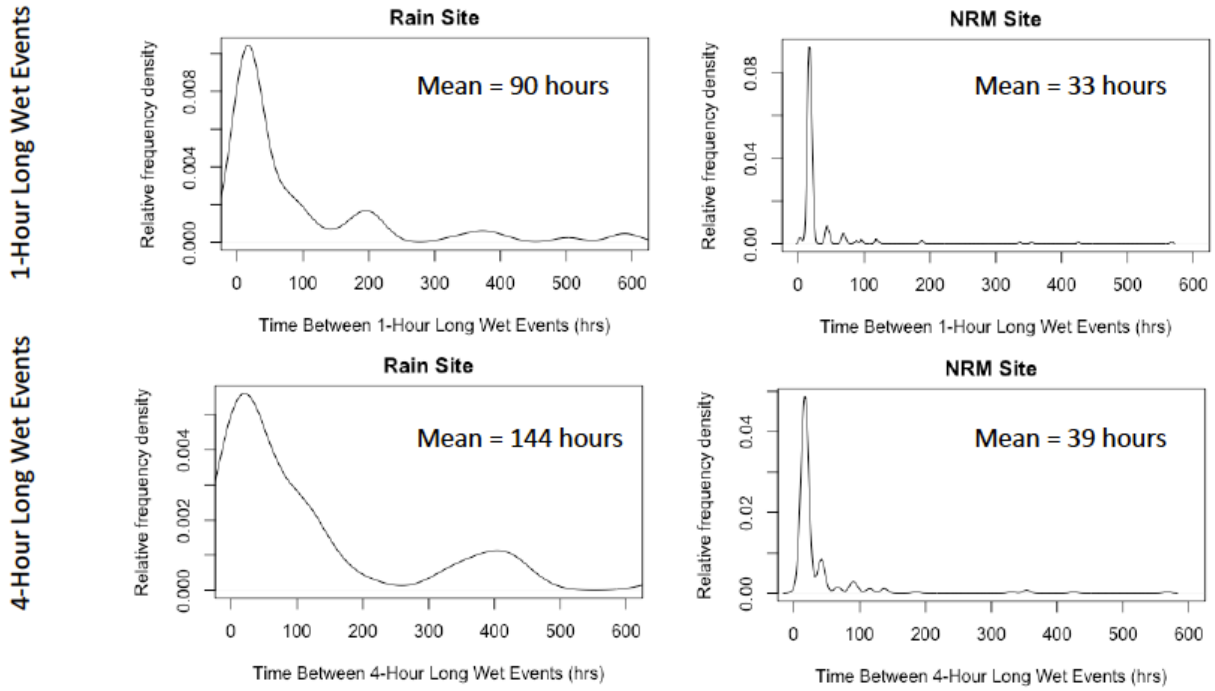

Figure S1.1. Frequency of dry periods between wet events at each site. Top two panels show the length of dry periods between wet events of at least one hour in length. Bottom two panels show length of dry periods between wet events of at least four hours in length.

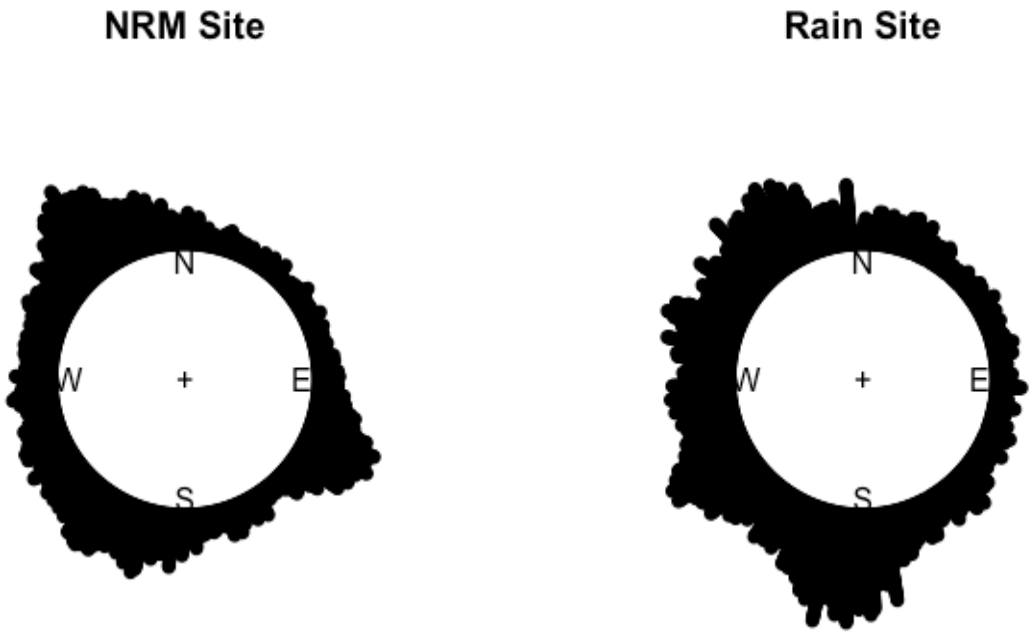

Figure S1.2. Wind vectors at the two sites during the study period. Length of lines on border represents the frequency (number of hours) that the wind was coming from that direction.

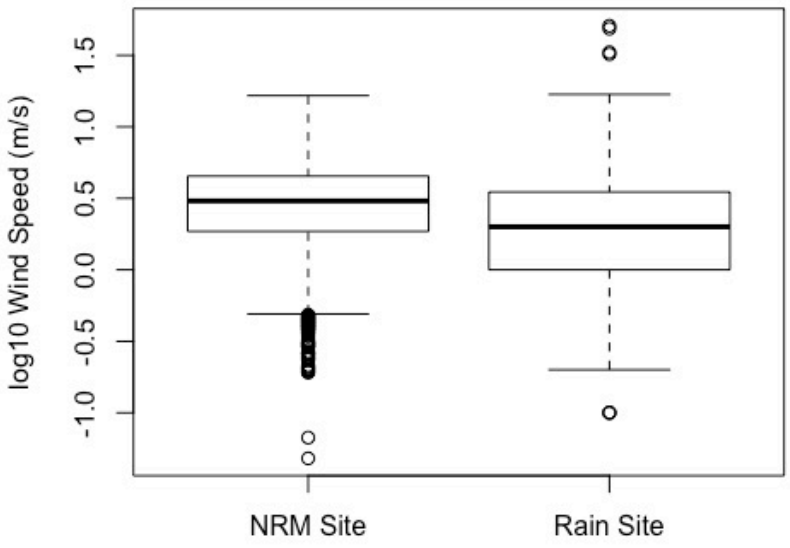

Figure S1.3. Log_{10} windspeed (m/s) at the two sites during the one year study based on hourly averages. $Mean_{NRM} = 3.35$ m/s; $Mean_{RAIN} = 2.27$ m/s; $T = 36.1$, $P < 0.001$. (T statistics are calculated using non-transformed data.)

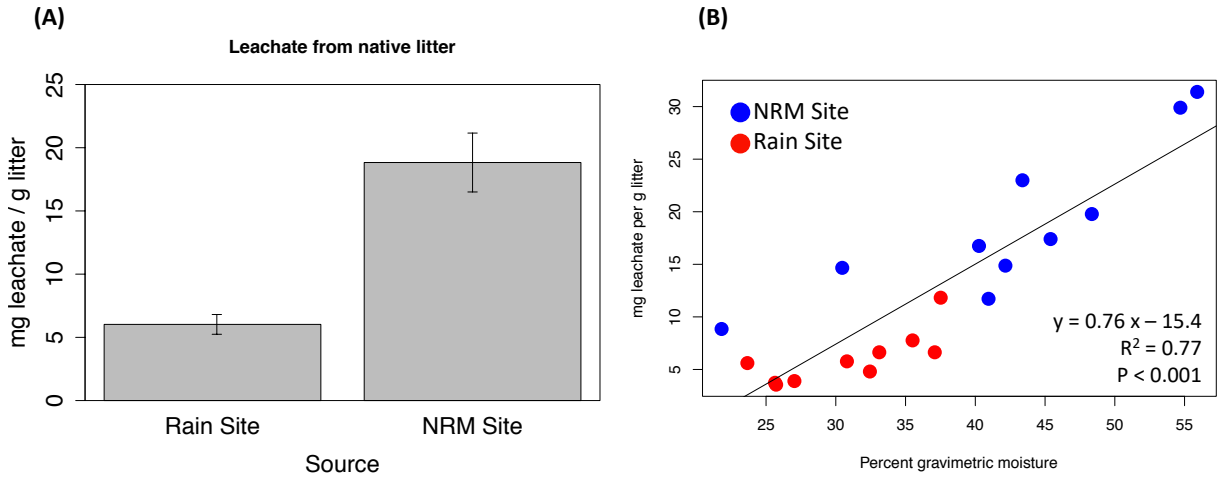

Figure S1.4. (A) Mass loss due to leaching for a subset of early-stage tillers when submerged for 24 hours in ultrapure water after sealing the ends with glue. (B) Leachate per g of litter for the same tillers expressed as a function of gravimetric moisture. The greater mass loss from tillers at the NRM Site seen in (A) appears to be driven by greater moisture uptake (likely reflecting a more porous cuticle), not necessarily the presence of more leachable carbon.

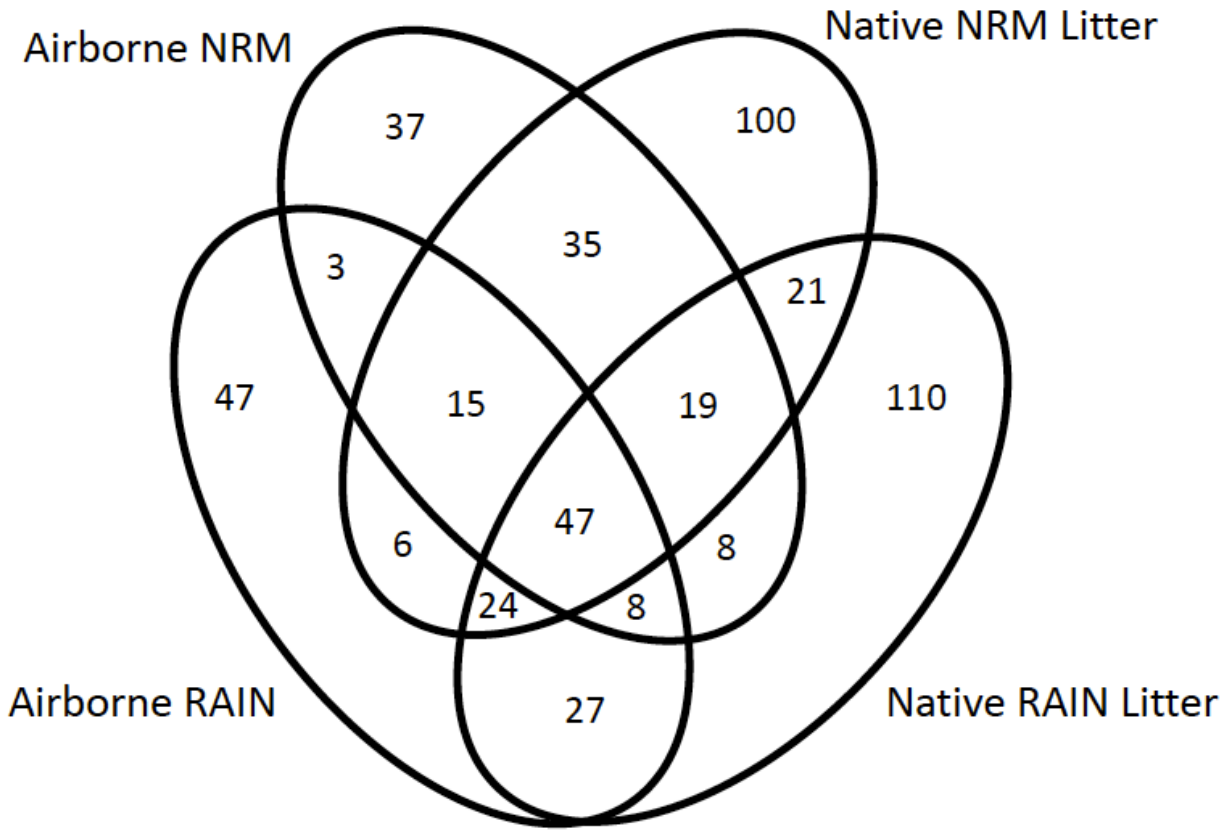

Figure S1.5. Venn Diagram showing overlapping fungal OTUs. For simplicity, early- and late-stage tillers are combined within each site.

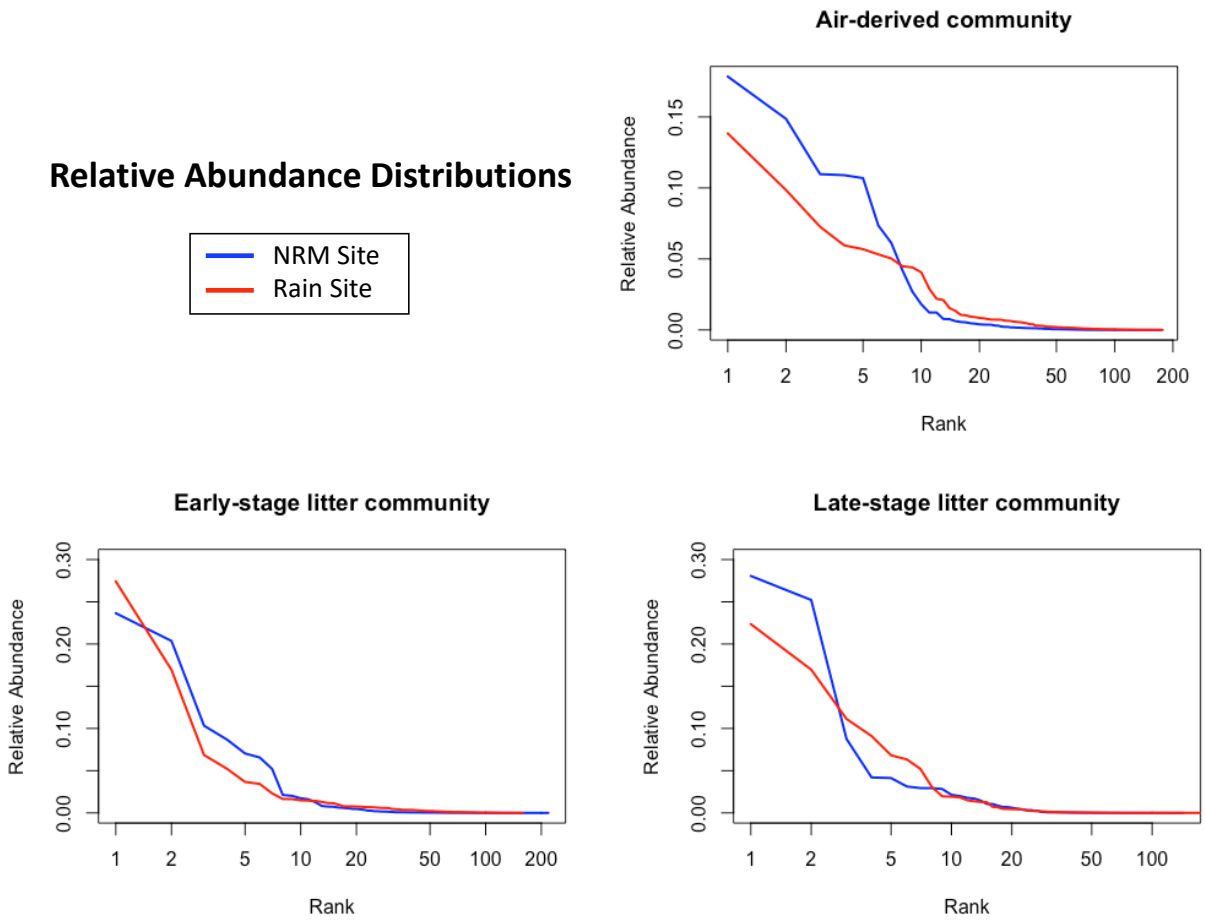

Figure S1.6. Relative abundance distributions of taxa on tillers at each of the three litter stages. Early- and late-stage figures show only abundances on native tillers.

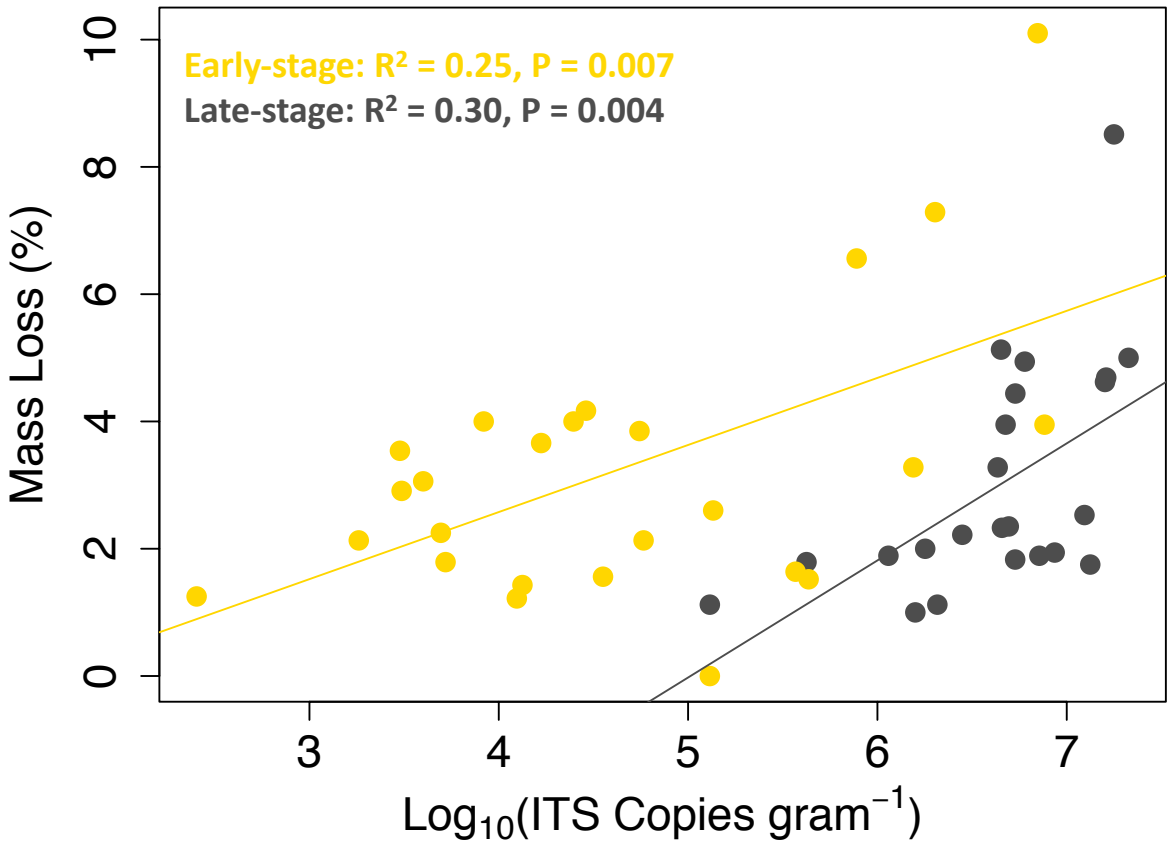

Figure S1.7. Mass loss as a function of final fungal biomass (indicated by ITS copies) for early- and late-stage senesced tillers.

CHAPTER TWO:

PHOTODEGRADATION OF PLANT LITTER CUTICLES ENHANCES MICROBIAL DECOMPOSITION BY INCREASING UPTAKE OF NON-RAINFALL MOISTURE

At home we had so often heard the sun glibly called the source of all life; here in the desert it certainly wasn't.

Henno Martin describing the Namib Desert
The Sheltering Desert (1957)

INTRODUCTION

Plant litter decomposition is a critical carbon cycling process in terrestrial ecosystems worldwide and is an important component of coupled climate models. In many systems however, we still lack a strong understanding of the ways various mechanisms interact to drive litter decomposition and carbon efflux. This is particularly true in drylands, which make up 40% of the Earth's land surface and can account for half of the interannual variability in global carbon storage (Poulter et al., 2014), limiting our ability to predict how carbon cycling is affected by climate change. Improving existing ecosystem and climate models depends on our ability to identify and describe the processes controlling litter decomposition rates in these moisture-limited systems.

Many litter decay models that perform well in wet and forested areas underestimate decomposition rates in drylands (Adair et al., 2008), suggesting that

current models may be missing important mechanisms that dominate in arid and semi-arid systems. Compared to most mesic systems where rainfall-supported biotic activity is the primary driver of litter decomposition, in drylands, abiotic processes play an outsized role in driving decomposition. The process of photodegradation—the direct or indirect decomposition of litter by solar radiation—may be particularly important in drylands due to the paucity of clouds and minimal tree canopy cover in drylands combined with low and erratic precipitation which reduces the activity of decomposing microbes (Austin and Vivanco, 2006). Incorporating photodegradation into existing litter decay models can substantially improve model predictions (Adair et al., 2017).

Solar radiation can influence litter decomposition through multiple photodegradation mechanisms. Direct photolysis of organic compounds like lignin, cellulose, and hemicellulose can lead to litter breakdown and the abiotic release of volatiles including CO_2, CH_4, and CO from leaf litter (Brandt et al., 2009; Day et al., 2019). Photodegradation may produce intermediaries such as peroxides and reactive oxygen species that can further degrade lignin and other organic components of litter (Messenger et al., 2009; King et al., 2012); this process can increase leaching and production of volatiles. Solar radiation can also influence litter decomposition by altering the size or composition of litter-associated microbial communities, which can in turn reduce litter decay rates (Pieristè et al., 2020). Finally, by cleaving strong double bonds in recalcitrant compounds like lignin, solar radiation can make litter

more susceptible to subsequent microbial degradation (King et al., 2012; Wang et al., 2017b). This last process, known as photopriming or photofacilitation, can lead to more rapid rates of mass loss than either abiotic photodegradation or microbial decomposition alone (Wang et al., 2015; Gliksman et al., 2017). Since photopriming links two major decomposition processes in drylands (biotic degradation and photodegradation), understanding its mechanisms is essential to accurately describing carbon turnover in these systems.

While photopriming can occur in arid and mesic systems alike, in drylands, its importance may be amplified by the frequency of non-rainfall moisture (NRM; fog, dew, and water vapor), which is a key regulator of microbial respiration (Dirks et al., 2010; Evans et al., 2020). Several recent studies have shown that NRM and photodegradation interact with one another through photopriming mechanisms, even on diurnal timescales. Lin et al. (2018) found that CO_2 production and lignin degradation were significantly greater when microcosms experienced an alternating cycle of UV radiation during the day and dark wet conditions at night. Similarly, by manipulating nighttime humidity and daytime solar irradiance in a Mediterranean shrubland, another study found synergistic effects of NRM-supported microbial activity and photodegradation on diel timescales (Gliksman et al., 2017). Since NRM can occur as often as 95% of nights in some grasslands (Ritter et al., 2019) and can account for the majority of litter mass loss (Evans et al., 2020), understanding how NRM and

photodegradation interact is critical to improving models that incorporate both of these important processes in litter decomposition in dry grasslands.

We set out to test a novel mechanism of photopriming by which solar radiation degrades the water-resistant cuticle of plant litter, increasing moisture uptake during NRM events and subsequently enhancing biotic decomposition. Plant cuticles act as waterproof barriers that minimize water loss while plants are alive (Shepherd and Griffiths, 2006), and we hypothesized this might also constrain how effectively litter can absorb NRM following senescence. Photodegradation may assist in this breakdown as plant cuticles contain many photo-reactive compounds that are susceptible to degradation by solar ultraviolet (UV; 280-400 nm) radiation (Messenger et al., 2009; Bruhn et al., 2014). One study found that the concentration of surface waxes in litter strongly predicted CO_2 and CH_4 emissions; emissions were high initially and declined as litter decayed (Day et al., 2019). Since litter moisture content strongly predicts biotic activity during NRM events (Jacobson et al., 2015) and this moisture content depends in part on the permeability of the cuticle, we hypothesized that as UV degrades the cuticle, it becomes more permeable to non-rainfall moisture, which then enhances microbial decomposition during NRM events. We refer to this process as "physical photopriming" since the primary mechanism is through a change in a physical property of the litter (water absorption rate) rather than a chemical property (such as lignin:N ratios) as proposed in the traditional photopriming paradigm.

To test this hypothesis, we conducted a combination of laboratory tests and field experiments in the Namib Desert of western Namibia. In one experiment, we manipulated solar UV and visible (400-700 nm) radiation during a 36-month litter decomposition study in the field, measuring mass loss, cuticle integrity, and litter's moisture uptake potential over time. To account for the confounding effects of photodegradation-induced changes to litter chemistry, we conducted a second experiment where we artificially removed the cuticle of grass tillers, measuring mass loss after six months. Finally, we corroborated these findings with observations of photodegradation on *in situ* grass litter in the field. We integrate these findings into a conceptual model that describes the process of UV-driven cuticle degradation and subsequent uptake of NRM leading to enhanced decomposition.

METHODS

Study system

We conducted this study in the Namib Desert, Namibia, a hyperarid, grass-dominated, coastal fog desert in Southwest Africa. The Namib Desert is an ideal site to study the interaction between NRM and photodegradation because it receives extremely high solar irradiance and hosts substantial NRM-driven litter decomposition (Jacobson et al., 2015; Evans et al., 2020). In addition, absolute decomposition rates are still rather low, allowing us a wide window of time to study the early stages of

cuticle degradation with finer precision. We conducted the study at the Gobabeb Namib Research Institute on the northern edge of the Namib Sand Sea in western Namibia (23°33.6'S 15°02.5'E), using a series of experimental manipulations and field observations to test our hypothesis. The site's meteorology has been described in detail elsewhere (Eckardt et al., 2013; Evans et al., 2020; Logan et al., 2021). Briefly, Gobabeb receives 25 mm mean annual rainfall, though that is highly variable from year to year. The site receives approximately 1500 hours of wetness per year and 99% of wet hours are attributable to NRM, not rainfall (Evans et al., 2020). Mean annual temperature is ca. 20 °C with mean daily maximum and minimum temperatures of 30 °C and 13 °C, respectively (Logan et al., 2021). Average daily unweighted ultraviolet-A (UVA ; 315-400 nm) and ultraviolet-B (UVB; 280-315 nm) irradiances are 435.5 and 11.86 W m^2, respectively (Figure S2.1).

We focused our study on *Stipagrostis sabulicola*, the dominant grass species across the dune system (Seely and Louw, 1980), with globally distributed con-generics. *Stipagrostis sabulicola* is a long-lived perennial grass with a thick waxy cuticle (Roth-Nebelsick et al., 2012). Hummocks of *Stipagrostis* can be several meters across and persist for decades though individual tillers will senesce and fall after several years (Figure S2.2A-B). Coarse standing dead tillers (>2 mm diameter) make up approximately 42 percent of the total hummock dead plant matter (Figure S2.3). The cuticle of leaves and stems are non-hydrophobic, facilitating the collection of water

droplets during fog and dew events that then fall off and are absorbed by a shallow root network (Ebner et al., 2011; Roth-Nebelsick et al., 2012).

We conducted four experiments or field observations (Figure 2.1): (1) a solar radiation manipulation where we measured mass loss, cuticle integrity, and litter moisture uptake potential under different solar radiation regimes, (2) a cuticle removal experiment, (3) field observations of solar radiation-induced damage and fungal growth, and (4) measurement of litter moisture uptake during an actual dew event in the field.

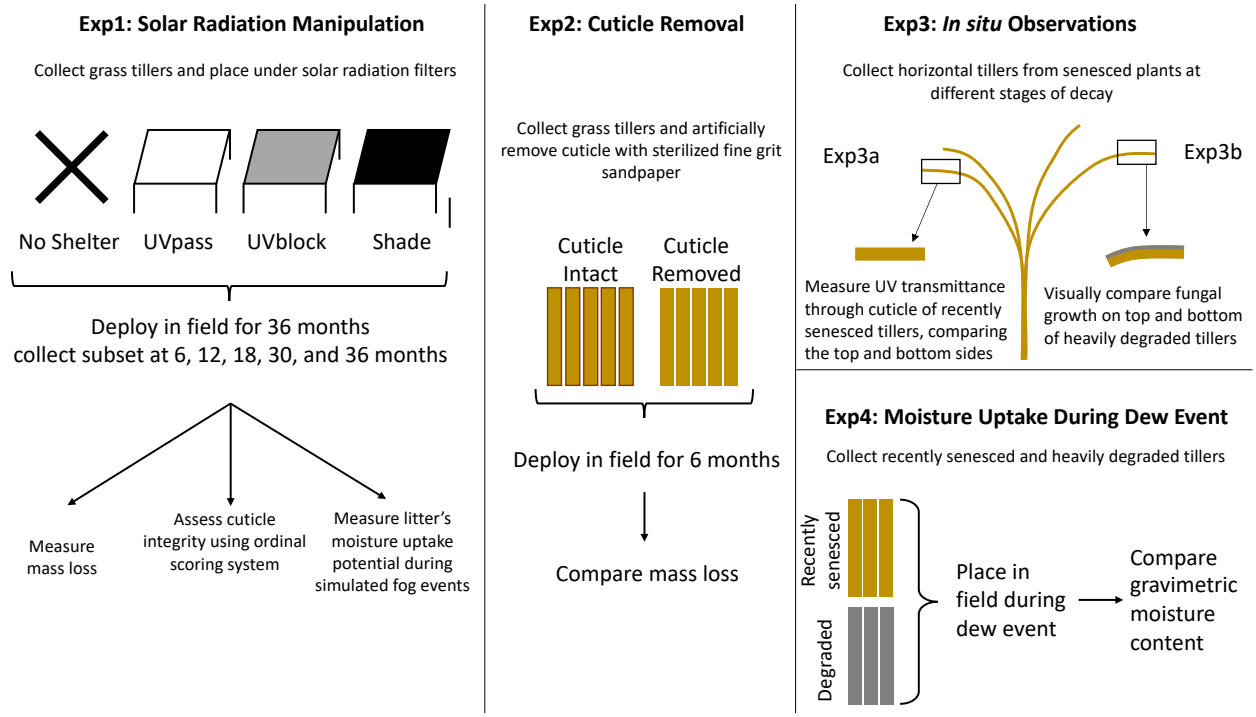

Figure 2.1. Study design summarizing the four experiments. (Exp1) 36-month solar radiation manipulation; (Exp2) cuticle removal experiment; (Exp3) *in situ* observations of grass tillers in the field comparing the sun-facing and shaded sides; (Exp4) measuring gravimetric moisture content following a dew event in the field. Individual tillers were only used for one experiment.

Exp 1: Solar Radiation Manipulation

To determine how solar radiation affected litter mass loss and cuticle integrity, we conducted a 36-month field manipulation of solar radiation. We collected recently senesced, standing *S. sabulicola* tillers from Station Dune at Gobabeb, dried them at 35 °C for 24 hours, cut them to 9 cm lengths, weighed them, and deployed them under radiation filters. To eliminate microclimate variations inherent in litter bags, we placed tillers in litter racks, which are custom made wooden frames covered with a dewaxed shellac for waterproofing (Figure S2.2G). This approach has been used before (Evans et al., 2020; Logan et al., 2021). We established four treatments: a shade treatment which utilized plexiglass that was spray painted white to block direct solar radiation, a UV-attenuation ("UVblock") treatment using Lexan polycarbonate (SABIC Innovative Plastics, Riyadh, Saudi Arabia) which blocks radiation below 400 nm but transmits 90% of radiation >400nm, a "UVpass" control made from clear Arkema G-UVT (Loop Acrylics, Chicago, USA) that has >80% transmittance of radiation above 300 nm, and a "no shelter" control to ascertain the effects of microclimate changes induced by the shelters. Spectra for the UVpass treatment and the UVblock control are shown in Figure S2.4 as measured on a UV-2401 PC spectrophotometer (Shimadzu, Kyoto, Japan). To determine the efficacy of the treatments in the field, we measured UV radiation under the shelters several times during the summer and winter using a broadband UV radiation sensor measuring unweighted radiation (250-400 nm) under

the treatments and normalizing it to clear sky measurements (Apogee UV Sensor Model SU-100, Apogee Instruments, Logan, UT, USA). We report values as percent of blocked UV radiation relative to the full exposure control (Figure S2.5).

Shelters were constructed from PVC pipe, with a 70 x 70 cm radiation filter on top (Figure S2.2F), except for the "no shelter" control. Since we were interested in studying the role of NRM and UV together, we took particular care to avoid confounding changes in the microclimate under the filters due to localized warming, altered dew points, and interception of fog droplets during fog events. Radiation filters faced north and were sloped on a 45° angle so rising air would be directed away from samples, even on windless days. The result was that we attenuated direct solar radiation during the majority of the day but some diffuse radiation spilled in on the sides and some direct radiation was present when the sun was at very low angles in the early morning and evening. In total, this resulted in a 62% reduction in total UV radiation under both of the UVblock and shade treatments. To assess how filters altered the microclimates beneath them, we placed iButton Hygrochrons (iButtonLink LLC, United States) to measure temperature and relative humidity) and leaf wetness sensors (S- LWA-M003, Onset Computer Corporation, United States) underneath two shelters and compared values relative to those at two spots in the open over several days.

We deployed 240 tillers evenly distributed among the four treatments. At five time points (6, 12, 18, 30, and 36 months), we weighed all remaining tillers and removed one fifth of them (selected using a stratified random sampling approach) for subsequent microbial analysis to be described elsewhere. As a result of this sampling procedure, many tillers were weighed multiple times, so we analyzed the data statistically with repeated measures ANOVAs using the 'lmer' function in R. We used time, UV treatment, and initial dry mass as predictors of mass loss and compared all models using corrected Akaike information criterion (AICc), selecting the one with lowest AICc.

To determine whether mass loss was coincident with cuticle degradation, we assessed the integrity of the cuticle of tillers from the solar radiation manipulation. Others have found that cuticular permeability to water is not strongly correlated with the thickness of the cuticle or wax coverage (Riederer and Schreiber, 2001) but rather, physical characteristics like cracking can make leaf surfaces more porous (Pitcairn et al., 1986); hence, we visually assessed cuticles for physical damage to determine whether tillers under the radiation treatments differed in their degree of cuticle integrity. At each collection time, we photographed the front (sun-facing) and back (shaded) side of each tiller using a ProScope Micro Mobile microscope (Bodelin Technologies, Oregon City, OR, USA) attached to an iPhone 6S, photographing the same location on tillers each time. We then created a 5-point ordinal scoring system to

classify the tillers based on the degree of physical damage to their outer surface. The criteria were based on physical changes to the cuticle surface including the presence and extent of cracks, waxes flaking, photobleaching, and removal of the cuticle surface. Tillers with more physical damage were given higher scores: 1 represented the fully intact cuticle of a recently senesced tiller and 5 represented a tiller with multiple cracks along the surface, no visible cuticular waxes, complete bleaching, and near ubiquitous fungal growth along the surface. Example photos of each stage as well as a more detailed description of the criteria are included in the supplementary material (Figure S2.6). Scores were determined by single observer, blinded to the treatments and crossed checked by a second observer. There were 672 photo pairs (one photo of each side of the tiller) for a total of 1344 photos. Since we used an ordinal score, we used a Kruskal Wallis test in the base package of R to determine whether scores changed over time and differed among the radiation treatments, but we used the arithmetic mean for ease of visualization when plotting figures.

Finally, to determine whether the cuticle degradation we observed coincided with an increased ability of tillers to absorb atmospheric water, we placed tillers in an artificial fog chamber and measured gravimetric moisture content of the tiller segments following a simulated fog event. The fog chamber is an acrylic box that uses a reptile fogger to generate a spray of fine water droplets in a constant temperature and humidity environment (Figure S2.7). We used a subset of tillers collected at each

collection time from the field. Tillers were cut to 5 cm lengths, dried at 55°C for 16 hours, weighed, and had their ends wrapped in parafilm so water could only enter the tiller via the cuticle surface, not exposed vasculature. We then placed the tillers in the chamber for a set amount of time (84 minutes at 24°C and 90-95% humidity), after which time they were removed, gently wiped with a Kimwipe to remove excess liquid water that had not been absorbed into the tissue, and reweighed. We shifted the position of the tillers in the chamber every 20 minutes so that fog would be evenly distributed to each tiller in the chamber. To control for variation in surface area among tillers with different diameters, we report moisture uptake values normalized to surface area as mg H_2O mm^{-2} in all analyses.

Exp 2: Direct cuticle removal

Since cuticle degradation in our solar radiation experiment could occur with photochemical-induced changes in litter quality, we sought to verify that the cuticle itself played a role in mass loss by conducting a second experiment where we physically removed the cuticle from a set of tillers and measured mass loss in the field after six months. We collected 48 standing, recently senesced *S. sabulicola* tillers from Station Dune near Gobabeb, air dried them at 40°C for 24 hours, and cut them into 9 cm lengths. We randomly selected 24 tillers from which we removed the outer surface using fine 220 grit sandpaper (sterilized with 100% ethanol), ensuring that all sides

were sanded equally. On average, 15.7% of the tiller mass was removed by sanding. Mass loss for tillers with cuticle removed was measured relative to their mass after removing the cuticle. Half of the tillers were left with the outer surface intact as controls. We then weighed the tillers, and deployed them in the field for six months to measure mass loss with the cuticle intact versus removed. Tillers were deployed in open litter racks in the UV manipulation experiment described above, evenly distributed among the shade, UVblock, UVpass, and "no shelter" treatments.

Exp 3a: *In situ* assessment of UV-driven cuticle degradation

We corroborated results from our experimental manipulations by assessing solar radiation-induced degradation of litter cuticles in the field using a fluorescence-based measure of cuticle transmittance of UV radiation. We used a UVA-PAM fluorometer (Kolb et al., 2005; Bilger et al., 2014), which was originally developed to non-invasively measure epidermal UV transmittance of leaves. The UVA-PAM measures fluorescence (λ > 650 nm) induced by UV (F_{UV}; λ_{max} = 375 nm) and normalizes it to fluorescence induced by blue-green light (F_{BG}; λ_{max} = 470 nm) to control for variation in underlying chlorophyll concentration (Barnes et al., 2015). According to this technique, we inferred that higher F_{UV}:F_{BG} values represented greater UV penetration through the cuticle. By comparing the upper (sun-facing) and lower (shaded) sides of senesced *S. sabulicola* tillers in the field, we used F_{UV}:F_{BG} as a measure of UV-induced cuticle

degradation, with higher values indicating greater UV damage. Since we did not calibrate our optical measurements against physical measurements of cuticle thickness or density, we use F_{UV}:F_{BG} only as a relative index of cuticle degradation by UV radiation.

We collected 24 horizontal stems from the Namib Sand Sea near Gobabeb. Tillers had to be no more than 20° from horizontal, not touching the ground, recently senesced, and show no signs of fungal growth on the surface following a visual assessment. By using stem material that had bent under its own weight instead of leafy material, we were able to control for morphological differences since each side should have started with the same level of UV-absorbing pigments and cuticular structures while the plant was alive. Upon collection, a short notch was cut in the upper (sun-facing) side of each tiller to identify orientation later. In the lab, we used the UVA-PAM to take triplicate readings at each of three different points on both sides for a total of nine readings for the sun-facing side and nine readings for the shaded side. We averaged these technical replicates to produce one top and one bottom value for each tiller and used a paired t-test to compare F_{UV}:F_{BG} values on the two sides, treating the tiller as the unit of replication (n=24).

Exp 3b: Fungal growth estimates

To determine whether surficial fungi grew more on the sun-facing or shaded side of tillers, we randomly sampled senesced tillers with pigmented fungal growth collected on one afternoon. We only collected tillers that were no more than 20° from horizontal and recorded whether they had visible fungal growth on the top, bottom, or both. We used a chi-squared test to determine whether fungi were more common on one side than the other.

Exp 4: Moisture uptake during a dew event

Finally, to verify whether tillers with degraded cuticles absorbed more water during actual NRM events in the field, we placed five late-stage decomposing tillers (Figure S2.2E) and five recently senesced tillers (Figure S2.2C) into litter racks in the field (Far East Dune; 23°47.04'S 15°46.86'E, 25 June 2015) and weighed them to determine gravimetric moisture content after exposure to an overnight dew event. We then used a t-test to compare moisture content between the degraded and intact tillers.

RESULTS

Exp 1: Solar Radiation Manipulation

The attenuation of solar UV radiation significantly reduced litter mass loss relative to both controls, while subsequent shading to reduce visible light had no

discernible effect on mass loss (Figure 2.2A). The best model (lowest AICc) for mass loss in our solar radiation experiment included time as well as significant interactions between time and treatment and between time and initial mass (Table 2.1). Decomposition in all treatments proceeded very slowly at first and accelerated over time, unlike the classical exponential decay model typical of most mass loss curves (Figure 2.2A). Notably, mass loss in the UVblock and shade treatments did not differ throughout the study. We saw an effect of the shelters themselves on mass loss since the No Shelter control had greater mass loss than did the UVpass control (Figure 2.2A). Temperature and leaf wetness status underneath shelters were lower than in the open in some evenings, though relative humidity did not show a consistent directional shift (Figure S2.8).

Table 2.1. ANOVA table for the mass loss model from the solar radiation manipulation (Exp1) with lowest AICc.

Source	SS	df	F	P
Initial Mass	0.22	1	0.1738	0.6769
Time	477.14	1	372.1289	<0.001
Treatment	4.03	3	1.0483	0.3708
Initial Mass * Time	35.25	1	27.4941	<0.001
Treatment * Time	93.47	3	24.2988	<0.001

Table 2.2. ANOVA table of moisture uptake (mg H_2O/mm^2) for the solar radiation manipulation (Exp1).

Source	SS	df	F	P
Treatment	$3.77x10^{-9}$	3	1.31	0.276
Time	$2.49x10^{-8}$	1	26.0	<0.001
Treatment * Time	$1.76x10^{-9}$	3	0.611	0.609
Residuals	$1.08x10^{-7}$	112		

Cuticle integrity decreased overtime in all treatments (Figure 2.2B) and the sun-facing sides had more damage than the shaded sides (Figure S2.9; $P_{wilcox} < 0.001$). Solar radiation treatment was significant only on the sun-facing side of the tillers ($P < 0.001$), not the shaded side ($P = 0.30$). On the sun-facing side, the magnitude of cuticle integrity damage was consistent with the amount of sun exposure, with the shaded tillers having the most intact cuticles followed by those under the UVblock treatment, then UVpass control, and finally the no shelter control, which had the most degraded cuticles (Figure 2.2B).

Water uptake potential was influenced by both time and solar radiation but there was no significant interaction between the two (Table 2.2). Tillers that had been decomposing in the field for longer, absorbed more water (Figure 2.2C). Treatment did not have a significant effect on moisture uptake rates (Table 2.2), but tillers under the shade treatment tended to have lower moisture uptake than did the three treatments that received ambient visible light (Figure 2.2C), while none of the three treatments with ambient light differed from one another ($P>0.1$, Figure 2.2C). On average, tillers in the shade treatment absorbed 17.7% less water (mg H_2O/mm^2) than did those from the three treatments exposed to visible light.

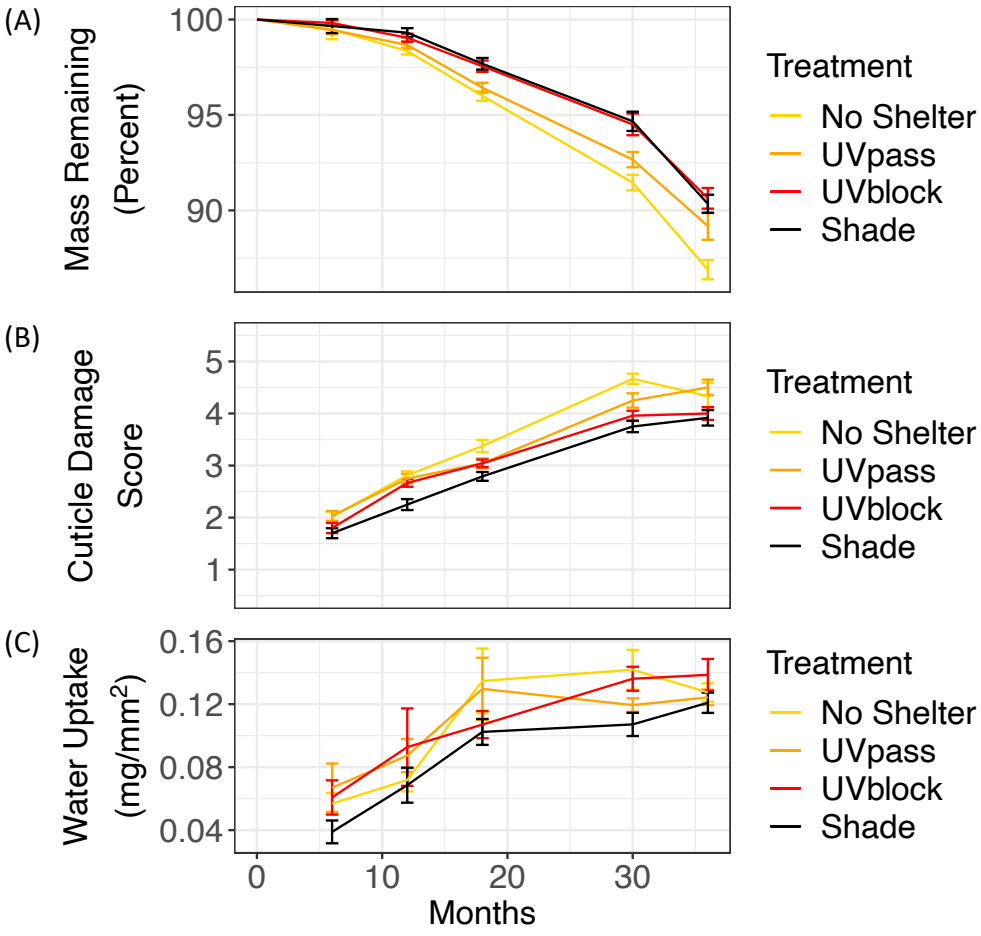

Figure 2.2. Results from the solar radiation manipulation (Exp1), showing changes in tiller properties over time. The three panels show progression of the same tillers. (A) mass loss; (B) cuticle damage based on visual assessment of tillers (figure shows only the sun-facing side of tillers, see Figure S2.8 for the shaded side); (C) moisture uptake potential for tillers as measured during a simulated fog event. Plotted values are means ±1 S.E.M.

Exp 2: Cuticle Removal Experiment

In our cuticle removal experiment, tillers that had their cuticle artificially removed had 4.25 times greater mass loss than did control tillers with intact cuticles

(Figure 2.3). Mass loss after six months did not differ among the UV treatments (Table 2.3).

Table 2.3. ANOVA table of mass loss for the cuticle removal experiment (Exp2).

Source	SS	df	F	P
Cuticle Treatment	186.40	1	88.072	<0.001
UV Treatment	12.75	3	2.009	0.128
Cuticle * UV	6.25	3	0.985	0.410
Residuals	84.66	40		

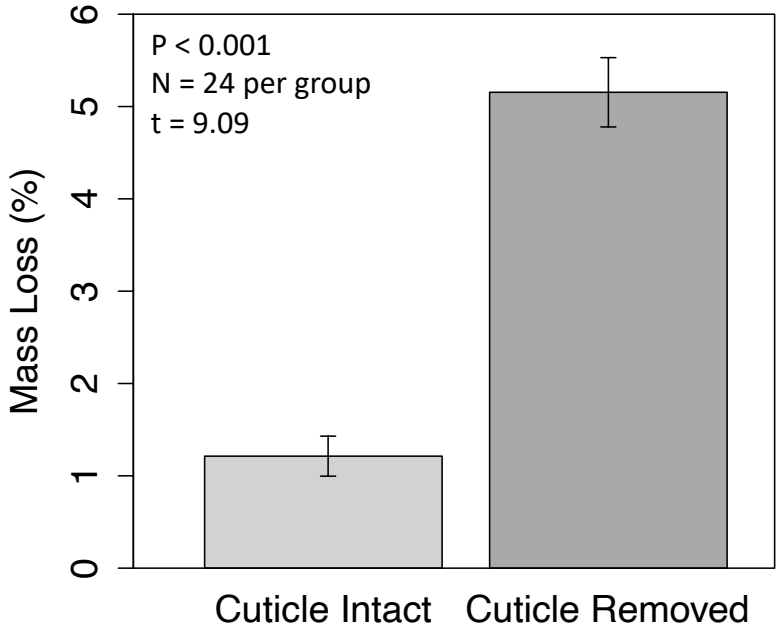

Figure 2.3. Results from Exp2 showing mass loss after six months for tillers with intact cuticles and those with cuticles artificially removed by sanding. Solar radiation treatment was not significant (P>0.05), so we pooled samples by cuticle treatment here. Plotted values are means ±1 S.E.M.

Exp 3: *In situ* observations of tillers

UV transmittance (F_{UV}:F_{BG}) across the cuticle of recently senesced tillers was higher on the upward sun-facing side than the downward shaded side (Figure 2.4A; $T_{paired} = 4.59$, $P < 0.001$). This signal was driven by variation in F_{UV}, not F_{BG}, indicating that this variation was due to differences in cuticle transmittance of UV radiation, not differences in the underlying chlorophyll concentration between the upper and lower portions of the stems (Figure S2.10).

On older tillers we observed in the field, pigmented fungi were consistently more likely to be found on the sun-facing side of stems than on the shaded side (Figure 2.4B-C; $\chi_2^2 = 49.1$, $P < 0.001$). Of 51 randomly sampled horizontal tillers that had visible fungal growth anywhere on them, 40 (78%) showed evidence of fungal growth only on the upward-facing side while only one tiller (2%) had fungal growth on the bottom but not the top.

Exp 4: Moisture uptake during a dew event

During an overnight dew event in the field, tillers with heavily degraded cuticles had a gravimetric moisture content 3.8 times higher than did tillers with intact cuticles (Figure 2.5) ($P = 0.008$). In fact, even after a full night of exposure to dew, tillers with intact cuticles had the same water content as a set of recently senesced tillers collected

during a dry period, suggesting that tillers with intact cuticles absorbed no detectable water, even after several hours in a wet environment.

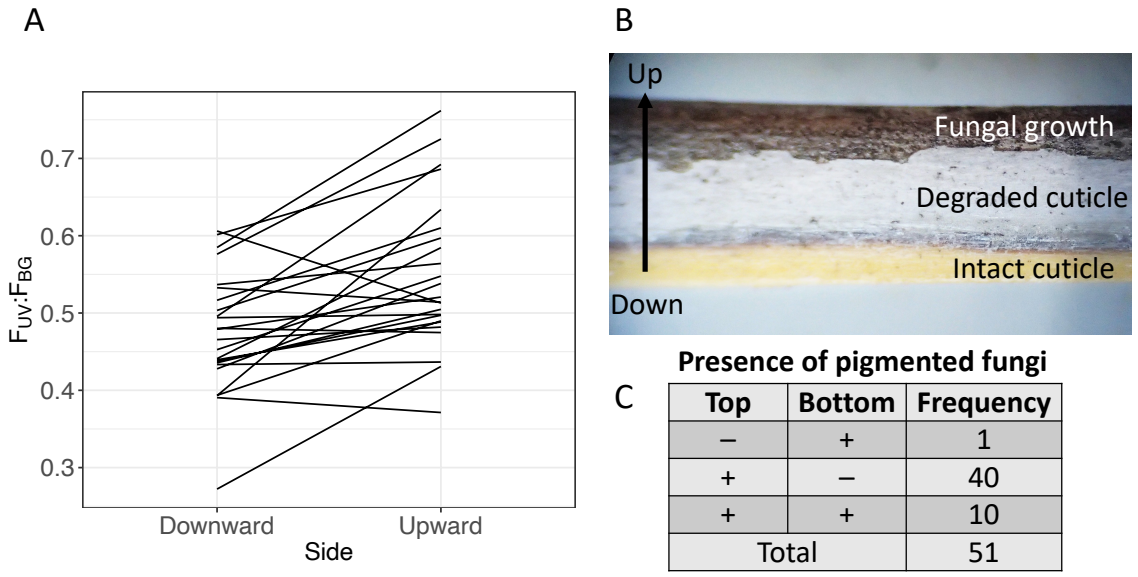

C

Presence of pigmented fungi

Top	Bottom	Frequency
–	+	1
+	–	40
+	+	10
Total		51

Figure 2.4. Results for Exp3 showing (A) transmission of UV radiation through the cuticle for both the upward facing (sun-exposed) and downward (shaded) side of recently senesced horizontal stems that had no visual sign of fungal growth (paired t-test $p<0.001$). Higher values reflect greater UV penetration into the tissue, consistent with greater UV-driven photodegradation. (B) Example of a late-stage tiller showing extensive fungal growth on the sun-facing side but not in the shade. Note photobleaching and cracking of the cuticle on the side. (C) Presence of pigmented fungi on randomly sampled horizontal tillers in the field, showing fungal growth is much more common on the upper side than on the lower side of horizontal tillers ($\chi_2^2 = 49.1$, $P < 0.001$).

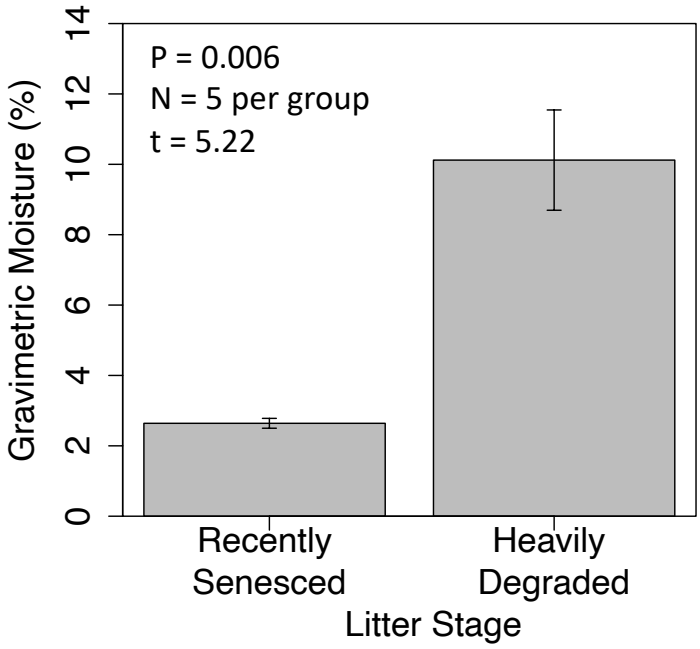

Figure 2.5. Results from Exp4 showing gravimetric moisture content of recently senesced tillers (with intact cuticles) and older tillers (with heavily degraded cuticles) following a night of heavy dew deposition. Plotted values are means ±1 S.E.M.

DISCUSSION

Photopriming is an important component of litter decomposition in arid and mesic systems (King et al., 2012). To date, most photopriming studies have focused on how solar radiation alters litter chemistry (e.g. degrading lignin in plant cell walls), making litter more easily degraded by microbial decomposers (Austin et al., 2016). We expand on this work by introducing a conceptual model that differentiates between this classic chemical photopriming mechanism and a novel physical photopriming mechanism we describe in this study (Figure 2.6). According to the classical "chemical photopriming" pathway (Figure 2.6, bottom and middle box), solar radiation degrades

recalcitrant structural components such as lignin through both direct photolysis and reactive intermediaries (King et al., 2012). These processes then accelerate decomposition by alleviating the lignin bottleneck and making litter components more available for biotic decomposition (Austin and Ballare, 2010; Austin et al., 2016). However, lignin is not typically a component of plant cuticles (Riederer, 2006), so in the early stages of decomposition, the bulk of structural lignin is shielded from solar radiation, protecting it from photodegradation until the exterior portion of the litter is degraded. This may limit the ability of the classic lignin-degradation-based photopriming pathway until other processes can expose internal structural lignin to solar radiation. Here, we present evidence of another mechanism (a "physical photopriming" pathway), whereby solar radiation degrades photoreactive compounds in the cuticle of litter early in the decay process, increasing water absorption during wet events and subsequent biological decomposition (Figure 2.6, top and middle box).

Results from our study are consistent with other studies that show an interaction between photodegradation and NRM-supported microbial decomposition. Several studies have found that thermal and photochemical breakdown during the day can enhance NRM-driven microbial activity at night (Wang et al., 2015; Gliksman et al., 2017; Lin et al., 2018). In these previous studies, as with ours, solar radiation's primary contribution to mass loss was not thought to involve the production of volatiles or leachates through direct photochemical oxidation, but rather through a

photopriming mechanism that enhanced biotic degradation. While some previous work has shown that solar radiation and biotic activity interact on diurnal scales (e.g. at night, microbial decomposers consume the photochemical breakdown products from the prior day), we found a mechanism through which solar radiation and biotic activity would interact over much longer timescales. In our study, photodegradation played an important role in cuticle degradation for months prior to development of significant fungal decomposer communities. In this sense, the physical photopriming mechanism we describe here is more important early in the litter decay process and may decrease in importance over time, as biotic decomposition becomes less limited by litter moisture content.

One of the most striking patterns we observed in our field study was the peculiar shape of our mass loss curve, showing accelerating rather than decelerating mass loss over the three-year study (Figure 2.2A). This could be explained in part by very low absolute rates of litter decomposition in the Namib Desert. Even after three years, tillers under our highest treatment (the "No Shelter" control) had an average mass loss of only 13.1% (Figure 2.2A). The accelerating mass loss likely reflects this being a snapshot of the initial phase of decomposition, highlighting a pattern that is not often seen in other studies that lack the temporal resolution necessary to see this shape when decomposition proceeds more rapidly. While we cannot know for certain, we may have seen a typical exponential decay curve had the experiment continued for

several more years. The changes in cuticle integrity and moisture uptake potential we observed prior to the start of exponential decay, highlight the importance of cuticle degradation early in the decomposition process.

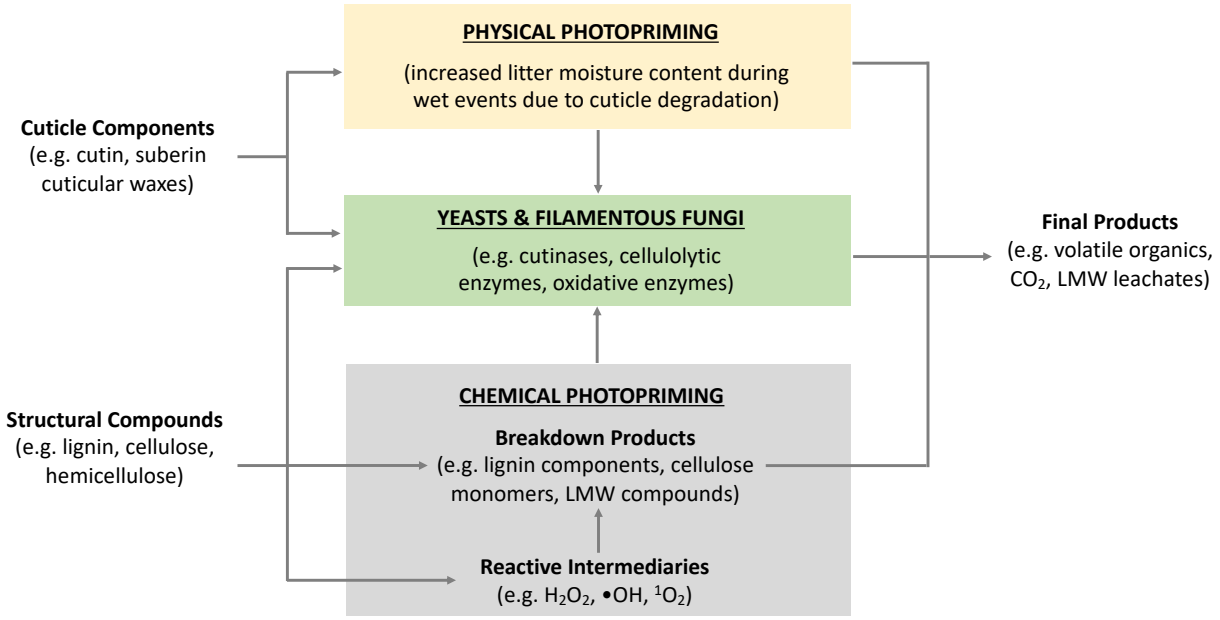

Figure 2.6. Conceptual model showing litter photopriming mechanisms and how they interact with biological degradation by fungi. Classic photopriming where solar radiation degrades recalcitrant compounds like lignin, is described as chemical photopriming since the primary mechanism of action is through a chemical change in litter degradability (grey box). This process can occur through direct and indirect pathways. Concurrently, physical photopriming (gold box) changes litter's ability to absorb non-rainfall moisture (a physical process) through cuticle degradation. Yeasts and filamentous fungi directly degrade both the cuticle and interior structural components of plant litter as well as the breakdown products of photodegradation (green box). This model does not preclude other processes like thermal degradation, sand abrasion, and insect herbivory that can also alter cuticle integrity and accelerate mass loss. LWM = low molecular weight.

Importantly, on *in situ* tillers in the field, fungi were more likely to be found on the sun-facing side than the shaded side of tillers, despite the potentially increased stress caused by direct exposure to solar radiation (Figure 2.4B-C). In other studies, UV radiation has been found to inhibit fungal growth (Fourtouni et al., 1998) though this is not always the case as UV-A radiation can stimulate sporulation in some fungi (Manning and Tiedemann, 1995) . It is unlikely that the stark contrast in fungal growth we observed between the upper and lower sides of tillers was a result of direct stimulation of fungal growth in response to UV radiation, especially when a more shaded portion of the exact same substrate was available only millimeters away on the shaded side of the tillers.

By using both a No Shelter control and our UVpass control (a filter with ~90% transmittance of UV radiation), we were able to examine the effect that altered microclimates under our radiation filters had on litter decomposition. Mass loss was significantly greater under our No Shelter control than under our UVpass control (Figure 2.2A), showing a shelter-effect. Relative humidity was not strongly altered by the shelters, but leaf wetness sensors detected less liquid water condensation underneath a subset of shelters during some nights (Figure S2.8). This was probably due to the shelter's interception of laterally transported fog droplets and the likely cause of decreased mass loss rates under the filters. Nevertheless, the clear effect of UV exclusion on mass loss and litter physical properties among tillers, after controlling

for the effect of microclimate differences (i.e. by comparison to the UVpass control), demonstrates that solar radiation plays an important part in cuticle decay and overall litter decomposition, independent of confounding microclimate variations.

While both UV radiation and visible light affected litter cuticle integrity, UV appeared to be the most important component of solar radiation responsible for cuticle degradation-driven mass loss. The clearest effect of solar radiation we saw in any treatment was the clustering by UV radiation treatment in our mass loss experiment (Figure 2.2A). This is consistent with other studies that have shown that, while short wavelength visible light can accelerate litter decomposition (Pieristè et al., 2019), UV radiation is often a stronger driver (King et al., 2012). Our measurements of the optical properties of *in situ* tillers also implicate UV in cuticle degradation since our fluorescence-based measure found clear differences in UV transmittance through the cuticle. Future studies may examine the specific wavelengths responsible for cuticle degradation via this mechanism and how this may differ among plant species.

While our study focused on the role of solar radiation in early-stage cuticle degradation, other drivers can also degrade litter cuticles, increasing litter's ability to absorb moisture. Many fungi and bacteria produce cutinases (Chen et al., 2008) and the non-lignin-bound cutin and suberin found in plant cuticles are often microbially degraded during the early stages of litter decomposition (Angst et al., 2016). Indeed, 20% of randomly sampled, *in situ* horizontal stems with fungal colonization in the

Namib had substantial visible fungal growth on both the sun-exposed and the shaded sides (Figure 2.4C) and even the underside of tillers in our most shaded treatment showed evidence of increasing cuticle degradation over time, although they received no direct sunlight (Figure S2.9B). Surficial fungi may even interact with solar radiation on diurnal timescales. By exposing grass litter to an alternating cycle of darkness and UV radiation, Lin et al. (2018) found that photopriming can occur on a timescale of days. In the Namib, fog droplets can coalesce on the top of leaning grass tillers where solar radiation is more direct. This could lead to a diurnal interaction between surficial fungi and photodegradation that could accelerate cuticle breakdown. While results of our radiation manipulation clearly implicate the role of UV radiation in cuticle degradation, we could not directly quantify the extent of biotic cuticle degradation. Future studies can examine how the activity of yeasts and other fungi on the litter surface interact with solar radiation to degrade cuticles in the early stages of litter decomposition.

The physical photopriming process which we describe here likely goes hand-in-hand with classical chemical photopriming (Figure 2.6), but the relative importance of each mechanism likely varies among systems. For example, in mesic systems where water is less limiting and plant litter consists primarily of lignin-rich tissue (i.e. wood), microbial decomposition may be more limited by litter recalcitrance making alleviation of the lignin bottleneck the most important mechanism of photodegradation (Austin et

al., 2016). Alternatively, in arid systems which are dominated by relatively labile grasses, photodegradation of the cuticle that we describe here may take on a more important role. Teasing out which of these mechanisms dominates in different systems will require studies that track how both physical and chemical properties of litter change during decomposition among species and across systems.

By demonstrating the role of the cuticle in litter decomposition, our study links existing literature on plant litter traits in decomposition models with studies of NRM and photodegradation. Physical traits like cuticle thickness and specific leaf area can predict litter mass loss rates as well as or even better than chemical traits (Zukswert and Prescott, 2017; Erdenebileg et al., 2020). Future studies may build on this work by incorporating interactions between plant traits, NRM, and photodegradation into existing litter decay models. For example, plant species vary in how long cuticles persist following senescence and this may affect their susceptibility to photodegradation (Throop and Archer, 2009). Attempts to incorporate photodegradation (Adair et al., 2017), NRM (Evans et al., 2020), and plant traits (Cornwell et al., 2008) into litter decay models have improved carbon loss estimates, but so far, these efforts have focused on only one of these drivers at a time. Combining data from plant trait databases such as the TRY Database (Kattge et al., 2020) and solar radiation networks (https://www.esrl.noaa.gov/gmd/grad/surfrad/netlinks.html) may provide the opportunity to study interactions between these different drivers using

existing datasets and may improve predictions of carbon loss in dryland systems where litter decay is notoriously underestimated by existing models (Adair et al., 2008).

We showed that NRM and solar radiation interact through a novel mechanism to accelerate decomposition during the early, standing phase of litter decay in a dryland grass. Arid and semi-arid lands make up 40% of Earth's land surface and, in many of these systems, standing dead grass litter can make up more than half of total plant material (Seely and Louw, 1980; Zhou et al., 2009). This standing dead phase is a critical and sometimes years-long phase during which litter can be "primed" for subsequent accelerated decomposition once it falls to the surface (Wang et al., 2017a). Moisture regimes are changing in drylands worldwide, especially in NRM-dominated systems (Forthun et al., 2006; Niu et al., 2010; Haensler et al., 2011; Dai, 2013; Kutty et al., 2019), so understanding how NRM and photodegradation interact to drive litter decomposition can play a crucial role in predicting how drylands respond to environmental change, enhancing our ability to manage these globally important ecosystems.

APPENDIX

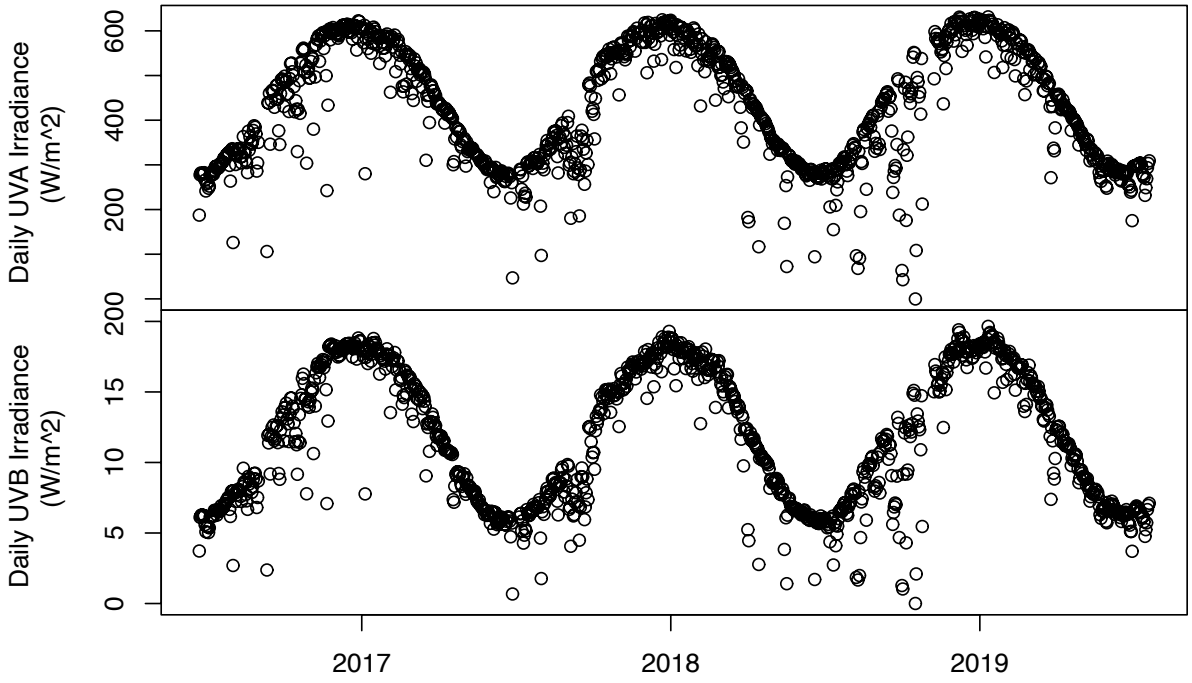

Figure S2.1. UVA and UVB radiation measured by Kipp and Zonen UV pyranometers at Gobabeb. Data from the Baseline Surface Radiation Network courtesy of Dr. Roland Vogt (https://mcr.unibas.ch/dolueg2/index.php?project=gobabeb&var=d).

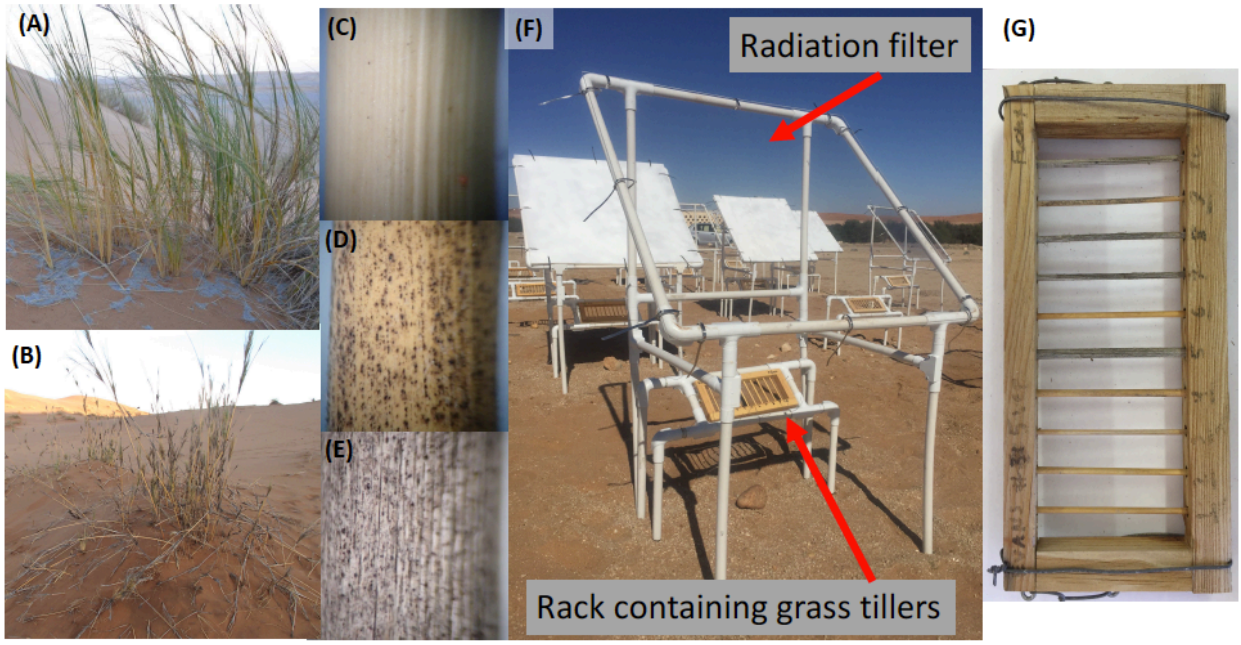

Figure S2.2. (A) Live *Stipagrostis sabulicola* in the Namib Sand Sea forming hummocks. (B) Dead *S. sabulicola* stems will remain standing and intact for years following leaf senescence. (C-E) close-up photographs of *S. sabulicola* tillers showing cracks and fissures becoming more common as litter progresses from recently senesced (E) to heavily degraded (G). (F) Solar radiation filters with litter rack underneath. (G) An example litter rack. The "rungs" of the "ladders" are *S. sabulicola* stems ~ 0.5 cm in diameter and 9 cm long.

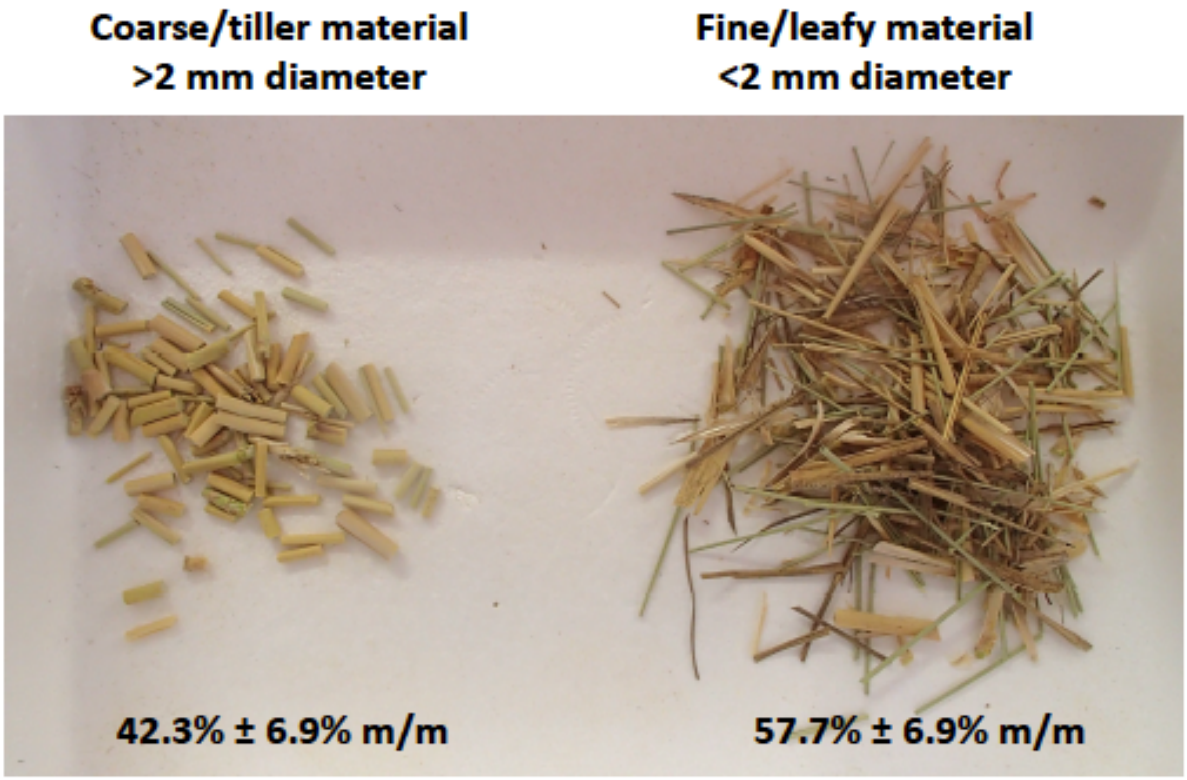

Figure S2.3. Coarse (>2 mm diameter) and fine (<2 mm diameter) fractions of *S. sabulicola* tillers (N = 5). Photo is a representative example.

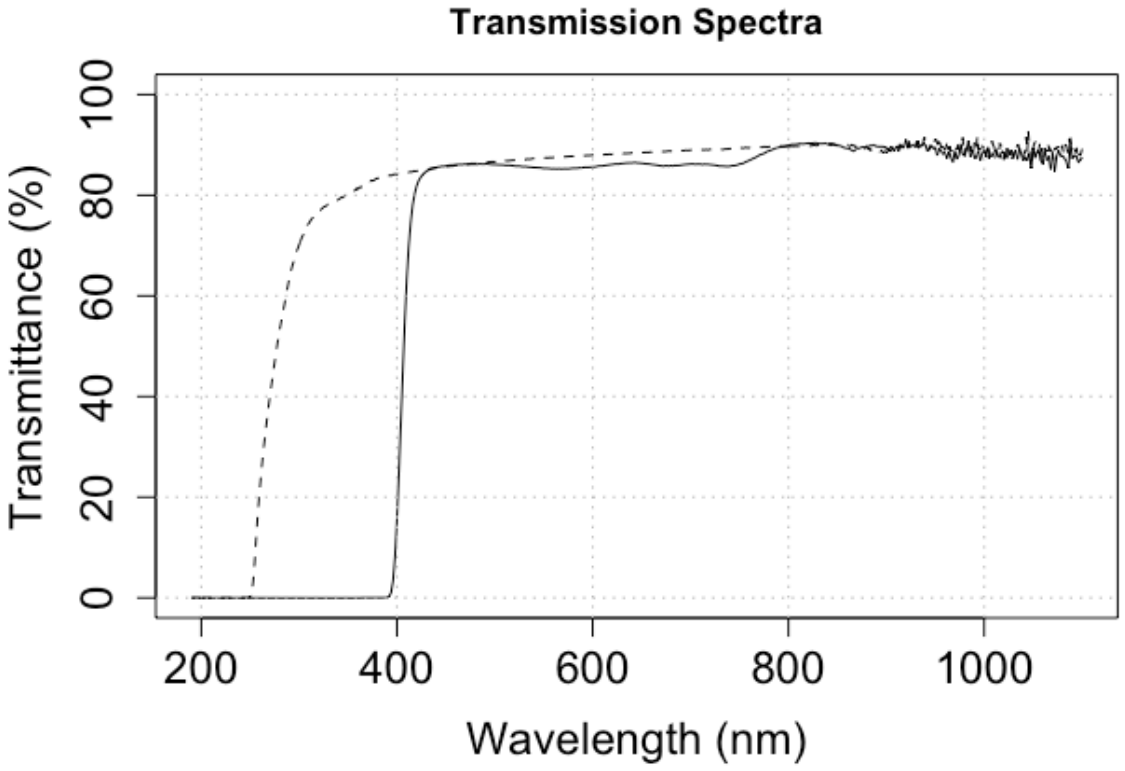

Figure S2.4. UV transmission spectra of UVblock (solid) and UVpass (dashed) filter materials, measured on a UV-2401 PC spectrophotometer (Shimadzu, Kyoto, Japan) .

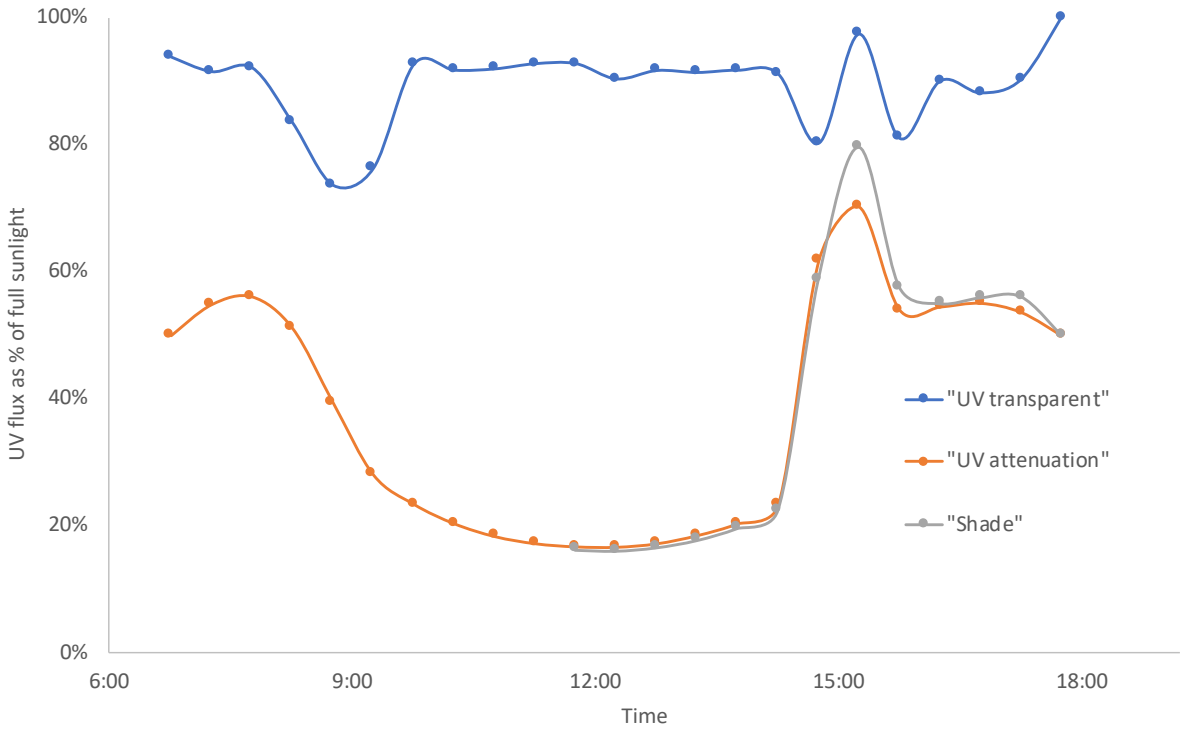

Figure S2.5. Broadband UV-A + UV-B irradiation under each treatment over the course of a day. Values are expressed as percentages relative to unobstructed sun light.

Figure S2.6. Example microscope photographs of tillers at five different stages of cuticle degradation, corresponding to physical damage to the cuticle surface. The sun-facing and shaded side of tillers from the solar radiation manipulation (Exp1) were photographed and each assigned an ordinal score from 1-5 based on physical changes to cuticle surface including the presence and extent of cracks, waxes flaking, bleaching, and removal of the cuticle surface.

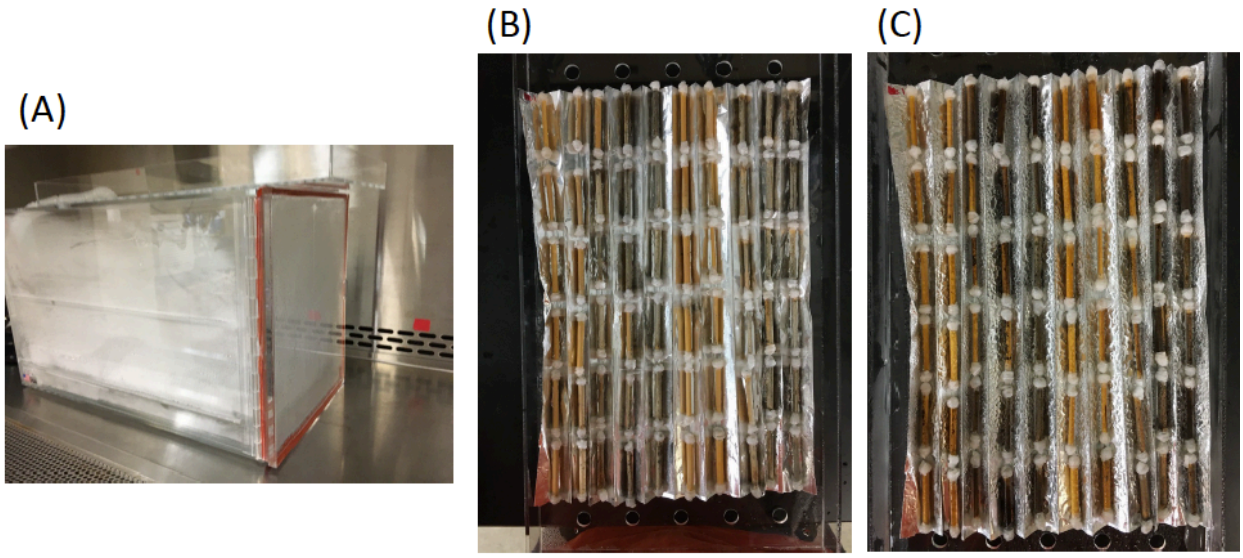

Figure S2.7. (A) Artificial fog chamber used for measuring tillers' potential to absorb water during NRM events. The chamber has been running for several minutes in this photograph and is filled with a steady stream of fog droplets. (B) Tray of dry tillers before being placed into fog chamber (ends are sealed with parafilm to prevent water from being absorbed by the vasculature. (C) Tray of tillers after exposure to simulated fog event (notice liquid water beaded up on tillers).

Figure S2.8. Temperature (top), Relative Humidity (middle), and leaf wetness percentage (bottom). For each plot, measurements made under two replicate shelters are plotted relative to the average of two "no shelter" controls at the same time. The plots show some effect of microclimates

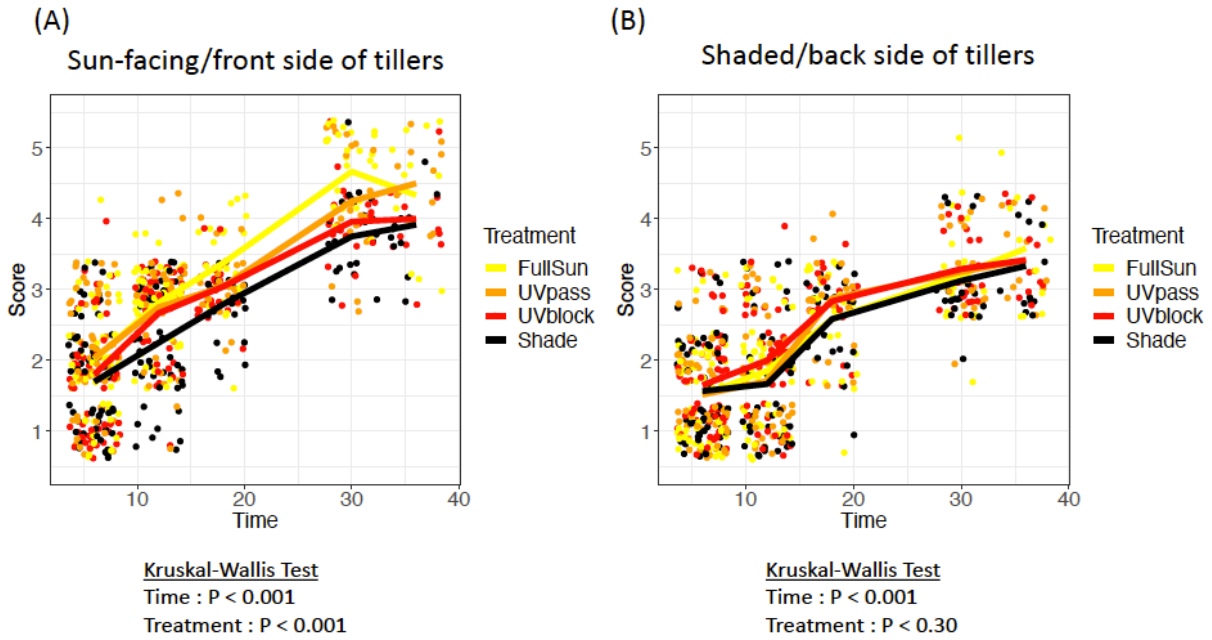

Figure S2.9. Cuticle damage scores for both the sun-facing (A) and shaded (B) side of tillers from Exp1 (1 = intact cuticles; 5 = heavily degraded cuticles). Data are plotted with "jitter" to show individual data points. Lines are mean values.

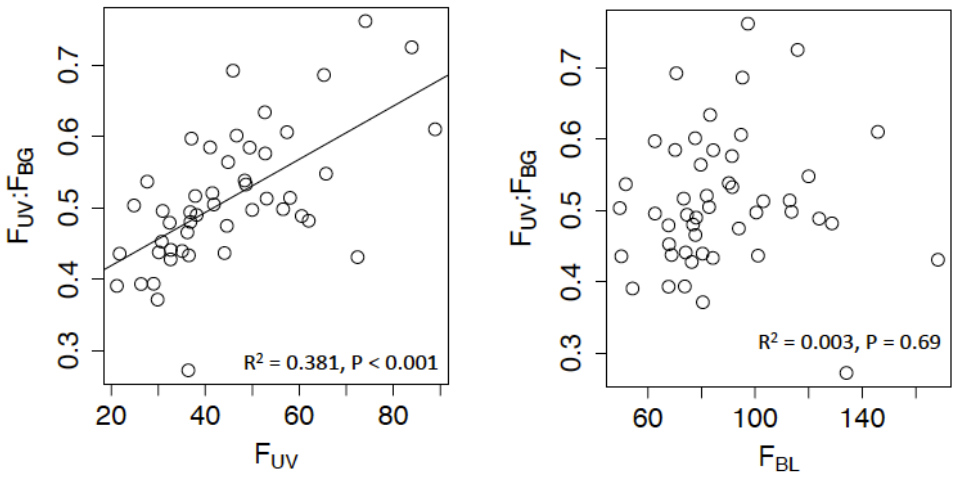

Figure S2.10. From Exp3a, variation in F_{UV}:F_{BG} as a function of F_{UV} (left) and F_{BG} (right) shows that the F_{UV}:F_{BG} varies primarily due to differences in transmittance of UV through the cuticle rather than difference in the underlying chlorophyll concentration of tillers.

CHAPTER THREE:

PHOTODEGRADATION ACCELERATES LITTER DECAY BUT DOES NOT ALTER FUNGAL COMMUNITY COMPOSITION IN A HYPERARID DESERT

Living and dead matter were so obviously at variance here, and the living matter so obviously triumphant in its adaptability over the dead elements and their rigid laws that the barren wilderness seemed to us more essentially alive than green trees rustling in the wind.

Henno Martin describing the Namib Desert
The Sheltering Desert (1957)

INTRODUCTION

Solar radiation is an important driver of litter decomposition. By photochemically breaking down plant litter constituents (a process known as photodegradation), solar radiation can accelerate litter decay rates, leading to substantially greater carbon turnover than would occur from biotic decay alone. Photodegradation is well documented in arid and mesic systems alike (King et al., 2012) and models that ignore the contribution of photodegradation can drastically underestimate litter decay rates and carbon fluxes (Chen et al., 2016; Adair et al., 2017). However, solar radiation, particularly ultraviolet-B (UV-B) radiation, is also a strong physiological stressor and can reduce the size of or alter the composition of decomposer communities, slowing litter decay (Pancotto et al., 2005; Pieristè et al., 2020). The net effect of solar radiation on litter decomposition is therefore a product of both the stimulatory effects of photodegradation and negative effects of

photoinhibition. Understanding how these two processes interact with one another under different conditions will enhance our understanding of carbon turnover.

Photodegradation can accelerate plant litter decay through a variety of direct and indirect pathways. Some plant structural components, including lignin, have highly irregular structures and multiple double bonds making them resistant to enzymatic attack but susceptible to oxidative damage by photodegradation. Solar radiation can break these bonds either through direct photolysis, in which UV triggers the release of CO_2, CH_4, and CO from leaf litter (Brandt et al., 2009; Day et al., 2019), or indirect photolysis in which solar radiation produces reactive intermediaries such as peroxides and reactive oxygen species that can further degrade lignin and other organic components of litter (Messenger et al., 2009; King et al., 2012). By degrading recalcitrant compounds in litter, solar radiation can increase the availability of biodegradable litter components, increasing decomposer growth (Baker and Allison, 2015; Austin et al., 2016). By degrading the litter cuticle, UV radiation can even change litter's physical properties such that it absorbs more water during fog and dew events, increasing decomposer growth (Logan et al. in review). These processes by which solar radiation increases litter's susceptibility to subsequent biotic decay (known as photopriming or photofacilitation), are a primary way it can accelerate litter decay, but radiation's contribution to early litter decay can vary widely depending on plant traits, climate, and solar irradiance levels.

UV radiation is a strong mutagen and physiological stressor, so it has the potential to inhibit biotic decomposition, but fungi have a suite of adaptations to ameliorate the damaging effects of solar radiation. By embedding pigments such as melanin in their cell walls, fungi can shield themselves from some of the harmful effects of both desiccation and radiation stress (Cantrell 2017). Within the cytoplasm, small water-soluble molecules called mycosporines act as sunscreens by absorbing UV-B radiation while also serving as antioxidants, scavenging for reactive oxygen species that can be produced by UV interacting with cellular components (Oren & Gunde-Cimerman 2007). These stress-reduction strategies however are energetically costly and investing in radiation tolerance can slow growth (Lustenhouwer et al., 2020). This is why even when total microbial biomass is not affected by solar radiation, exposure to UV radiation can cause shifts in the makeup of the decomposer community in ways that affect how efficiently the community can degrade litter (Pieristè et al., 2020).

Importantly, many of the traits that help organisms cope with high radiation also mitigate the effects of desiccation stress. This includes melanization (Cordero and Casadevall, 2019), production of antioxidants that scavenge for reactive oxygen species (Oren and Gunde-Cimerman, 2007), and upregulation of DNA repair mechanisms (Mattimore and Battista, 1996). Since arid environments are characterized by both intense thermal, radiation, and desiccation stress, fungi in these environments may be less susceptible to the effects of solar radiation than are their counterparts in more

mesic systems. As a result, photoinhibition may be less important in environments that experience greater aridity. This could partially explain why some studies do not find inhibitory effects of solar radiation on fungal communities in deserts (Gallo et al., 2009). Studying how solar radiation affects litter-associated decomposer communities at the extreme end of the aridity spectrum can help illuminate the mechanisms of photoinhibition, allowing us to see how decomposers respond to the dual stressors of radiation and desiccation.

We studied how solar radiation affects litter-associated fungal communities in a hyperarid grassland with high radiation stress. We artificially reduced solar radiation, measuring mass loss and fungal community composition. To determine whether UV radiation had different effects than visible light, we had included both UV-attenuation and fully shaded treatments. We hypothesized that the ubiquity of stress-tolerant fungi in this system (Jacobson et al., 2015; Logan et al., 2021) would mean litter-associated fungi would be relatively insensitive to solar radiation. We also conducted a second experiment in which we sterilized a subset of litter, removing the existing microbial community prior to deploying it, to see whether solar radiation affected litter decomposition rates as new fungi colonized litter. Understanding how decomposers respond to solar radiation stress in extremely water limited systems can help us understand how photodegradation and photoinhibition interact with aridity to control litter decomposition rates in dryland systems.

METHODS

We conducted two experiments to assess how solar radiation affected litter decomposition rates and the composition of fungal communities. First, we constructed filters to selectively attenuate solar radiation and deployed them in the field for a 36-month litter decomposition experiment with fungal communities intact. At the end of the experiment, we used next generation sequencing to determine the composition of the litter-associated fungal communities under each treatment. Next, to determine how solar radiation contributed to litter decomposition when the fungal load was reduced, we performed a second mass loss experiment, this time autoclaving a subset of litter to remove existing decomposers at the start of the experiment.

Study System

We conducted our study at the Gobabeb Namib Research Institute in the Namib Desert, Namibia. Gobabeb is situated at the northern end of the Namib Sand Sea, a 3 million ha dune system devoid of permanent human settlements. Mean annual rainfall at Gobabeb is 27 mm, though this shows high year-to-year variability (Eckardt et al., 2013). Non-rainfall moisture (fog, dew, and water vapor) is much more frequent than rain (Jacobson et al., 2015) and supports the majority of litter decomposition (Evans et al., 2020). We studied decomposition of *Stipagrostis sabulicola*, the dominant grass in

the Namib Sand Sea with globally distributed con-generics (Seely and Louw, 1980). *S. sabulicola*'s litter chemistry is described by Logan et al. (2021).

Exp1: The effect of solar radiation on litter decay rates

To assess the contribution of solar radiation to litter decomposition, we constructed a series of radiation filters to selectively block different wavelengths of the solar spectrum. The results of this mass loss experiment are also reported in part elsewhere (Logan et al. in review). We used four treatments: a shade treatment which utilized plexiglass that was spray painted white to block direct solar radiation, a UV-attenuation ("UVblock") treatment using Lexan polycarbonate (SABIC Innovative Plastics, Riyadh, Saudi Arabia) which blocks radiation below 400 nm but transmits 90% of radiation >400nm, a "UVpass" control made from clear Arkema G-UVT (Loop Acrylics, Chicago, USA) that has >80% transmittance of radiation above 300 nm, and a "no shelter" control to ascertain the effects of microclimate changes induced by the shelters themselves. Spectra for the UVpass treatment and the UVblock control are shown in Figure S3.1 as measured on a UV-2401 PC spectrophotometer (Shimadzu, Kyoto, Japan). To determine the efficacy of the treatments in the field, we measured UV radiation several times throughout the year using a broadband UV radiation sensor measuring unweighted radiation (250-400 nm) under the treatments and normalizing it to clear sky measurements (Apogee UV Sensor Model SU-100, Apogee Instruments,

Logan, UT, USA). We report values as percent of blocked UV radiation relative to the full exposure control (Figure S3.2).

Shelters were constructed from PVC pipe, with a 70 x 70 cm radiation filter on top (Figure S3.3), except for the "no shelter" control. Radiation filters faced north and were sloped on a 45° angle so rising air would be directed away from samples, even on windless days, to minimize localized greenhouse warming. The result was that we attenuated direct solar radiation during the majority of the day but some diffuse radiation entered on the sides and some direct radiation was present when the sun was at very low angles in the early morning and evening. In total, this resulted in a 62% reduction in total UV radiation under both of the UVblock and shade treatments. To assess how filters altered the microclimates beneath them, we placed iButton Hygrochrons (iButtonLink LLC, United States) to measure temperature and relative humidity) and leaf wetness sensors (S- LWA-M003, Onset Computer Corporation, United States) underneath two shelters and compared values relative to those at two spots in the open over several days. Microclimate effects of shelters are reported in Figure S3.4.

We collected recently senesced, standing *S. sabulicola* tillers from Station Dune at Gobabeb, dried them at 35 °C for 24 hours, cut them to 9 cm lengths, weighed them, and deployed them under the radiation filters. To avoid shading and other microclimate effects of litter bags, we placed tillers in litter racks, which were specially

built wooden frames covered with a dewaxed shellac for waterproofing (Figure S3.3). This approach has been used previously (Logan et al., 2021; Evans et al., 2020). We deployed 240 tillers, evenly distributed among the four treatments. The experiment ran for 1092 days and at five time points (roughly 6, 12, 18, 30, and 36 months), we weighed all remaining tillers and removed one fifth of them (selected using a stratified random sampling approach) for amplicon-based analysis of the fungal community. To determine the effect of radiation treatment on decomposition, we used the 'lmer' function in the *lme4* package (Bates et al., 2015) to conduct repeated measures ANOVAs in R, using time, radiation treatment, and initial mass as predictors of mass loss.

Exp 2: Photodegradation with reduced fungal community

In addition to examining fungal communities' response to solar radiation, we wanted to know the effect of photodegradation on mass loss when the decomposer community was reduced. To do this, we autoclaved a subset of *S. sabulicola* tillers and placed them beneath the radiation filters. We placed two autoclaved and four non-autoclaved tillers under each filter. This experiment was started after the first so we were only able to measure mass loss out to 18 months after deployment. Autoclaving was performed in the field using a homestyle pressure cooker for 2 hours and effectiveness was confirmed by plating tillers onto Malt Extract Agar. Although we

eliminated fungi that were present at senescence, tillers could still be colonized by wind-dispersed fungi during the course of the experiment (Evans et al., 2019). As a result, tillers in our sterilized treatment had reduced, but not absent, decomposer communities present throughout the experiment.

Molecular Methods

To determine whether litter-associated fungal communities differed by radiation treatment, we collected a subset of tillers at each sampling time in the primary mass loss experiment and extracted DNA for amplicon sequencing. Despite multiple extraction and PCR methods, fungal biomass was too low to get extractable DNA from tillers at the early collection points so we confined our analysis to tillers collected at 30 months and 36 months (N = 90). We extracted DNA from litter using a MoBio MagAttract PowerSoil DNA kit (QIAGEN, Maryland, USA) on a Kingfisher Flex system (ThermoFisher Scientific, Massachusetts, USA). We sequenced the ITS region with Earth Microbiome Project primers (ITS1-F: CTTGGTCATTTAGAGGAAGTAA; ITS2: GCTGCGTTCTTCATCGATGC) (www.earthmicrobiome.org/protocols-and-standards/its/) (Gilbert et al., 2014), using 250-bp paired-end sequencing on the MiSeq Illumina (V2) platform at Michigan State University's Research Technology Support Facility Genomics Core. Fungal contigs were created in USEARCH version 11.0 using fastq_mergepairs and quality checked with fastq_eestats2. Sequences were

cut to a minimum length of 250 bp and quality filtered to a maximum expected error score of 1 using fastq_filter. To avoid the downsides associated with both reference-based and *de novo* OTU clustering, we identified Amplicon Sequence Variants (ASVs) (Callahan et al., 2017). ASVs were *de novo* chimera checked and filtered to remove low abundance ASVs (fewer than 8 reads) using unoise3.

After quality filtering, we had a total of 249,310 reads. We eliminated samples with fewer than 1000 reads and then rarefied to 1069 reads. Previous culture-based and amplicon-based studies have shown that fungal communities on *S. sabulicola* in the Namib Desert consist of relatively few fungi, with fewer than ~25 dominant taxa constituting the majority of sequences (Logan et al., 2021) so this sampling depth should allow us to capture the most abundant taxa while still retaining enough samples for robust statistical analysis. We performed statistical analysis of ASVs in R. We did not use a phylogenetic distance measure (i.e. UniFrac) because phylogenetic relationships among many of the fungi in our samples are in flux and the relatively short ITS region we sequenced does not allow us to confidently measure phylogenetic distance for several taxa without including additional information from other gene regions (Raja et al., 2017). Instead, PERMANOVAs and NMDS ordinations were generated using Bray-Curtis distance, which accounts for both presence and abundance of taxa. Distances were calculated using the 'distance' function in the *phyloseq* package (McMurdie and Holmes, 2013). To compare relative abundances of specific taxa

among the different solar radiation levels, we used the *DESeq* function in the '*DESeq2*' package (Love et al., 2014). Because *DESeq* does not allow zero abundances, we transformed data by adding one to each ASV abundance per sample beforehand. Since fungal reference databases have considerable errors in taxonomic identifications (Hofstetter et al., 2019), anytime we identify an ASV by name, it means we have manually verified its identity by using the NCBI's Basic Local Alignment Search Tool, using a conservative cutoff of ≥ 97% similarity and ≥ 80% coverage (Raja et al., 2017), using only type species as references (Ko et al., 2011).

RESULTS

Mass loss from tillers with intact fungal communities

In our 36-month solar radiation manipulation using litter with intact fungal communities, mass loss was greater under ambient UV controls compared to the UVblock and Shade treatments (Figure 3.1) (Table 3.1). While mass loss was slower when we filtered UV radiation, subsequent filtering of visible light did not affect the decomposition rate (i.e. the UVblock and Shade treatments did not differ). Unlike the exponential decay relationship typically seen in litter decomposition studies, rates of mass loss accelerated over the 1092-day experiment.

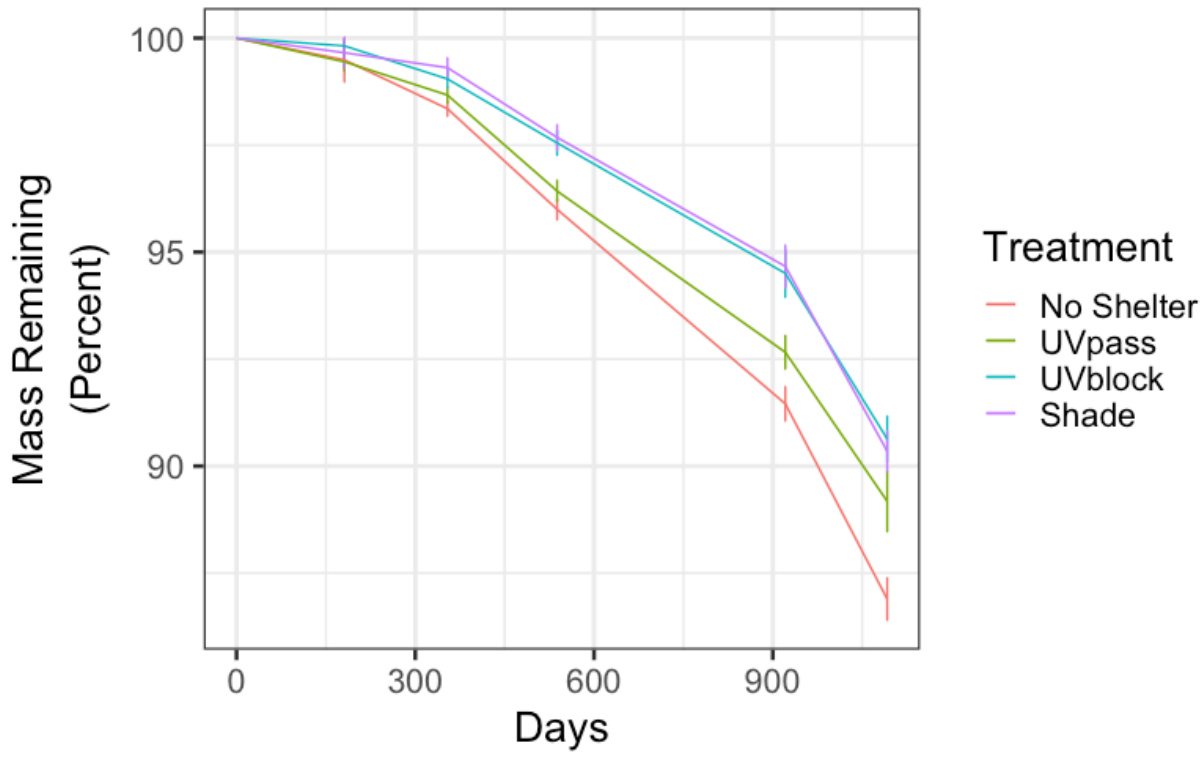

Figure 3.1. Mass loss in the primary solar radiation manipulation with intact fungal communities. Lines are means ± 1 S.E.M. N = 240 tillers at the start of the experiment, but 48 were removed at each collection time.

Table 3.1. ANOVA table of mass loss in the 36-month solar radiation experiment using native fungal communities. N = 240 tillers.

Source	SS	df	F	P
Initial Mass	0.22	1	0.1738	0.6769
Time	477.14	1	372.1289	<0.001
Treatment	4.03	3	1.0483	0.3708
Initial Mass * Time	35.25	1	27.4941	<0.001
Treatment * Time	93.47	3	24.2988	<0.001

In our second mass loss experiment, in which we reduced the initial size of decomposer communities, we found that reduced solar radiation decreased mass loss rates. This held true for both sterilized and non-sterilized litter (Figure 3.2), but the

effect of radiation depended on autoclave treatment (p=0.01 Radiation*Autoclave; Table 3.2), with autoclaving affecting how mass loss responded to visible light. Specifically, the Shade and UVblock treatments had similar mass loss rates for tillers with full fungal communities but on sterilized tillers, decomposition differed between four all treatments, with greater mass loss under greater radiation exposure (Figure 3.2).

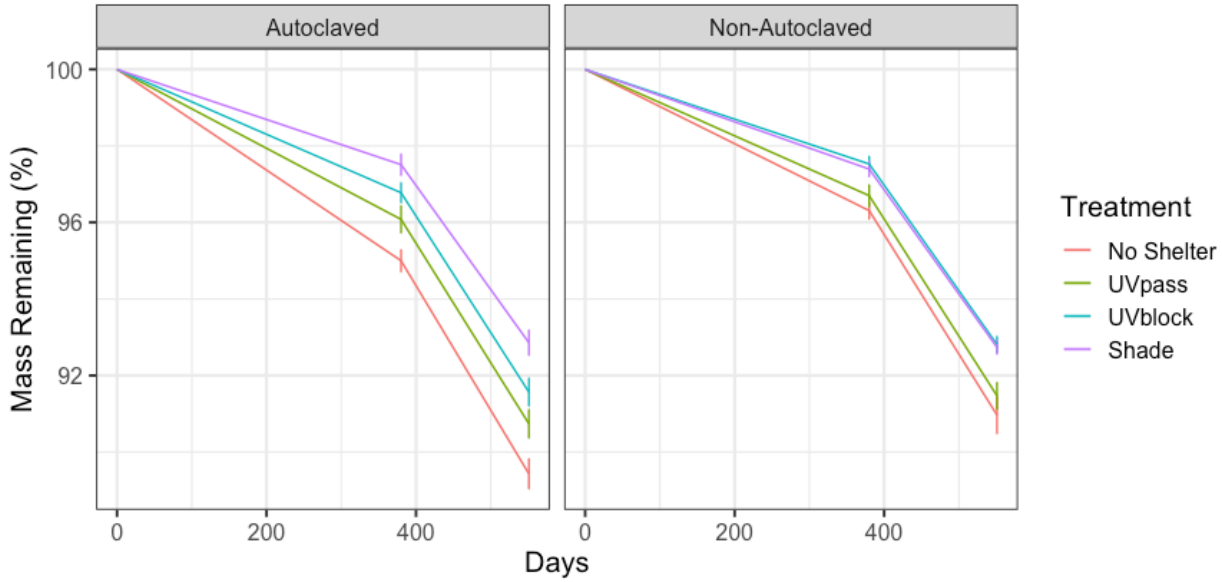

Figure 3.2. Mass loss from tillers with reduced fungal communities that were autoclaved prior to deployment (left) and tillers with intact fungal communities (right). Lines are means ± 1 S.E.M. N = 143.

Table 3.2. ANOVA table of mass loss in the reduced fungi (autoclaved) solar radiation experiment. N = 143.

Source	df	SS	F	P
Radiation Trt	3	0.0173	33.0	<0.001
Autoclave Trt	1	0.00350	20.0	<0.001
Time	1	0.183	1043	<0.001
Radiation*Autoclave	3	0.00204	3.87	0.010
Radiation*Time	3	0.000656	1.25	0.292
Autoclave*Time	1	0.000067	0.384	0.536
Radiation*Autoclave*Time	3	0.000054	0.104	0.958
Residuals	270	0.0473		

Solar radiation's effect on fungal communities

We identified a total of 144 fungal ASVs in *S. sabulicola* tillers, with Ascomycota making up the vast majority of sequence reads. When we aggregated the treatments by UV level (No Shelter and UVpass controls = Ambient UV; UVblock and Shade = Reduced UV), mean richness was 11.8 ASVs tiller^{-1} in the two ambient UV treatments and 14.1 ASVs tiller^{-1} in the reduced UV treatments ($t = 2.48$; $P < 0.015$) though total richness was comparable (94 ASVs in ambient UV treatments and 106 ASVs in reduced UV treatments). This is consistent with other studies that have found relatively few fungal taxa in this system compared to communities in mesic systems (Jacobson et al., 2015; Evans et al., 2020; Logan et al., 2021). A core group of 56 ASVs were present under both the ambient and reduced UV treatments and these represented an average of 98.9% of reads per sample (Figure 3.3). The other 88 ASVs

(those found only on either ambient or reduced UV treatments) represented only 1.1% and 1.0% of reads on tillers in those treatments respectively.

Table 3.3. Identities and relative abundance of the eight ASVs with mean read abundances >1% per sample. Relative abundance is reported as the proportion of total reads on each sample attributable to that ASV, averaged across all four treatments.

ASV	Division	Species	Relative Abundance
ASV_6	Ascomycota	*Alternaria sp.*	3.4%
ASV_2	Ascomycota	*Aureobasidium pullulans* complex	25.5%
ASV_4	Ascomycota	*Aureobasidium pullulans* complex	7.3%
ASV_8	Basidiomycota	*Cryptococcus/Filobasidium sp.*	1.7%
ASV_1	Ascomycota	*Neophaeothecoidea proteae*	40.9%
ASV_3	Ascomycota	*Neophaeothecoidea proteae*	6.5%
ASV_5	Ascomycota	*Phaeococcomyces mexicanus*	4.6%
ASV_7	Ascomycota	*Phaeococcomyces mexicanus*	2.5%

Table 3.4. Results of PERMANOVA test of differences in fungal community composition (Bray-Curtis distance) across the four radiation treatment levels and days in the field. Only samples at 30 months and 36 months had extractable DNA, so Time denotes only the difference between those two time points, not the full length of the experiment. N = 90 samples.

Source	df	SS	F	P
Treatment	3	0.632	1.18	0.292
Time	1	0.117	0.653	0.601
Treatment*Time	3	0.552	1.03	0.394
Residuals	82	14.7		

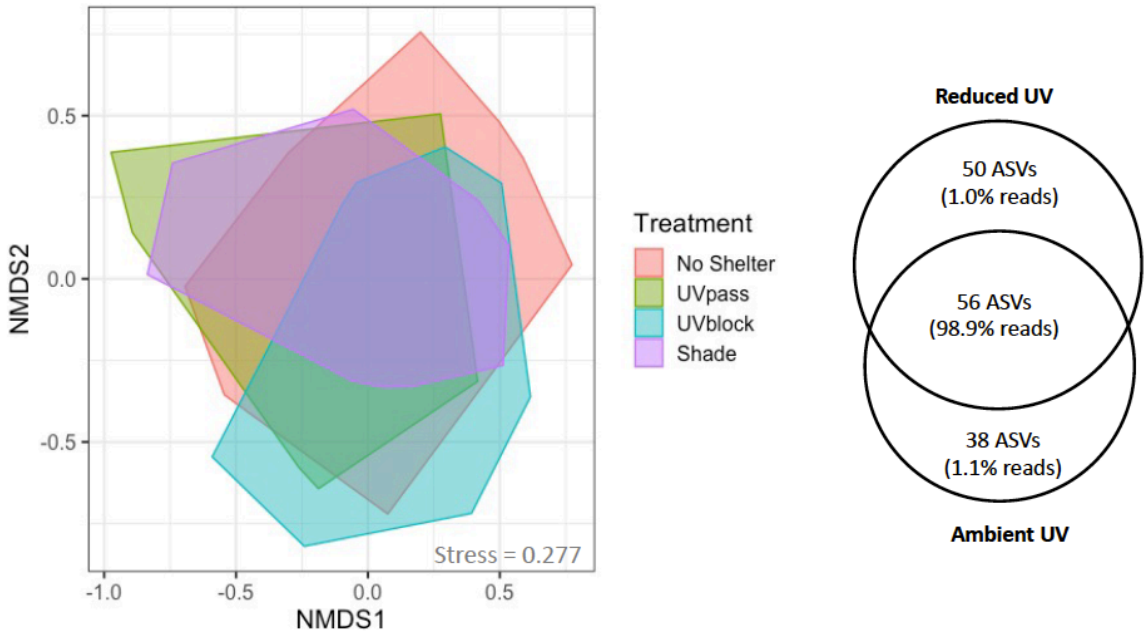

Figure 3.3. (left) NMDS (Bray-Curtis distance) of fungal community composition at 30 months and 36 months (both time points are combined since there was no significant difference in fungal communities at the two times). Shapes are convex hulls for each treatment. (right) Venn diagram of Amplicon Sequence Variants found in only the Ambient UV treatments (i.e., No Shelter and UVpass controls), only the Reduced UV treatments (i.e., UVblock and Shade treatments), and those found at both UV levels. The percentages in parentheses show mean relative abundance of those ASVs per sample averaged across all samples. Percentages do not sum to 1 due to rounding.

Across all treatments, the fungal community was dominated by a small group of highly abundant taxa. Eight ASVs belonging to five taxa had mean relative abundance >1% reads per tiller and collectively, these made up an average of 92.4% of reads per sample (Figure 3.4) (Table 3.3). Two ASVs that were identified as *Neophaeothecoidea proteaei* constituted 47.4% of total reads and another two ASVs identified as *Aureobasidium pullulans* complex constituted 32.8% of total reads.

Fungal community structure was not significantly different among the radiation treatments (Figure 3.3) (Table 3.4). This was the case whether we treated the four treatments separately or aggregated by UV level (Table S3.1). Community composition did not differ between the 30-month and 36-month collection points, so we combined the time points for subsequent analysis (Table 3.4). When we looked at the relative abundances of individual taxa using *DESeq*, four of the 144 ASVs had significantly different abundances ($P < 0.05$) under the ambient UV treatments versus the reduced UV treatments. All four were more abundant in the reduced UV treatments, compared to the ambient (Table 3.5). However, these taxa were not abundant overall, collectively constituting 0.59% of total reads under ambient UV conditions and 1.5% of reads under the reduced UV treatments.

Table 3.5. Identities and relative abundance of the four taxa that had significantly different abundances under ambient compared to reduced UV treatments. Relative abundance percentages are based on average read abundance per tiller. Adjusted p-values are from DESeq comparison of abundances among the two UV levels.

ASV	Species	Rel. Abundance (Ambient UV)	Rel. Abundance (Reduced UV)	Adjusted P-value
ASV_14	*Symmetrospora* sp.	0.18%	0.45%	0.025
ASV_15	Unknown Teratosphaeriaceae	0.26%	0.36%	0.012
ASV_16	*Aureobasidium pullulans* complex	0.15%	0.52%	0.01
ASV_34	*Symmetrospora* sp.	0.0042%	0.11%	0.011

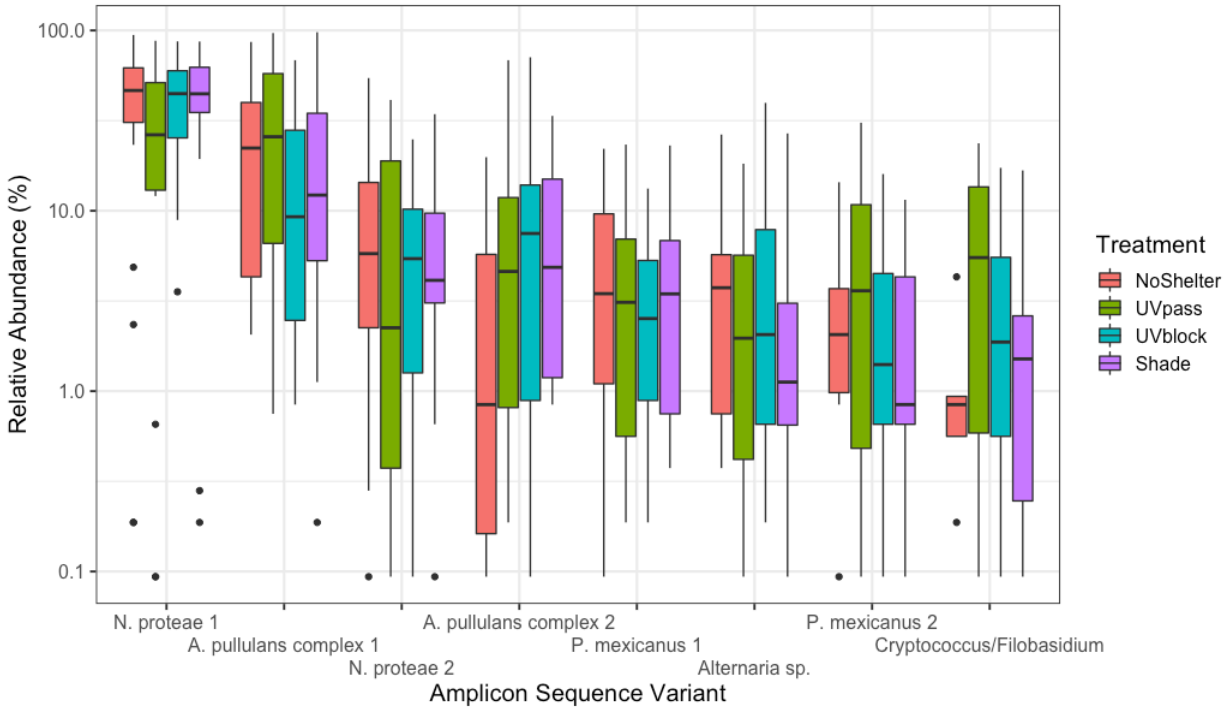

Figure 3.4. Mean relative abundance of reads from the eight ASVs with mean relative abundances >1% per tiller. Collectively the eight ASVs sum to a mean relative abundance of 92.4% of reads per tiller. Repeat names occur because, sometimes, multiple ASVs were identified as belonging to the same taxon, at least to the level we were able to confidently identify.

DISCUSSION

We show that solar radiation accelerates litter decomposition in a hyperarid desert, but the composition of litter-associated fungal communities is largely insensitive to our experimental mainuplations of solar radiation. While some rare taxa increased in abundance when radiation was reduced, the dominant fungi on litter appeared unaffected by radiation at levels observed in the field. That we did not

observe a strong effect of solar radiation on fungal communities may be because the species pool available to colonize litter (either from endophytes or via airborne dispersal following plant senescence) is pre-filtered to select for taxa that are highly resistant to radiation stress. Fungi that decompose litter in the Namib must tolerate the prolonged dry periods as well as the intense solar radiation, and the combined effect of these two selection pressures may be a highly UV-tolerant fungal community.

Many of the dominant fungi we identified on litter in this hyperarid desert are well-known polyextremophiles with wide geographic and niche ranges. *Phaeococcomyces mexicanus* has been found as an epiphyte on desert shrubs (Moreno-Rico et al., 2014), a leaf endophyte (Ricks and Koide, 2019), and in Antarctic snow (de Menezes et al., 2019) and is related to the black yeasts, which are notoriously tolerant of environmental stressors associated with both low water activity and radiation (Gostinčar et al., 2010). Members of the basidiomycetous yeast genus *Cryptococcus/Filobasidium* have been primarily isolated from soils and plant florets but have also been found in alcoholic drinks and the intestines of lab mice and pigeons (Kwon-Chung, 2011) as well as in Antarctic soils, suggesting high a tolerance of cold and desiccation, at least among some strains (Arenz et al., 2006). Members of the *Aureobasidium pullulans* complex (which represent the second and third most abundant ASVs) are well known polyextremophiles found in hypersaline water, glacial ice, aviation fuel tanks, and in epiphytic and endophytic lifestyles worldwide (Gostinčar et

al., 2014). That these taxa were relatively insensitive to solar radiation was unsurprising. In fact, at least two other photodegradation studies have reported no change in *Aureobasidium* spp. abundances after manipulating UV radiation in the field (Newsham et al., 1997; Gallo et al., 2009) (we could not find any studies that reported radiation tolerances of our most abundant fungus, *Neophaeothecoidea proteae*, partially because the genus was first described in 2014).

In general, the dominant litter-associated fungi under all radiation levels are highly stress-tolerant taxa with fairly wide geographic and niche ranges. This corroborates previous work we have done which found that both litter-associated and airborne/fog-dispersed fungal communities in the Namib contain many stress-tolerant and extremophilic taxa (Jacobson et al., 2015; Evans et al., 2019; Logan et al., 2021). This also supports the hypothesis that the fungal community is relatively insensitive to changes in solar radiation because the available species pool consists largely of robust, stress-tolerant taxa, and would explain why even after 36 months, the dominant fungi on shaded tillers were the same as those that thrived in direct sunlight.

To our knowledge, this study is the first to report litter-associated fungi's responses to UV radiation in an extremely hyperarid system (MAP <50 mm). In this setting, we did not find evidence of photoinhibition of fungal decomposition that has been described at other sites. Reducing UV-B radiation altered litter-associated fungal and bacterial communities in a sub-Antarctic shrub community (Pancotto et al., 2003)

and a deciduous forest (Pieristè et al., 2020), since some taxa were more susceptible to UV radiation stress than others. Increasing UV-B radiation also altered the dominant fungi on litter in a subarctic heath system (Gehrke et al., 1995). Each of these three studies was conducted in systems that, while not all considered mesic, were wetter than ours (MAP = 499, 852, and 310 mm respectively). A study conducted along an arid riparian zone (MAP = 250 mm) found that reducing solar radiation had no detectable effect on fungal community composition (Gallo et al., 2009). In this study, litter was colonized by similar extremophilic taxa to those we found, including *Aureobasidium* spp. and *Alternaria* spp. While we cannot draw definitive conclusions from these few studies, these findings support the hypothesis that under more arid conditions, litter-associated fungi are more tolerant of radiation stress and therefore experience less photoinhibition. Whether this is due to trait correlations between radiation and desiccation response mechanisms, pre-filtering of the available species pool, or other drivers, is an area for future research.

Four ASVs had greater relative abundances when UV radiation was reduced (Table 3.5), though a literature search yielded no clear explanation based on their known ecology. One ASV belongs to Teratosphaeriaceae, a family whose members are found in highly acidic soils and alpine and Antarctic desert rock surfaces, several of which are highly melanized (Ruibal et al., 2009; Hujslová et al., 2013). *Symmetrospora* sp. is a recently described yeast typically found on leaf surfaces though also isolated

from decaying wood, beetle guts, and elsewhere (Haelewaters et al., 2020). Finally, one ASV was identified as *Aureobasidium pullulans* complex, the polyextremophilic fungus discussed above that is known for its hardiness. Collectively these results do not suggest that these fungi would be particularly susceptible to radiation stress. Logan et al. (2021) found a similarly surprising pattern where some fungi that showed preference for a hotter, more arid site in the Namib had congenerics who appeared more abundant at a cooler, wetter site. This could be due to strain-level variation in stress responses among taxa, though this is unlikely since traits relevant to stress tolerance are often conserved at much higher taxonomic levels (Treseder and Lennon, 2015). More likely, this represents a limitation in our ability to confidently delineate biologically meaningful differences in abundance among rare taxa with relatively few reads. That the most abundant taxa showed no difference in abundance among radiation treatments and those that did show significant differences were relatively rare and had no clear pattern of greater susceptibility to radiation stress suggests that, on the whole, litter-associated fungal communities in this system have a high tolerance for radiation stress.

Tillers with their initial fungal communities removed by autoclaving showed strong differences in mass loss rates under the different radiation treatments. These results must be interpreted carefully because, while we removed the endophyte community present at the time of deployment, air-dispersed fungi likely still colonized

them after deployment (Wenndt et al. in press). In addition, autoclaving can alter litter chemistry and physical properties, which can affect subsequent decomposition (Howard and Frankland, 1974; Berns et al., 2008). Since we did not measure the size of the fungal community on these tillers upon collection, we can only say that the size of the microbial communities in the early stages was smaller than on the non-sterile controls (we could not destructively sample these tillers because they are part of another ongoing, long-term study and so were redeployed to the field after being weighed). While this limits our ability to compare between the sterilized and non-sterilized litter, the strong effects of solar radiation (including both visible and UV radiation), even when fungal loads are reduced, lends support for the conclusion that abiotic photodegradation plays an important role early in the litter decay process. Given our finding that the dominant fungi were equally abundant under different radiation levels, and tillers with reduced fungal loads had strong differences among the radiation treatments, we suggest that alteration of fungal communities by solar radiation (and subsequent slowing of mass loss) may be relatively unimportant in hyperarid systems compared to direct photochemical changes to the litter.

While we did not observe large changes in the community of dominant taxa under our treatments, this does not mean they were completely insensitive to solar radiation. Exposure to UV and near-UV radiation can induce significant changes in fungal physiology (Manning and Tiedemann, 1995). For example, many fungi increase

pigment production when exposed to radiation stress (Palacio-Barrera et al., 2019) and several of the most abundant fungi in our study are known to produce dark, melanin-based pigments including *Aureobasidium pullulans complex* (Gostinčar et al., 2014), *Alternaria alternata* (Häggblom and Unestam, 1979), and *Phaeococcomyces* sp. (Butler, 1987). Stress-tolerant fungi tend to grow slower and have lower decomposition rates in the field, because energy that could have otherwise been devoted to growth is spent on stress protection mechanisms (Lustenhouwer et al., 2020). Had the fungi in our study had strong physiological responses to radiation exposure, it would likely have decreased their decomposition ability and may have reduced overall fungal biomass by slowing growth rates (Pieristè et al., 2020), both of which would have slowed decomposition. Instead, we saw the opposite pattern. That decomposition was greater under high radiation treatments does not preclude the possibility that these physiological stress responses occurred, but it does mean that any inhibitory effects radiation might have had on fungi's decomposition ability were overshadowed by the strong stimulatory effects of increased photodegradation. This is consistent with previous work demonstrating the importance of direct photochemical changes to litter in hyperarid systems (Logan et al. in review).

The proliferation of trait-based approaches in microbial ecology has made it easier to answer questions linking community composition with biogeochemical cycles (Lustenhouwer et al., 2020; Põlme et al., 2021). Since litter-associated fungal

communities in the Namib are small (fewer than 20 dominant taxa) compared to those in mesic soils (Tedersoo et al., 2014; Logan et al., 2021), these systems may be particularly amenable to using culture-based assays of fungal traits to examine community-level responses to environmental stressors (Wenndt in press; Jacobson et al., 2015). Combining these approaches with metabolomics and other trait-based tools to examine how individual taxa respond to radiation stress (as well as correlations with desiccation and thermal stress tolerances) can expand our understanding of how the biotic and abiotic effects of solar radiation interact with one another to drive litter decomposition.

Photodegradation and photoinhibition act in concert to determine the net effect of solar radiation on litter decomposition. Recent modeling efforts have shown that incorporating photodegradation and photoinhibition into the litter decay components of earth system models can improve model performance in drylands (Chen et al., 2016; Adair et al., 2017). We show that in particularly arid systems, the stimulatory effects of photodegradation may be more important than the inhibitory effects of photoinhibition because of fungal decomposers' high tolerance of radiation stress. If indeed fungal communities under extreme aridity are more resilient to radiation stress, as our study suggests, then increasing aridity in some regions as a result of climate change may influence how resilient decomposer communities are to radiation stress and potentially modifying the influence of solar radiation on carbon turnover.

APPENDIX

Table S3.1. Results of PERMANOVA test of differences in fungal community composition (Bray Curtis distance) across UV treatment and days in the field. This table differs from Table 3.4 in that this combines the No Shelter and UVpass controls into one treatment and the UVblock and Shade treatments into another, giving only two treatment levels based on UV radiation exposure. Only samples at 30 months and 36 months had extractable DNA, so Days denotes only the difference between those two time points, not the full length of the experiment. N = 90 samples.

Source	df	SS	F	P
UV level	1	0.164	0.913	0.404
Days	1	0.114	0.637	0.622
UV level*Days	1	0.270	1.15	0.179
Residuals	86	15.4		

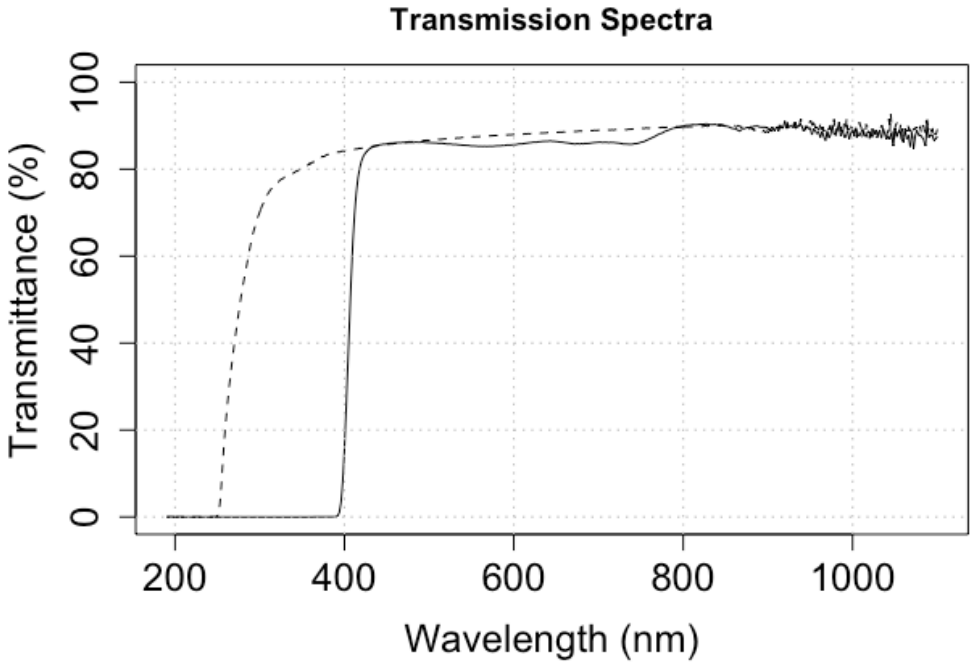

Figure S3.1. UV transmission spectra of UVblock (solid) and UVpass (dashed) filter materials, measured on a UV-2401 PC spectrophotometer (Shimadzu, Kyoto, Japan).

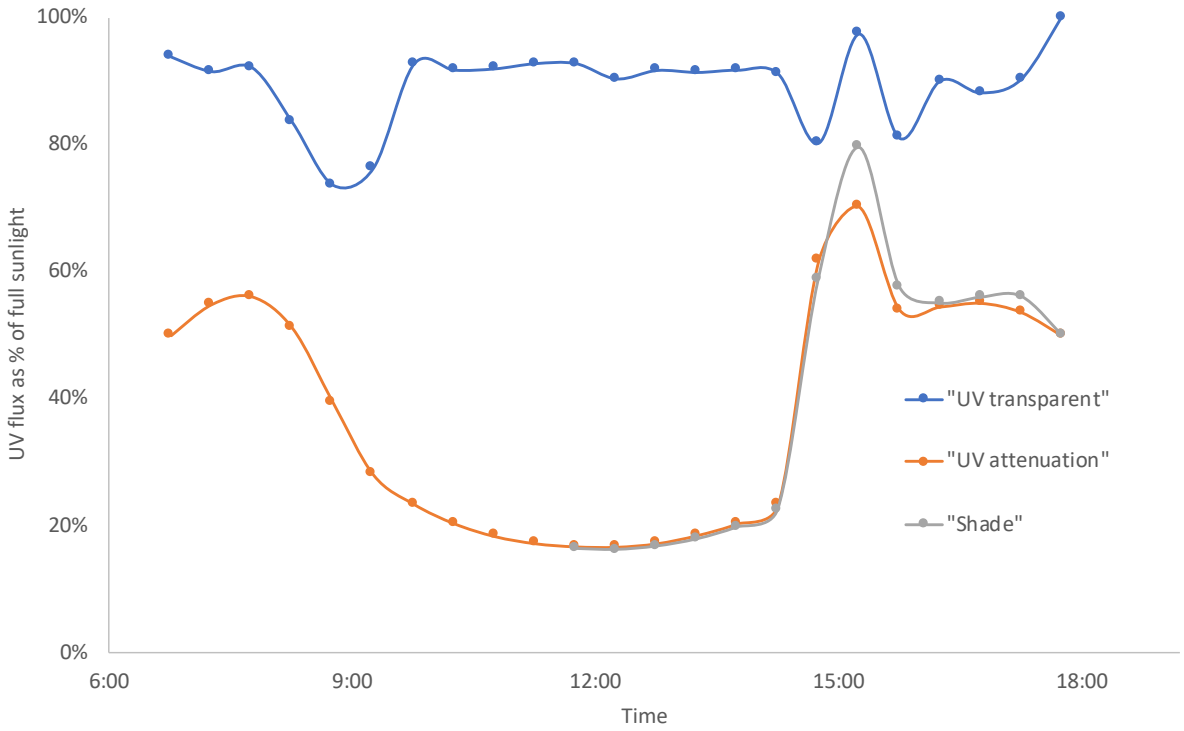

Figure S3.2. Broadband UV-A + UV-B irradiation under each treatment over the course of a day. Values are expressed as percentages relative to unobstructed sun light.

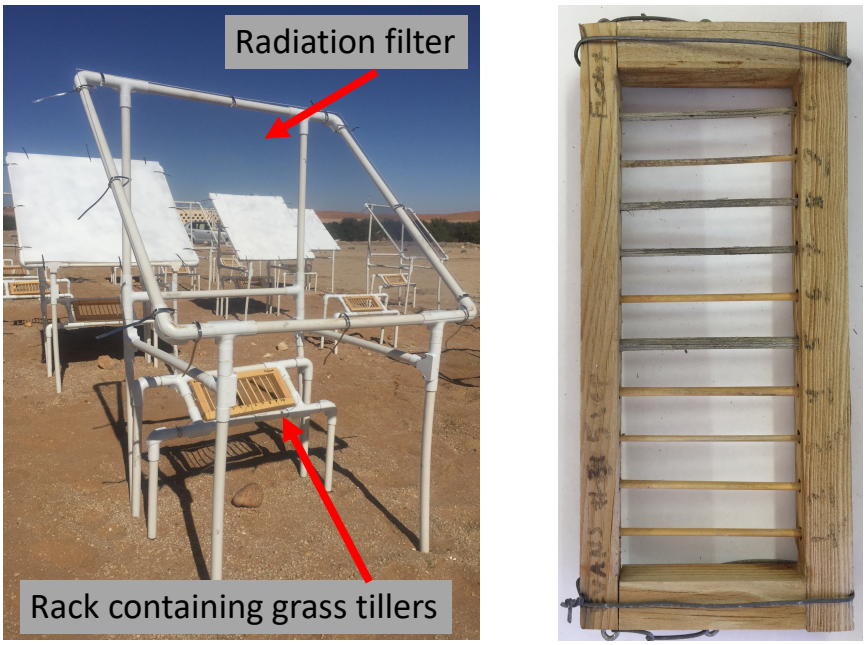

Figure S3.3. (Left) Solar radiation filters with litter rack underneath. (Right) An example litter rack. The "rungs" of the "ladders" are *S. sabulicola* stems ~ 0.5 cm in diameter and 9 cm long.

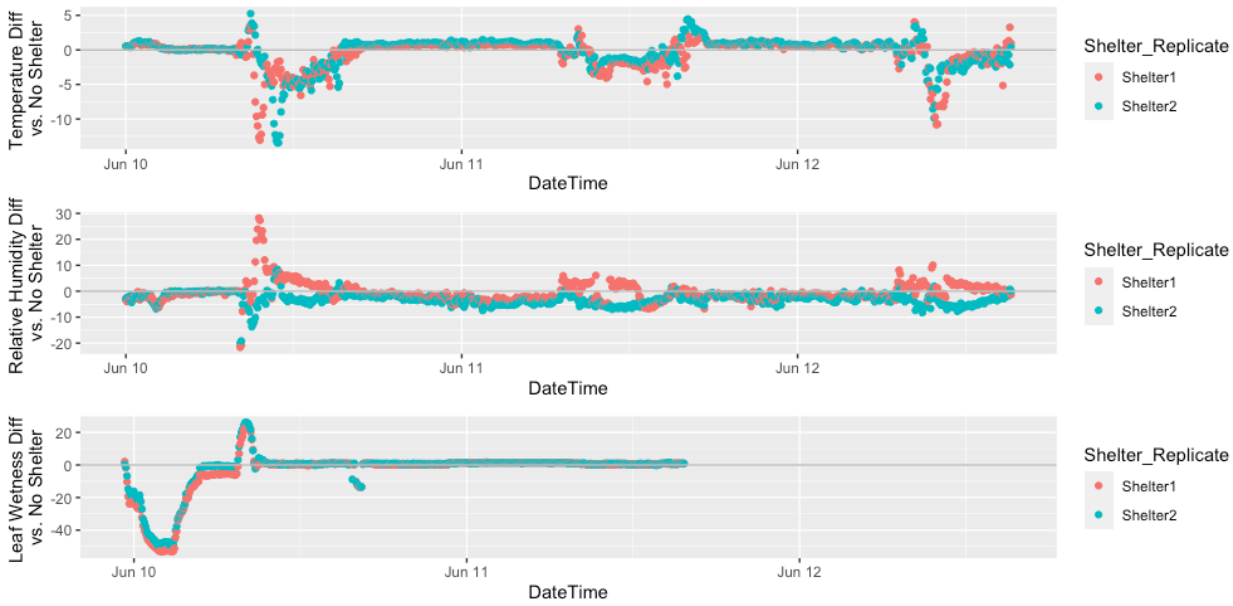

Figure S3.4. Temperature (top), Relative Humidity (middle), and leaf wetness percentage (bottom). For each plot, measurements made under two replicate shelters are plotted relative to the average of two "no shelter" controls at the same time. The plots show a small shelter effect of microclimates on some nights.

CHAPTER FOUR:

ACCOUNTING FOR NON-RAINFALL MOISTURE AND TEMPERATURE IMPROVES LITTER DECAY MODEL PERFORMANCE IN A FOG-DOMINATED DRYLAND SYSTEM

If indeed deserts are 'simple systems' we should now… be able to understand their workings quite well and to apply this understanding in models of predictive value.

Immanuel Noy-Meir (1981)

INTRODUCTION

Drylands play an important part in the global carbon cycle, but we still lack a strong understanding of carbon cycling in these systems. Historically, ecosystem models have underestimated dryland litter decomposition rates (Parton et al., 2007; Adair et al., 2008). This is partly because the models are driven by rainfall, assuming little to no decay between precipitation events. While rainfall pulses play a large role in dryland systems (Noy-Meir, 1973; Seely and Louw, 1980), considering rain alone does not fully capture litter decomposition in these systems. This may be partially because much decomposition occurs at and above the soil surface, and aboveground litter decomposition is less sensitive to large rain pulses than is belowground decay (Jacobson and Jacobson, 1998; Austin, 2011). Abiotic processes including photodegradation, aeolian erosion, and thermal degradation that drive aboveground litter decomposition can degrade litter regardless of moisture conditions (Austin, 2011) and rain events as little as 1 mm can facilitate microbial activity (Collins et al.,

2008). Finally, non-rainfall moisture (fog, dew, and water vapor: NRM) can support substantial biotic decomposition of plant litter, even in the absence of rain (Dirks et al., 2010; Jacobson et al., 2015; Wang et al., 2017a). These findings demonstrate that carbon and nutrient cycling in drylands are not restricted to precipitation pulses and that NRM is an crucial driver of dryland biogeochemical cycles. As our understanding of the importance of NRM in arid and semi-arid ecosystems evolves, we need to update our conceptual and predictive models to incorporate these important drivers of ecosystem processes.

Despite growing recognition of NRM's importance, current litter decay models do not explicitly account for its ability to support decomposition. This is partly because field-based studies of NRM-driven decomposition are scarce and so far, have mostly focused on documenting single cases and understanding mechanisms. Recent studies have shown that the rate of NRM-driven decomposition depends on many factors including the frequency of humid conditions (Evans et al., 2020), the composition of decomposer communities (Logan et al., 2021), and interactions with other processes like photodegradation (Logan et al. in review; Wang et al., 2015; Gliksman et al., 2017). These insights have been very helpful in demonstrating that NRM-driven decomposition occurs and identifying its various mechanisms. However, before we can incorporate NRM into mechanistic earth system models we need multi-year studies that quantify the relationship between NRM and mass loss across a range

of environmental conditions (Bonan et al., 2013), something that has not been done to date.

One recent attempt to model NRM-driven decomposition has shed light on this challenge. Evans et al. (2020) developed a model that treated decomposition as a pulse process that could be triggered by either rain or NRM when conditions met a given criterion (i.e., when relative humidity was above a given threshold or when dew was present as determined by a leaf wetness sensor). They found that accounting for NRM produced mass loss estimates that were considerably higher than those from a rain-only model and that these new estimates were within the range observed in the field. This approach showed that NRM can improve mass loss estimates, but it included several simplifying assumptions that need to be tested before NRM can be incorporated into models more generally. First, they modeled annual mass loss by measuring instantaneous respiration rates and scaling them up to annual timescales. This showed that the NRM-driven biotic activity on the scale of individual events can be used to estimate long-term mass loss rates over several months, albeit with wide error estimates. A better approach would be to validate model predictions by formally integrating rates of mass loss at multiple sites and in multi-year field studies (Bonan et al., 2013). Studies where meteorology and decomposition are both measured and quantifiably linked to one another are currently lacking.

Second, their model treated decomposition as essentially a pulse process that could be triggered by either rainfall or NRM, but responded similarly to both (in other words, as long as the threshold condition was met, decomposition was considered to be "on"). While rainfall and NRM may induce similar decomposition rates for a similar moisture level, this approach does not allow the possibility of continuous responses. For example, litter moisture content varies with relative humidity (Tschinkel, 1973; Dirks et al., 2010) so a sensitivity function that allows instantaneous decay rates to vary depending on the magnitude of the NRM event may be more appropriate than a simple threshold trigger. Finally, their model did not include temperature dependence, despite decomposition being highly sensitive to temperature in almost all terrestrial systems (Sierra, 2012; Sierra et al., 2015). Relative humidity is closely linked to air temperature, and average temperature during NRM events is often considerably lower than during rain events (Logan et al., 2021). Developing more powerful NRM-driven litter decay models may therefore require incorporating continuous moisture responses and temperature sensitivities to accurately capture decomposition dynamics, though to date these remain untested.

We set out to determine whether incorporating NRM into a simple litter decay model improved model performance in an NRM-dominated system. We tested multiple potential relationships between meteorological variables and litter decay rates

in an attempt to parameterize a model of NRM-driven decomposition. We had two main objectives:

1. Use a novel dataset to evaluate multiple methods of modeling litter decomposition as a function of NRM.
2. Determine how important temperature sensitivity is in NRM-driven litter decomposition models.

We drew upon literature on soil organic matter decomposition and rainfall-driven litter decomposition to identify potential moisture and temperature sensitivity functions (Sierra et al., 2015). To evaluate models, we conducted a 30-month, multi-site litter decomposition study that spanned a ten-fold magnitude of NRM frequency. By placing litter across this gradient and making continuous meteorological measurements alongside mass loss, we were able to quantify the relationship between NRM and litter decay on a multi-year timescale for the first time. Finally, we used a Bayesian model-data integration approach to parameterize mass loss models using several temperature and moisture sensitivity functions and used model selection criteria to identify the best models.

METHODS

Empirical Measurements

We conducted our study in the central Namib Desert in western Namibia. The Namib Desert is a coastal fog desert, with a steep NRM gradient across a narrow geographic range (Eckardt et al., 2013). Rain is scarce in the Namib and NRM is expected to be responsible for the vast majority of litter decomposition (Evans et al., 2020). We leveraged the FogNet weather array, a network of meteorological stations throughout the central Namib Desert that is part of the Southern African Science Service Centre for Climate Change and Adaptive Land Management (SASSCAL; www.sasscalweathernet.org) and maintained by the Gobabeb Namib Research Institute (www.gobabeb.org) (Figure S4.1). Each station measures air temperature, relative humidity, wind speed and direction, soil temperature, leaf wetness state, rainfall, and fog precipitation on a Juvik fog screen. The sites are all located within 70 km of one another but span an order of magnitude in NRM frequency: wet conditions (fog or dew) occurs for 3.1% of the year (quantified by hours wet) at the driest site and 25.3% at the wettest, but a full characterization of meteorology across these sites was part of this study. Weather data were recorded once per minute and converted to hourly averages for analysis.

At six sites, we deployed senesced tillers of *Stipagrostis sabulicola* to monitor mass loss. *S. sabulicola* is the dominant grass in the Namib Sand Sea with globally distributed

congenerics (Roth-Nebelsick et al., 2012). Since litter-associated fungal communities can respond differently to NRM based on their history of exposure to different moisture regimes (Logan et al., 2021), we collected all tillers from the same site (Gobabeb) so the initial fungal community would be the same. To avoid potential microclimate effects of traditional litter bags (Xie, 2020), we measured mass loss by placing tillers in litter racks, custom-made wooden frames designed to hold grass tillers while keeping them completely exposed to ambient solar radiation and moisture conditions (Figure S4.2). Every six months for 30 months, we collected a subset of ten tillers at each site and weighed them. Tillers were destructively harvested at each time point, so in our final dataset, each tiller was weighed prior to deployment and once again when it was collected.

To assess the effects of NRM on litter decomposition throughout the decay process, we deployed litter at two stages of decay. Categories were based on previous observations of *S. sabulicola* decay *in situ* in the Namib (Logan et al., 2021). Early-stage tillers were tillers that had senesced in the preceding two months, had no visible fungal growth, and had visibly intact cuticles (Figure S4.2). Late-stage tillers were harvested from upright plants that have likely been standing for at least one year post-senescence and were characterized by coverings of light and dark-pigmented fungi and a cracked cuticle that was considerably more permeable to water. Previous work found similar measures of gross litter quality (including C:N ratios, total lignin, and lignin:N

content) between litter at these two stages, and found that the primary difference between the two is the level of fungal colonization and state of cuticle degradation, with late-stage tillers harboring much larger fungal communities (Logan et al., 2021). Since we only collected standing grass litter that had not fallen over yet, our terminology of "early" and "late" does not reflect the entire decomposition process but is meant to highlight relative successional differences between the litter stages based on time since senescence and saprophytic community size.

Model Description

To model the effect of NRM on litter decomposition, we began by modeling decay rates using a simple exponential model of the form:

$$M(t) = M_0\, e^{-k_{eff}\, t} \quad \text{(Equation 4.1)}$$

Where $M(t)$ is mass at time t, M_0 is initial mass, and k_{eff} is the effective litter decay constant. This approach captures typical litter decay dynamics, with a rapid initial decay phase followed by slower mass loss over time. We determined an effective decay rate for each site and litter stage, plotting this as a function of the total NRM time and accumulated rainfall at that site.

This approach, whereby we fit a separate effective decay rate for sites with different climates, is a common approach to describe how litter decomposition varies under different climatic conditions (Zhang et al., 2008). However, because it treats

mass loss as solely dependent on the decay rate and time, this approach achieves no generality about the underlying relationship between decomposer activity and climate or litter characteristics. Instead, each estimated effective decay rate is only valid under the specific set of environmental conditions from which it was derived. Thus, while this approach allows one to compare decay rates among sites with different climates, it does not permit testing of specific hypotheses about the nature of the climate-decay rate relationship, independent of sites. To allow better comparability to other studies, we first used this approach to estimate site-specific effective decay rates. We then added moisture and temperature dependence as described below to determine how this improved model performance.

We incorporated NRM and temperature dependence by allowing them to modify an intrinsic litter decay (k_{int}) term, which represents the rate of litter decay under ideal, non-limiting conditions according to:

$$\frac{dM(t)}{dt} = -k_{int}\, g(t)\, h(t)\, M(t) \qquad \text{(Equation 4.2)}$$

Or equivalently,

$$M(t) = M_0\, e^{-k_{int}\, t\, g(t)\, h(t)} \qquad \text{(Equation 4.3)}$$

Where h(t) and g(t) are sensitivity functions for NRM and temperature respectively. Unlike the simple model described by Equation 4.1, in this model, the litter decay rate (k_{int}) is the maximum rate under ideal temperature and moisture conditions, which is then modified downward by the sensitivity functions (with the exception of Q_{10}

temperature sensitivity function that allows increasing decomposition above a reference temperature). This allowed us to test specific hypothesized relationships between moisture and litter decay rates, both within and between sites depending on how we choose to fit the parameters (i.e. separate fits for each site or global parameter estimates). Using a one-pool model allowed us to simplify the intrinsic decay component of the model and focus on the effect of different temperature and moisture sensitivities. We discretized the model using hourly meteorological data, calculating the instantaneous rate of mass loss for each hour as:

$$\frac{M_{n+1}}{M_n} = 1 - \Delta t_n \, k_{int} \, g(t_n) \, h(t_n) \qquad \text{(Equation 4.4)}$$

Operationally, mass loss was calculated as the cumulative product of the instantaneous decay rate at each hour.

Sensitivity functions

Since litter decomposition can occur in response to both liquid water in the form of dew and fog (Jacobson et al., 2015) or from water vapor under humid conditions even in the absence of liquid water (Dirks et al., 2010), we tested separate sensitivity functions based on either relative humidity levels, or based on a measurement of the presence of liquid water. Sensitivity functions are presented in Table 4.1 and shown in Figure 4.1. The threshold model is binary, allowing decomposition to happen at the intrinsic litter decay rate if and only if relative humidity is above a specified threshold

(R_T). This simple approach has yielded mass loss estimates similar to those measured in the field previously (Evans et al., 2020). To account for possible saturation at high relative humidities, we also evaluated a logistic sensitivity model that allows the rate of decomposition potential to slow as relative humidity nears 100%. The exponential moisture model allows decomposition rates to increase exponentially with relative humidity, reflecting the relationship between litter moisture content and relative humidity that is often seen in both controlled (Tschinkel, 1973) and field conditions (Dirks et al., 2010). Each sensitivity function was normalized to 1 when relative humidity was 100%. Finally, we tested a fourth function based on the presence or absence of liquid water as measured by a leaf wetness sensor during which decomposition occurred at the intrinsic decay rate when conditions were wet and not at all when conditions were dry. Previous work showed that relative humidity can accurately predict leaf wetness state (Sentelhas et al., 2008; Evans et al., 2020), so we expected this model to perform similarly to the threshold model.

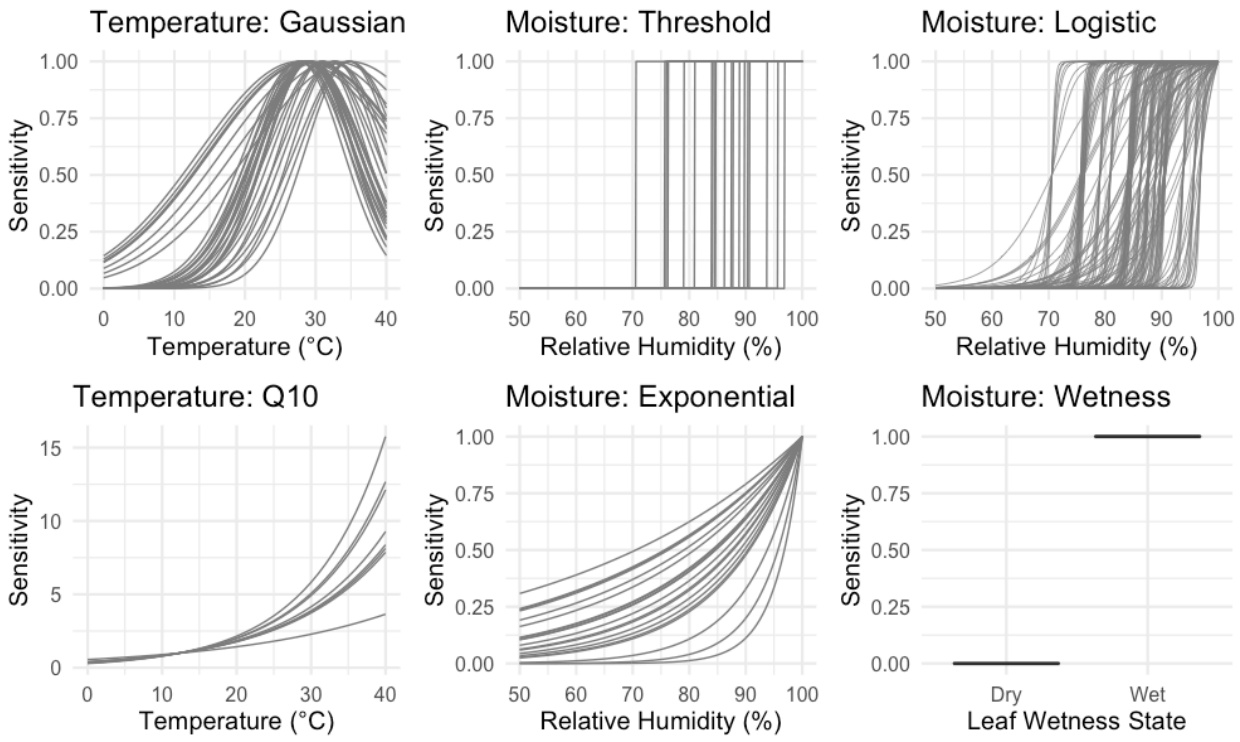

Figure 4.1. Temperature and NRM sensitivity functions included in the models. Each curve shows one parameter combination chosen by randomly sampling around a specified set of priors as identified in Table 4.2. The wetness moisture function has no parameter and is simply the proportion of time during each hour that the leaf wetness sensor detected the presence of liquid water.

Table 4.1. Moisture and temperature sensitivity functions. The first three moisture functions are based on relative humidity and the fourth is based on leaf wetness state. Moisture functions are normalized to 1 at 100% relative humidity and temperature sensitivity functions are normalized to 1 at T_{ref} and T_{opt}.

Class	Name	Model	Parameters
Moisture	Threshold	$h(RH) = if(RH > R_T)$	R_T = relative humidity threshold
Moisture	Exponential	$h(RH) = 2^{\frac{100-RH}{R_{0.5}-100}}$	$R_{0.5}$ = RH value at half saturation point
Moisture	Logistic	$h(RH) = \frac{1 + e^{r\,(R_{0.5}-100)}}{1 + e^{r\,(R_{0.5}-RH)}}$	r = logistic growth rate $R_{0.5}$ = RH value at half saturation point
Moisture	Wetness	$h(LWS) = LeafWetnessState$	None
Temp.	Q_{10} Model	$g(T) = Q_{10}^{(T-T_{ref})/10}$	Q_{10} = Q_{10} coefficient T_{ref} = Reference temperature
Temp.	Gaussian	$g(T) = e^{-0.5\left(\frac{T-T_{opt}}{stDev}\right)^2}$	stDev = standard deviation T_{opt} = Optimal temperature

To model temperature dependence, we tested two common temperature sensitivity functions: a Q_{10} model and a Gaussian distribution. Q_{10} sensitivity is a monotonically increasing function that is used to model many biological process including litter decomposition (Sierra et al., 2015). Each increase of 10°C above a reference temperature (T_{ref}, often the site's mean temperature), results in an acceleration of the process in question by given amount, called the Q_{10} coefficient. To account for possible negative temperature dependence above an optimum temperature (T_{opt}), we also tested a Gaussian temperature sensitivity function. A Gaussian function is often particularly well suited for describing aggregated responses of entire communities (Low-Décarie et al., 2017), as is the case for the fungal communities on

our tillers (Logan et al., 2021). Temperature sensitivity was normalized to 1 at T_{opt} in the Gaussian model and T_{ref} in the Q_{10} model. We tested each combination of moisture and temperature functions (as well as moisture-only and temperature-only versions) for a total of 15 different litter decay models.

To understand the nature of the different models and compare them across a range of conditions, we performed two model runs. First, we explored a large parameter space to determine how parameters interact with one another across a wide range of hypothetical conditions. This included parameter values outside of realistic ranges (for example, relative humidity thresholds from 5-99% and an intrinsic litter turnover time from 0.1-100 years). This allowed us to see how parameters interacted with each other within the different models and explore general properties of each model. Next, to assess which models performed best under realistic conditions, we constrained the parameter space to more accurately reflect real world parameter values. For this model run, we determined optimal values for each parameter based on lab and field incubations and then randomly varied parameter combinations around these values (see below). Parameter definitions as well as constrained values used in the second model run are reported in Table 4.2. Figure 4.1 shows the range of temperature and moisture sensitivities we used in the constrained model run.

Table 4.2. Parameter definitions and values used to constrain the second model run to realistic conditions. Means ± standard deviation are shown. For Q_{10}, T_{opt}, and stDev, models were actually run with two standard deviations (i.e. twice the value shown below).

Parameter	Definition	Model (type)	Value	Justification
Log_{10} Turnover Time (1/k)	Intrinsic turnover time (i.e. turnover time under ideal temp & moisture conditions)	All	1 ± 1 year	Estimated from maximum respiration rate from previous studies
T_{ref}	Reference temp for Q_{10} function	Q_{10} (temp)	12.3°C	Mean temp when wet
Q_{10}	Q_{10} sensitivity	Q_{10} (temp)	2.38 ± 0.292 °C	Temperature incubations (Figure 4.2)
T_{opt}	Optimum temperature for Gaussian distribution	Gaussian (temp)	29.7 ± 2.37 °C	Temperature incubations (Figure 4.2)
stDev	SD around T_{opt} for Gaussian distribution	Gaussian (temp)	6.59 ± 3.02°C	Temperature incubations (Figure 4.2)
$R_{0.5}$	RH value where moisture sensitivity is 50% of maximum	Exponential (NRM) Logistic (NRM)	90 ± 10%	Range of humidity conditions during which NRM typically occurs (Evans et al. 2020)
R_T	RH value above which decomp is "on"	Simple threshold (NRM)	90 ± 10%	Range of humidity conditions during which NRM typically occurs (Evans et al. 2020)
r	Rate of logistic growth	Logistic (NRM)	1 ± 1	Smaller values approximated a straight line; higher values resembled the simple threshold model

We used the Akaike information criterion (AIC) to compare the constrained models to one another to determine which was the best fit to the data. AIC is a model selection criterion that rewards goodness of fit based on a log likelihood function while penalizing models with greater parameters to reduce overfitting biases (Aho et al.,

2014). We report AIC values for all combinations of models from the constrained parameter run to compare model performance under realistic scenarios.

Constraining Parameter Space

To constrain temperature parameters, we performed a lab incubation of *S. sabulicola* tillers. We varied the temperature from 10-35°C at 5°C steps, allowing litter to equilibrate for 60 minutes before measuring respiration. We sprayed seven tillers with sterile deionized water until they were saturated to stimulate fungal activity and placed them in 55 ml acrylic tubes connected to a LI-8100A gas analyzer (LI-COR Biosciences, Lincoln, Nebraska, USA), measuring mean flux during 3 minute incubations. To measure the response of the specific fungal communities associated with litter used in the field study, all tillers used in the lab incubation were collected at Gobabeb, the same site where litter in the mass loss experiment was collected.

To calculate Q_{10}, we excluded the measurements at 35°C (when response becomes negative) and then used the 'Q10' function in the *respirometry* package in R to calculate a separate Q_{10} value for each tiller (Birk, 2021). For the reference temperature, we used the mean temperature when leaf wetness sensors were "wet" across all sites (12.3°C). This value was fairly constant among sites, varying by less than 0.9°C (Figure S4.3). For the Gaussian moisture sensitivity parameters, we used the 'optim' function in R to find the temperature optimum (T_{opt}) and standard

deviation (stDev) around the optimum after normalizing flux rates to the maximum rate measured for each tiller (R Core Team, 2020).

The turnover time represents the litter's intrinsic decay rate under ideal temperature and moisture conditions and is equivalent to the inverse of k_{int}, the exponential parameter in the decay function. To place a lower boundary on this value, we examined previous studies that measured respiration from *Stipagrostis sabulicola* under wet conditions and extrapolated to estimate a minimum turnover time (in years) under ideal, non-limiting conditions. Jacobson et al. (2015) reported respiration rates from wet *S. sabulicola* tillers as high as 1.5 μg CO_2-C g^{-1} litter hr^{-1}, corresponding to an intrinsic turnover time of ~0.63 years, assuming 50% of plant litter mass is carbon. This is within the range of intrinsic turnover rates reported for other grasses (Zhang et al., 2008). We therefore used a turnover time with a mean of 1 year around a log-normal distribution.

We varied the logistic growth parameter (r) of the logistic moisture sensitivity function from around 1, because at much lower values, it began to resemble a straight line and at higher values, it converged on the simple threshold model. Since we were interested primarily in how to model NRM's effect on litter decomposition, and since we had constrained temperature parameters based on our litter incubation experiment, we plotted parameter space combinations for moisture variables, averaged across the range of temperature parameters.

RESULTS

Meteorological Conditions and Temperature Incubations

Moisture conditions varied substantially among the sites. Hours of wetness during the 30-month study ranged from 284 hours year^{-1} (3.1% of total hours) at the driest site (Garnet Koppie) to 2333 hours year^{-1} (25.3% of total hours) at the wettest site (Kleinberg). Drier sites tended to be warmer, though mean temperature spanned a range of only 0.9°C among the sites (Table 4.3). Temperatures during NRM events were lower and less variable than temperatures during dry periods (Table 4.3). Wet conditions almost never occurred when temperature were above 20°C at any site (Figure S4.3). Average relative humidity differed among the sites and was correlated with hours of wetness. Rainfall occurred at all sites during the study period, ranging from 26.4–64.2 mm, but did not correlate with NRM frequency. The optimum temperature for respiration in the incubations was 30°C, showing a peak at 30°C with flux rate dropping at 35°C (Figure 4.2).

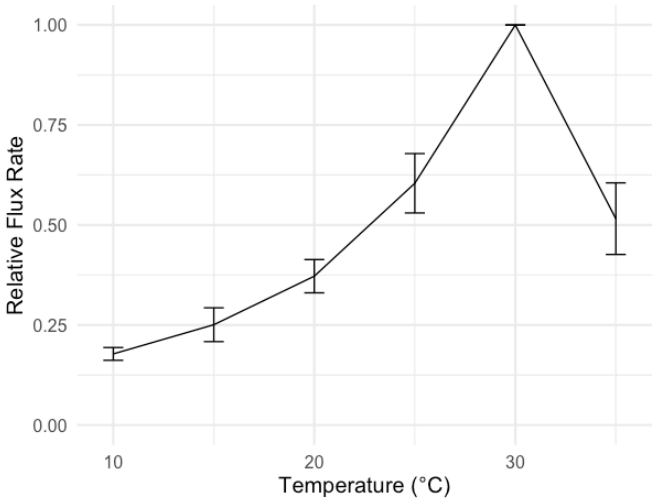

Figure 4.2. Temperature sensitivity of respiration from *S. sabulicola* tillers in a lab incubation, used to constrain temperature parameters (mean ± 1 S.E.M., n = 8). Flux rate is normalized to the rate at 30°C. Tillers were sprayed with deionized water until saturated and respiration was measured at 5°C intervals.

Table 4.3. Summary of meteorological conditions at each site during the study showing mean temperature when wet, mean temperature when dry, the proportion of total time when conditions were wet (as determined by a leaf wetness sensor), accumulated rainfall during the study period, and mean relative humidity throughout the year. Temperature ranges in parentheses report the middle 95% of data.

Site	$Temp_{dry}$ (°C)	$Temp_{wet}$ (°C)	Wet Hours	Prop. Time Wet	Rain (mm)	Mean Rel. Humidity (%)
GK	22.4 (12.67 - 32.34)	12.2 (6.88 - 19.17)	284	0.03	61.8	37.5
GB	22.2 (11.35 - 33.42)	12.4 (6.24 - 17.91)	666	0.07	64.2	44.8
S8	21.4 (10.92 - 32.49)	11.7 (5.66 - 17.4)	788	0.09	26.4	46.9
VF	21.7 (11.75 - 32.37)	12 (6.34 - 16.38)	920	0.10	33.7	50.2
MK	22 (12.73 - 32.09)	12.6 (8.00 - 16.59)	1456	0.13	44.5	53.6
KB	20.1 (11.01 - 30.91)	12.4 (6.69 - 17.07)	2333	0.25	56.6	67.7

Litter Mass Loss

In general, mass loss was greater at sites with more NRM and lower at sites with less NRM (Figure 4.3). There was a significant three-way interaction between

litter stage, site, and time (Table S4.1). Within each site, early-stage and late-stage litter decomposed at comparable rates for the first 18 months, but diverged after that depending on the site. After 24 months at the two driest sites, early-stage litter lost more mass than did late-stage litter. At the four wettest sites however, late-stage litter experienced the greater mass loss (Figure 4.3).

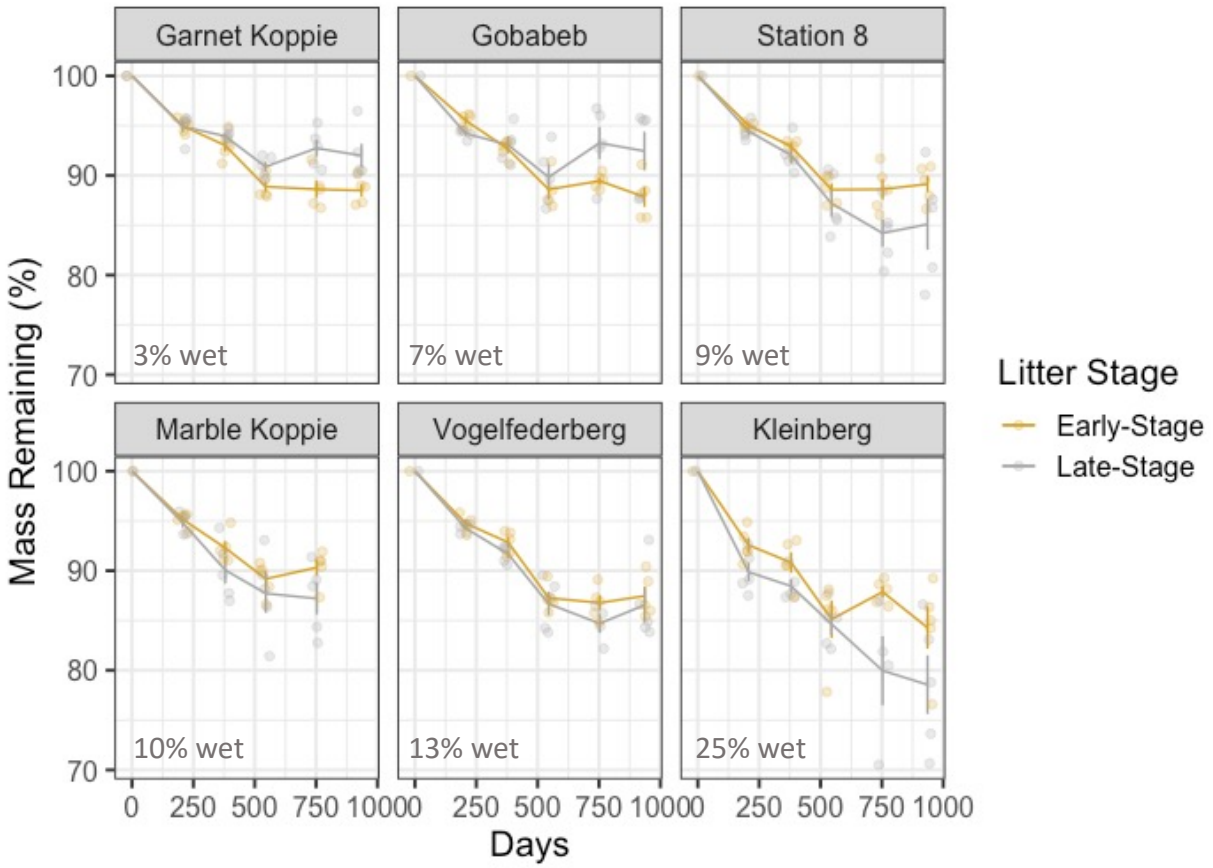

Figure 4.3. Mass loss for early-stage (yellow) and late-stage (grey) tillers at each site (mean ± 1 S.E.M.). Percentage values in the bottom of each panel show the average proportion of time throughout the year that the site has liquid water condensation, as determined by a leaf wetness sensor. Apparent increases in mass therefore reflect variation among the tillers, not actual increases in tiller mass, since a subset of tillers was destructively harvested at each collection time.

When we used a simple exponential decay model without temperature and moisture sensitivity (Equation 4.1), the effective decay rate at each site was correlated with NRM duration but not accumulated rainfall (Figure 4.4). Late-stage litter (i.e., tillers with more well-established fungal communities) responded more strongly to NRM than did early-stage litter; for every additional 1000 hours of wetness at a site, effective decay rate increased 0.0043 for early-stage litter and 0.014 for late-stage litter (Figure 4.4).

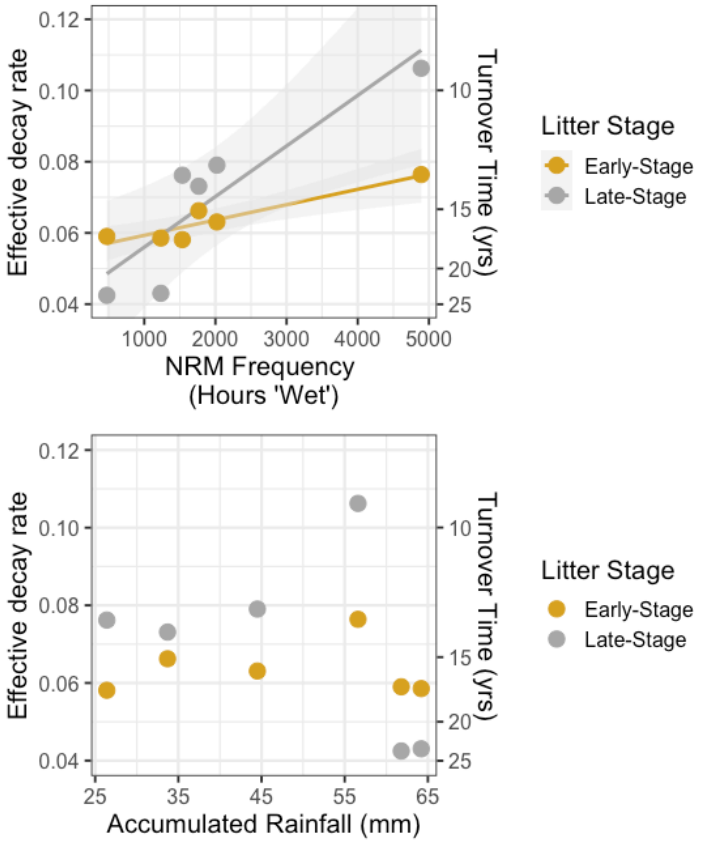

Figure 4.4. Effective decay rate calculated without temperature or NRM sensitivity (Equation 4.1) relative to NRM frequency and accumulated rainfall during the study period. Among sites, decay rate constant was strongly correlated with the proportion of time that a site experienced NRM conditions (Early-Stage: $R^2 = 0.87$, $P = 0.007$,

Figure 4.4 (cont'd). slope = $4.311*10^{-6}$; Late-Stage: $R^2 = 0.80$, P = 0.02, slope = $1.421*10^{-5}$) but was uncorrelated with total rainfall (Early-Stage: $R^2 = 0.01$, P = 0.87; Late-Stage: $R^2 = 0.14$, P = 0.46).

Model Parameter Space Exploration

For the three NRM sensitivity functions based on relative humidity, parameter values showed a tradeoff between turnover time and RH thresholds (Figure 4.5). Parameter combinations with the lowest AIC scores featured either slow turnover times and a low RH threshold (bottom right of plots) or faster turnover times and high RH thresholds (upper middle of plots). When we fit parameters separately for each site instead of globally, AIC values improved, but the actual values of the best parameter combinations did not change (Figure S4.4). Similarly, fitting parameters separately to early- and late-stage tillers did not produce different optimal parameters (Figure S4.5).

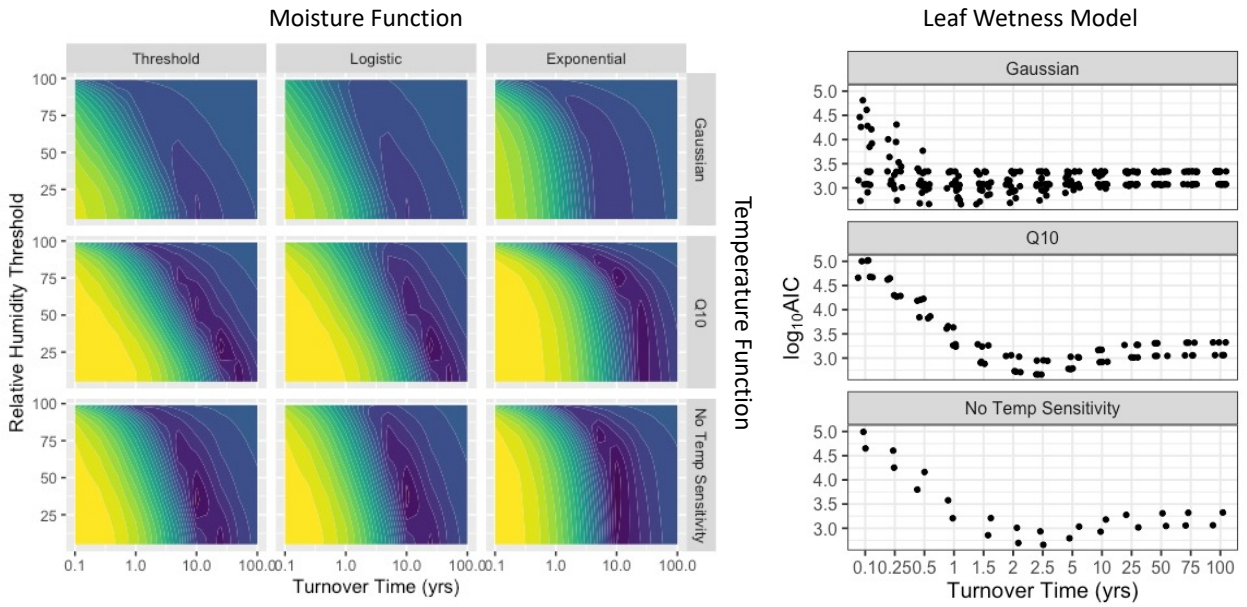

Figure 4.5. Parameter fits for the first model run showing parameter combinations across a wide range of hypothetical conditions. (Left) The three humidity-based NRM functions showing the relationship between turnover time ($1/k_{int}$) and relative humidity threshold (R_T or $R_{0.5}$). Colors represent $\log_{10}$AIC scores with purple denoting lower values and yellow denoting higher values. (Right) Parameter estimation for the leaf wetness-based moisture function showing $\log_{10}$AIC as a function of turnover time ($1/k_{int}$). Plots have different numbers of points because of different numbers of temperature parameters that were tested (the Gaussian temperature function has two, the Q_{10} function has one, and the bottom plot has no temperature parameters).

Models that included Q_{10} temperature sensitivity converged on slower intrinsic decay rates (i.e., longer turnover times) than did those using a Gaussian temperature sensitivity or temperature-independent models (Figure 4.5). The wetness sensitivity function yielded an optimal litter turnover time of 2.5 years under a moisture-only and Q_{10} temperature sensitivity model (Figure 4.5). Using a Gaussian temperature sensitivity yielded a faster intrinsic decay with an optimal turnover time from 0.5-1.5 years.

Model Performance Comparison

Models that included NRM sensitivity had better fits than did the simple litter decay model, but the best models included both NRM and temperature sensitivity (Figure 4.6). While model fit improved (AIC scores were lower) whenever NRM sensitivity was included, the degree to which NRM sensitivity improved fits depended on which temperature sensitivity function was included in the model. In particular, models with Gaussian temperature sensitivity performed better than did those with Q_{10} sensitivity or no temperature sensitivity. Surprisingly, after controlling for temperature response, each of the four moisture functions had similar AIC scores, with no single moisture model performing noticeably better than the others (Figure 4.6).

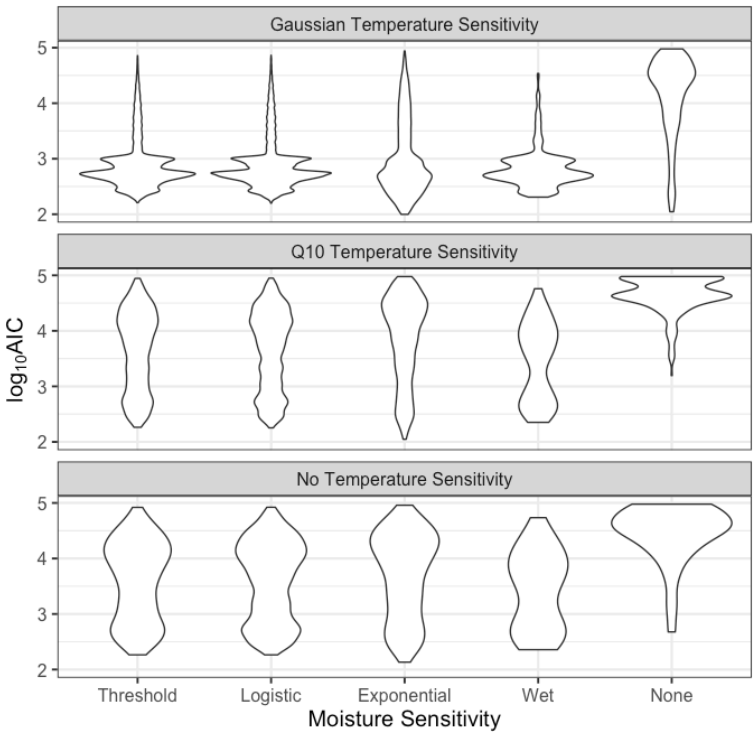

Figure 4.6. Model performance (log_{10}AIC scores) for each model combination of temperature and moisture sensitivities. Each observation represents one parameter combination after constraining them as described in Table 4.2. Lower scores denote better fits. This only shows models constrained using realistic parameter estimates.

Including temperature sensitivity alone (without NRM) did not improve model fit as well as modeling only NRM sensitivity (without temperature). All of the NRM-only models (Figure 4.6, bottom row) had better fits than did temperature-only models (Figure 4.6, right column), though each showed a wide range depending on the specific parameter combinations. In fact, an unconstrained model with Q_{10} temperature sensitivity but no moisture sensitivity converged on an optimal Q_{10} value <1, indicating a negative temperature dependence of litter decomposition (Figure S4.6), the opposite of what we observed in the temperature incubations.

When we compared one of the best models with temperature and NRM sensitivity (a Gaussian temperature function and an exponential moisture function) to a simple decay model that had no temperature or NRM sensitivity but varied effective decay rate among sites (Equation 4.1), we found that the temperature and NRM model performed better (Figure 4.7). The Gaussian-exponential model had lower AIC scores and the slope of the observed vs. predicted values was closer to 1, yielding more realistic mass loss predictions (0.85 for Gaussian-exponential model, 0.71 for simple decay model).

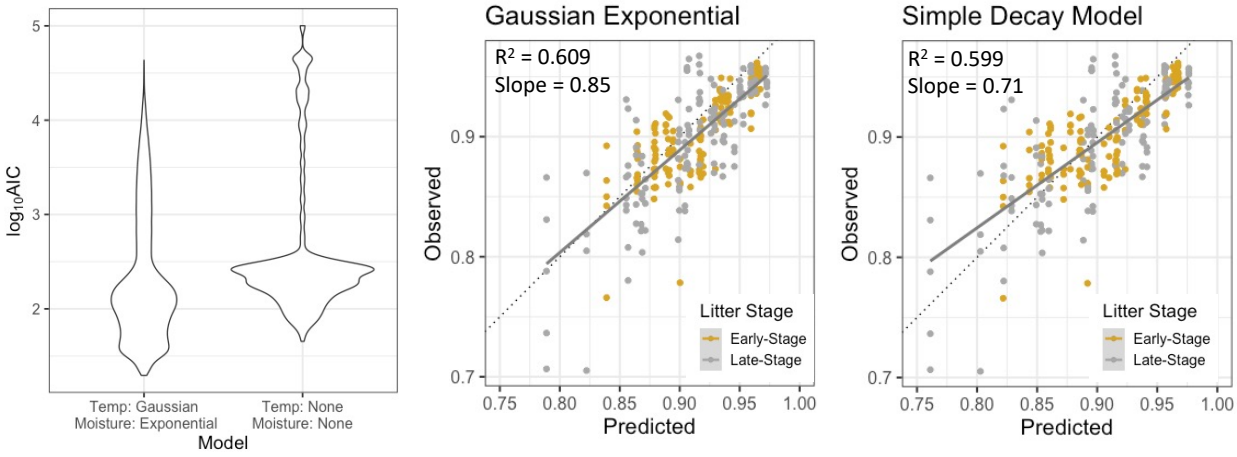

Figure 4.7. (Left panel) Fit of the model based on Gaussian temperature sensitivity and exponential moisture sensitivity versus a simple exponential decay model (without temperature or NRM sensitivity) in which K_{eff} is allowed to vary independently for each site. The simple decay model depicted here differs from the one in Figure 4.6 because this one uses K_{eff} and is not constrained to the same set of parameters from there. (Right two panels) Model predictions for the best version of the Gaussian-Exponential model versus the simple decay model with site-specific K_{eff} values. Solid lines are the best fit lines and dotted lines are the ideal 1:1 line.

DISCUSSION

Decomposition is a crucial component of earth system models and NRM is an important moisture source in arid and mesic grasslands worldwide. In a first attempt at modeling NRM-driven decomposition, Evans et al. (2020) showed that decay rates are faster when NRM is more frequent, but there has yet to be a scalable quantification of the relationship between NRM and litter decay rates across a range of conditions. Doing so is an important step to improving earth system models, which must be validated with field measurements made under realistic conditions (Bonan et al., 2013). Using a 30-month, multi-site experiment, we showed that explicitly accounting for both temperature and NRM sensitivity improved a litter decay model in an NRM-affected system and examined how multiple sensitivity functions performed relative to one another.

While incorporating either NRM sensitivity or temperature dependence improved model performance, it was the inclusion of both that led to the largest improvement. Decomposition's temperature sensitivity often depends on moisture conditions (Petraglia et al., 2019). For example, in soils, temperature typically increases decay rates when moisture is abundant, but higher temperatures can dry out soils, slowing decomposition (Bear et al., 2014). Similarly, in our system, NRM wets litter, but tends to form at cooler temperatures, when decomposition is slower. Once temperatures get high enough (in this case, above 20°C; Figure S4.3), wet conditions

cease, making the positive effects of temperature moot. We find that this nuance about NRM gives rise to unrealistic predictions when models include only one type of sensitivity but not the other. For example, in our unconstrained model run, a model with only temperature dependence, but no NRM sensitivity, converged on a Q_{10} temperature sensitivity <1, indicating negative temperature dependence (Figure S4.6), even though incubation data clearly show a positive relationship across the range of conditions tillers experience in the field (Figure 4.2). This shows that both temperature and NRM sensitivity were needed to realistically capture litter decay dynamics under NRM conditions, lest one mask the effects of the other with unrealistic consequences.

The choice of temperature sensitivity function is often very important in modeling biological processes and can lead to quite different predictions (Low-Décarie et al., 2017). We found that model performance was better using a Gaussian rather than a Q_{10} temperature sensitivity function. Surprisingly, we found that the different NRM sensitivity functions, including both continuous and threshold functions, described litter decay dynamics equally well. While the threshold, logistic, and wetness moisture sensitivity functions share a general form in which decomposition rates increase substantially above a specific relative humidity value, the exponential function simulates gradually increasing decay rates at different relative humidity values. In this sense, the exponential function more accurately mimics the moisture

absorption curves seen in field and lab studies (Tschinkel, 1973; Dirks et al., 2010; Evans et al., 2020). Despite these differences, however, each of these functions had similar fits. This suggests that, while explicitly including sensitivity to NRM is important, the specific manner in which NRM is represented in the model may be less important. This means that NRM-explicit litter decay models in the future may be able to represent NRM with fewer parameters by adopting a simple threshold approach, eliminating the need to parameterize multiple moisture components. Since relative humidity is a standard meteorological measure (unlike leaf wetness), future models should able to use existing data sources to incorporate NRM, eliminating the need to collect additional data with specialized instrumentation.

The humidity threshold at which litter moisture content can support biological decomposition depends on several factors including the permeability of the litter to water, the amount of time it spends in humid conditions, and the decomposer community's sensitivity to moisture (Logan et al., 2021; Tschinkel, 1973). In the absence of rain, litter moisture content rarely reaches biologically significant levels until relative humidity reaches at least 70-80%, often higher (Tschinkel, 1973; Dirks et al., 2010; Evans et al., 2020). That early- and late-stage litter had similar relative humidity thresholds for decomposition is surprising, given their apparent differences in moisture absorption during fog events (Logan et al. in review), and previous

hypotheses that NRM-driven decomposition rates may partially be a function of the material's ability to absorb moisture (Evans et al., 2020).

Despite converging on the same parameter values, model fits were much better for late-stage litter than for early-stage litter (Figure S4.5). This could reflect the fact that the larger fungal communities on late-stage tillers enable them to respond to moisture more strongly than early-stage tillers, which do not have a large enough decomposer community to have a strong biological response to NRM. This is consistent with the results from our simple decay model (without explicit temperature and moisture sensitivity), which showed that effective litter decay rates for late-stage tillers were 3.3 times more sensitive to changes in NRM frequency than were early-stage tillers (Figure 4.4). Since the major differences between the early- and late-stage tillers we used in this study are their degree of prior fungal colonization and their ability to absorb water, this reinforces the importance of fungal communities as mediators of decomposition's response to NRM (Logan et al., 2021) and suggests that plant litter properties related to moisture absorption may influence NRM-sensitivity (Logan et al. in review). Examining whether these properties have the same influence on NRM-driven decay of other plant species may increase the generalizability of the response functions we present here.

Developing models that realistically predict carbon turnover is a multi-step process that requires determining a model structure, parameterizing, and accounting

for external forcings (Luo et al., 2015). Our goal was to compare several potential structures for modeling NRM-driven litter decomposition, but fully incorporating NRM sensitivity into existing earth system models will require additional work. This includes identifying the appropriate temporal resolution at which to model NRM events. The timesteps used by earth system models have shortened considerably over the last two decades, to the point where processes that were once represented monthly are now modeled on hourly timescales or less (Bolker et al., 1998; Bonan et al., 2013; Sokolov et al., 2018). We used hourly averages of minute data to describe decomposition rates, but do not yet know what temporal resolution is necessary to fully capture NRM events. Future studies can compare estimates using minute data (that have the benefit of capturing the wetting and drying dynamics of litter at the start and end of NRM events) to daily timescales, that may estimate NRM-driven decomposition from daily mean relative humidity. In the case of longer (daily) timescales, temperature dependence would likely be best determined using the minimum daily temperature instead of mean temperature, since minimum temperatures are likely to occur at night when NRM is most common. Of course, these methods will require additional testing at multiple sites, but since our models were relatively insensitive to the specific nuances of how NRM was modeled, any of several approaches may be appropriate depending on the structure of the decomposition sub-model in question.

Incorporating NRM into the model structure of existing earth system models may also require integrating relative humidity with the moisture parameters typically included in other decomposition models. Relative humidity *per se* is often represented in the atmospheric component of models, but may not be directly incorporated into carbon sub-models, many of which treat soil water content (which regulates soil decomposition) as related to the ratio of rain to evapotranspiration (Necpálová et al., 2015). If NRM-driven decomposition can be captured by proxies constructed from evaporation, minimum temperature, and other values already included in carbon sub-models, it may be easier to incorporate this novel process into existing modeling approaches than if relative humidity must be explicitly incorporated, as that may require increasing linkages between atmospheric and carbon sub-models. Since relative humidity is an important driver of litter decay in many grasslands (Dirks et al., 2010; Evans et al., 2020) and is changing as a result of climate warming (Byrne and Gorman, 2018) (typically declining), incorporating it into earth system models as an explicit water source may be necessary to accurately predict litter turnover in grasslands, especially in NRM-affected systems. Fortunately, relative humidity is measured at meteorological stations worldwide and extensive data are available. Even in regions with data gaps, methods exist to estimate relative humidity from temperature datasets (Gunawardhana et al., 2017) and these can be incorporated into

earth system models to include NRM sensitivity without the need to collect additional data.

While our study focused exclusively on aboveground litter decay, NRM could affect belowground decomposition processes by decreasing litter inputs into the soil via standing litter decay as well as seeding a large diverse microbial community in the litter phase that could affect soil microbial communities. For example, even though solar radiation does not reach belowground, photodegradation can decrease belowground carbon stores in models, driven in part by increased carbon loss through CO_2 while litter is exposed to solar radiation (Chen et al., 2016). NRM-driven decomposition similarly removes carbon from the system before it reaches the soil surface, potentially decreasing inputs to belowground pools. Additionally, by promoting the development of larger (and specialized) microbial communities early in the decay process (Jacobson et al., 2015; Logan et al., 2021), NRM may accelerate belowground decomposition rates once litter is incorporated into the soil. Such soil-litter mixing can increase litter decomposition in dryland systems (Barnes et al., 2012, 2015; Hewins et al., 2013). Future studies can test the role of NRM-driven decomposition on both aboveground and belowground litter to identify how NRM affects linkages between these two pools.

Since our goal was to present a first attempt at incorporating NRM into litter decay models in an NRM-dominated landscape, we had to make several simplifications

that likely underestimated litter decay rates. First, we only looked at coarse tillers, not leafy material. Evans et al. (2020) showed that gravimetric moisture content of *S. sabulicola* tillers (like those we used) could reach 0.35 g H_2O g litter^{-1} while leafy material could absorb as much as 1.45 g H_2O g litter^{-1} during NRM events, resulting in considerably higher respiration rates for leaves. Similarly, windblown detritus (litter that has become physically disconnected from the plant) makes up a considerable proportion of total litter mass in the Namib (Seely and Louw, 1980) and can absorb substantial water under humid conditions (Tschinkel, 1973). While there have been no direct measurements of respiration from this windblown detritus that we know of, we have no reason to believe that it would not also decompose under NRM conditions. As a result, actual rates of NRM-driven decomposition across the whole ecosystem are likely higher than what we report here.

Secondly, we focused only on the meteorological drivers of litter decomposition, though others factors play important roles as well. Photodegradation (Austin and Vivanco, 2006; King et al., 2012), macrodetritivore activity (Louw and Seely, 1982), and soil-litter mixing (Hewins et al., 2013; Lee et al., 2014) are all important drivers of litter decomposition in drylands. Since our goal was the quantify the relationship between NRM and litter turnover, we focused solely on NRM, but future studies can build on this work by combining our approach with existing models. For instance, photodegradation can interact with NRM to accelerate carbon turnover, especially of

standing litter (Logan et al.; Wang et al., 2017a), and accounting for photodegradation can improve litter decay models (Chen et al., 2016; Adair et al., 2017). Combining these other mechanisms with the relative humidity-based litter decay model we present here may reveal additional interactions that can be validated by field studies. The fact that we were able to describe a large degree of litter decomposition by using a simple relative humidity-based and temperature-based model, however, demonstrates that NRM plays an important role in the litter decay process across a wide range of environmental conditions.

We show that NRM frequency is a major predictor of litter decomposition, and for the first time used data from a multi-site field study to develop temperature and NRM sensitivity functions for a litter decay model, improving predictions of litter decomposition in an NRM-affected system. Temperature and moisture regimes are changing as a result of anthropogenic climate change and our ability to predict how ecosystems respond depends, in part, on how well we can link biogeochemical cycles to their environmental drivers. NRM and rainfall are often controlled by different climatic drivers and may therefore respond differently under future climate change (Forthun et al., 2006; Haensler et al., 2011; Dai, 2013). By modeling the contribution of NRM to decomposition, in addition to that of rainfall, we can better predict how drylands will respond to changing moisture regimes, increasing our ability to manage these globally important systems.

APPENDIX

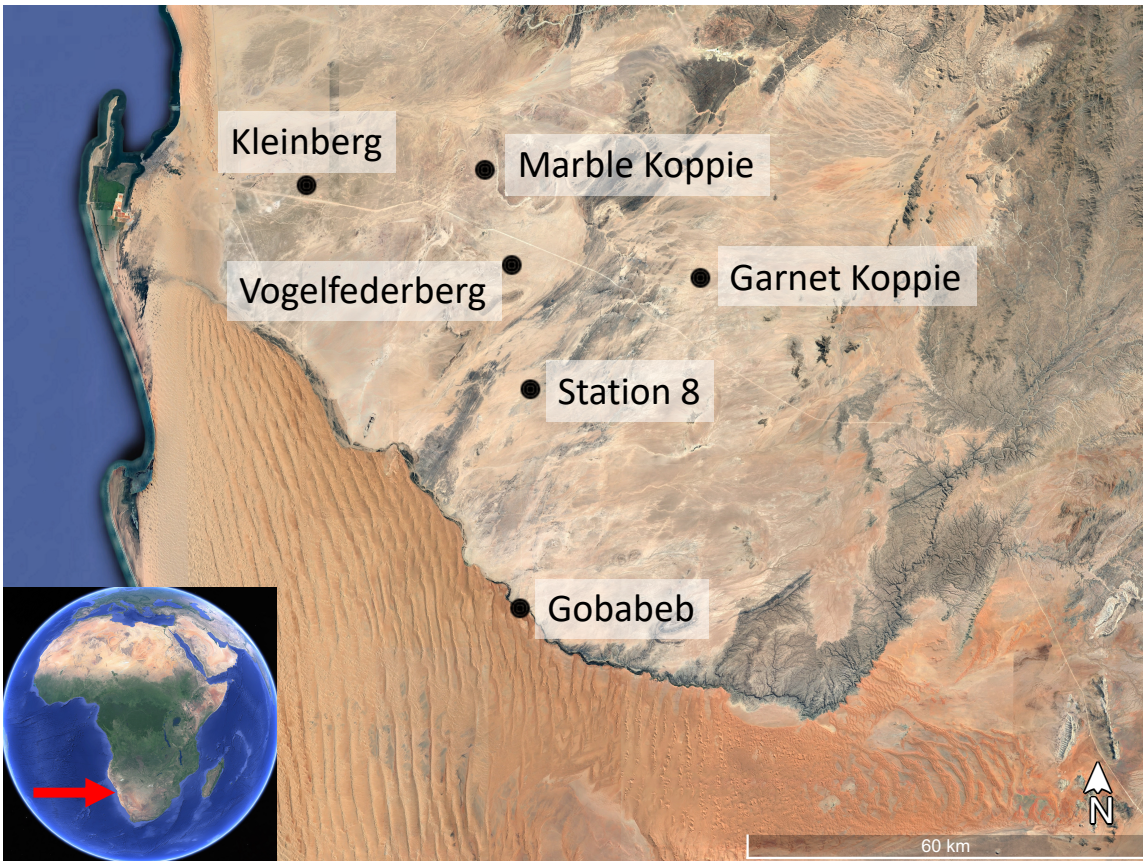

Figure S4.1. Location of the six FogNet sites used in this study. All samples were collected from dunes of the Namib Sand Sea at Gobabeb.

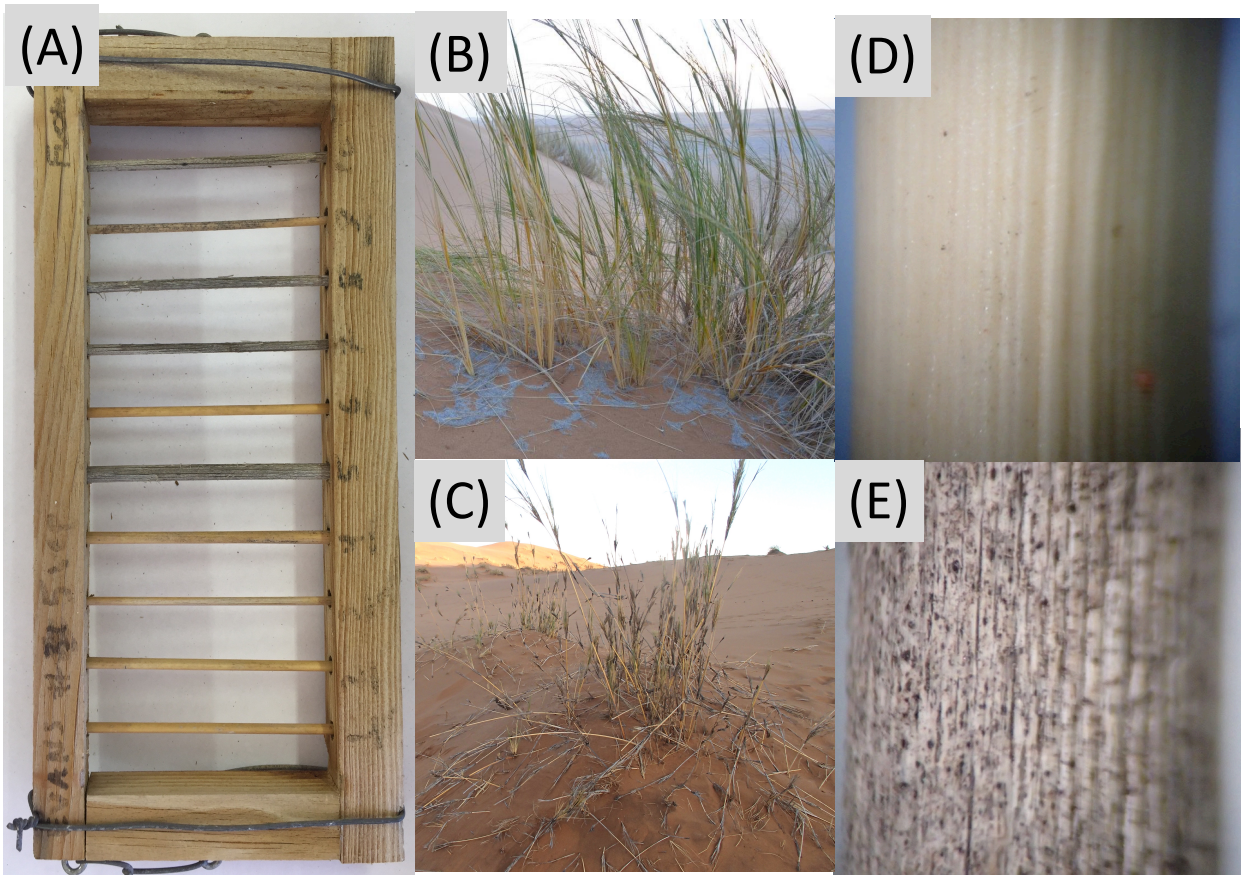

Figure S4.2. (A) Example of a litter rack used instead of litter bag. The "rungs" of the "ladders" are *Stipagrostis sabulicola* stems ~ 0.5 cm in diameter and 9 cm long; (B) Living *S. sabulicola* hummock growing in the dunes; (C) Dead *S. sabulicola* tillers like those used in this study; (D) Close up image of a recently senesced (early-stage) tiller with inact cuticles and little fungal growth; (E) Close up image of a late-stage tiller with cracked cuticle surface and substantial colonization by dark pigmented fungi.

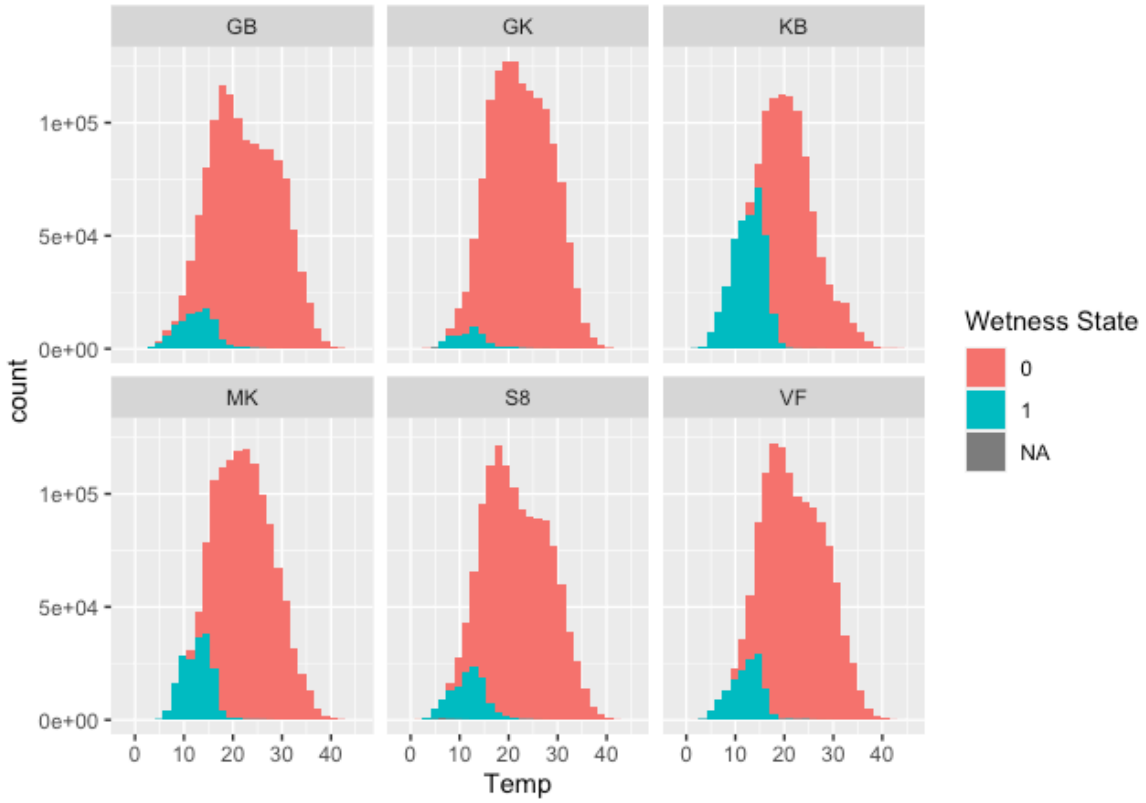

Figure S4.3. Frequency distributions of temperature when wet (blue) and dry (red) at the six sites during the study.

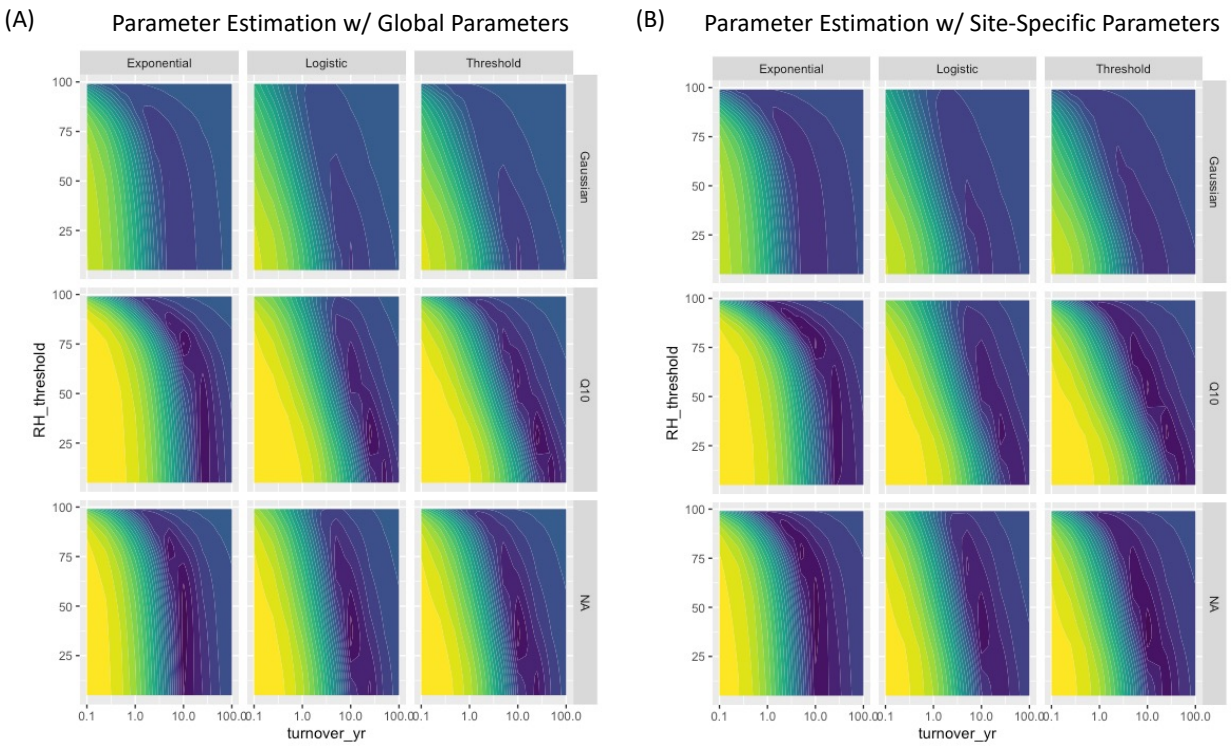

Figure S4.4. Parameter fits for the humidity-based moisture models using (A) global parameters that were fitted across sites, and (B) site-specific parameters. Colors represent AIC scores with purple denoting lower values and yellow denoting higher values. The left panel is identical to Figure 4.3 in the main text.

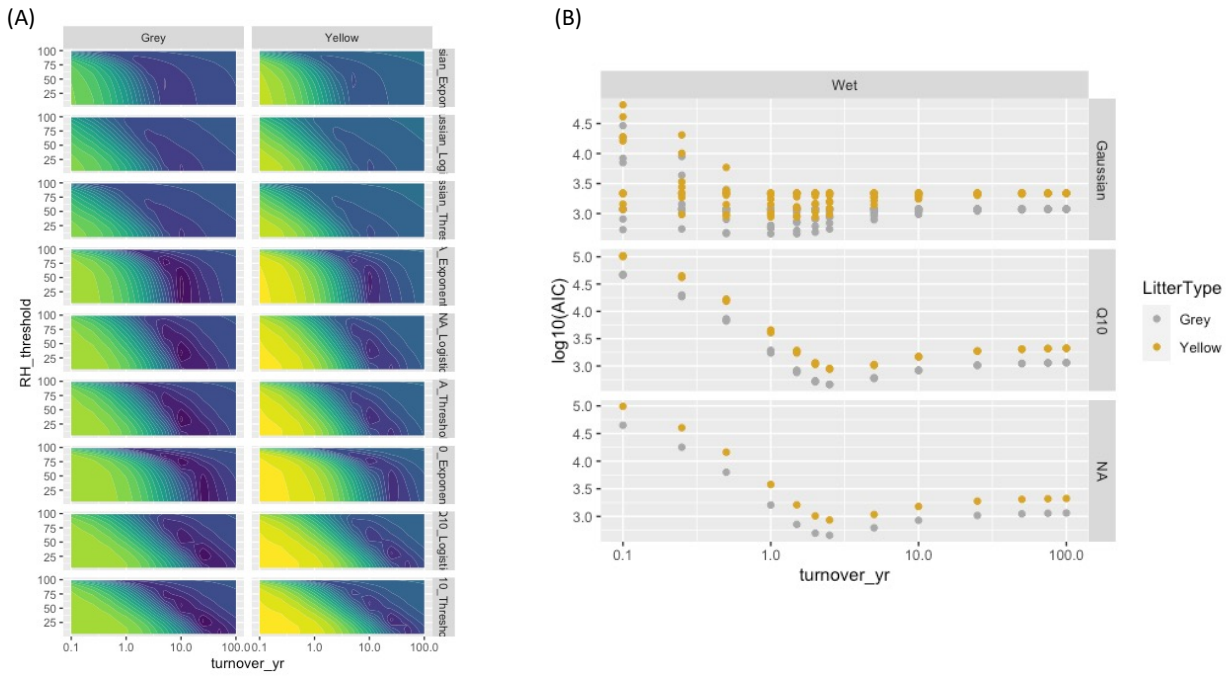

Figure S4.5. (A) Parameter fits for the humidity-based models for (left) late-stage litter and (right) early-stage litter. Colors represent AIC scores with purple denoting lower values and yellow denoting higher values. (B) Model fits for the wetness-based models, color-coded by litter stage (this is identical to the right panel of Figure 4.5, but color coded to show differences in litter stage).

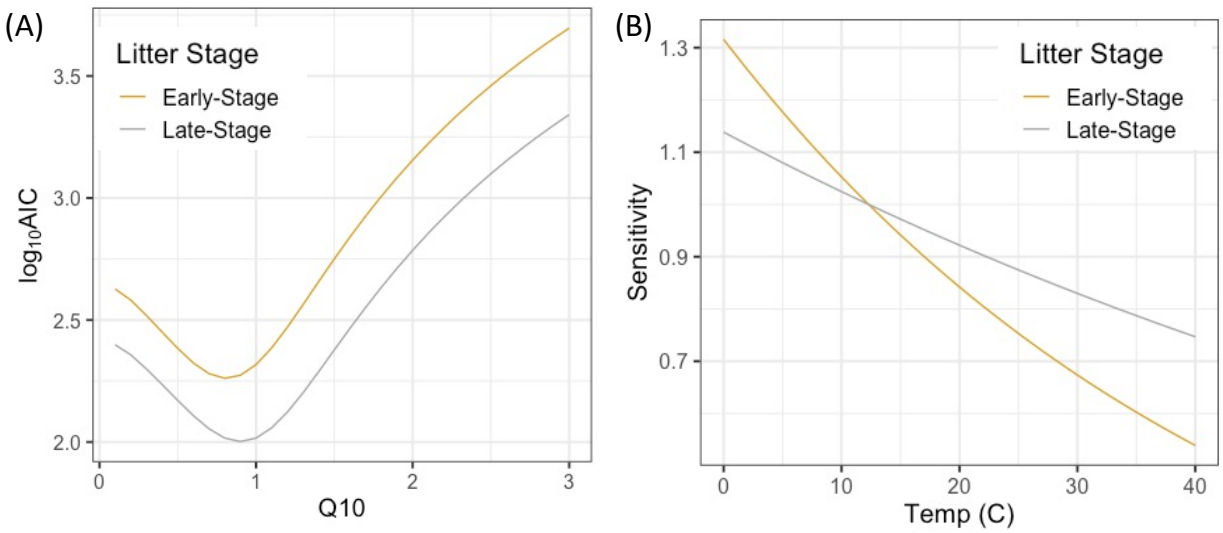

Figure S4.6. (A) Parameter estimation plot of Q_{10} coefficient for an Q_{10}-only model run (i.e. with no NRM sensitivity) showing model fit is best for Q_{10} values below 1. (B) Estimated Q_{10} sensitivity curves based on optimal value determined from panel A.

WORKS CITED

WORKS CITED

Adachi, Y., Watanabe, H., Tanabe, K., Doke, N., Nishimura, S., and Tsuge, T. (1993). Nuclear Ribosomal DNA as a Probe for Genetic Variability in the Japanese Pear Pathotype of Alternaia alternata. *Appl. Environ. Microbiol.* 59, 3197–3205.

Adair, C., Parton, W., Del Grosso, S., Silver, W., Harmon, M., Hall, S., et al. (2008). Simple three-pool model accurately describes patterns of long-term litter decomposition in diverse climates. *Glob. Chang. Biol.* 14, 2636–2660. doi:10.1111/j.1365-2486.2008.01674.x.

Adair, E. C., Parton, W. J., King, J. Y., Brandt, L. A., and Lin, Y. (2017). Accounting for photodegradation dramatically improves prediction of carbon losses in dryland systems. *Ecosphere* 8. doi:10.1002/ecs2.1892.

Aho, K., Derryberry, D., and Peterson, T. (2014). Model selection for ecologists: the worldviews of AIC and BIC. *Ecology* 95, 631–636.

Akimoto, Y., and Kusaka, H. (2015). A climatological study of fog in Japan based on event data. *Atmos. Res.* 151, 200–211. doi:10.1016/j.atmosres.2014.04.003.

Al-Suwaine, A. S., Bahkali, A. H., and Hasnain, S. M. (1999). Seasonal incidence of airborne fungal allergens in Riyadh, Saudi Arabia. *Mycopathologia* 145, 15–22.

Allison, S. D., Lu, Y., Weihe, C., Goulden, M. L., Martiny, A. C., Treseder, K. K., et al. (2013). Microbial abundance and composition influence litter decomposition response to environmental change. *Ecology* 94, 714–725. doi:10.1890/12-1243.1.

Angst, G., Heinrich, L., Kögel-knabner, I., and Mueller, C. W. (2016). The fate of cutin and suberin of decaying leaves, needles and roots – Inferences from the initial decomposition of bound fatty acids. *Org. Geochem.* 95, 81–92. doi:10.1016/j.orggeochem.2016.02.006.

Aradhya, M. K., Chan, H. M., and Parfitt, D. E. (2001). Genetic variability in the pistachio late blight fungus, Alternaria alternata. *Mycol. Res.* 105, 300–306.

Arenz, B. E., Held, B. W., Jurgens, J. A., Farrell, R. L., and Blanchette, R. A. (2006). Fungal diversity in soils and historic wood from the Ross Sea Region of Antarctica. *Soil Biol. Biochem.* 38, 3057–3064. doi:10.1016/j.soilbio.2006.01.016.

Ariyawansa, H. A., Hyde, K. D., Jayasiri, S. C., Buyck, B., Chethana, K. W. T., Dai, D. Q., et al. (2015). Fungal diversity notes 111–252 — taxonomic and phylogenetic contributions to fungal taxa. *Fungal Divers.* 75, 27–274. doi:10.1007/s13225-015-0346-5.

Austin, A. T. (2011). Has water limited our imagination for aridland biogeochemistry? *Trends Ecol. Evol.* 26, 229–35. doi:10.1016/j.tree.2011.02.003.

Austin, A. T., and Ballare, C. L. (2010). Dual role of lignin in plant litter decomposition in terrestrial ecosystems. *Proc. Natl. Acad. Sci. U. S. A.* 107, 4618–4622. doi:10.1073/pnas.0909396107.

Austin, A. T., Méndez, M. S., and Ballaré, C. L. (2016). Photodegradation alleviates the lignin bottleneck for carbon turnover in terrestrial ecosystems. *Proc. Natl. Acad. Sci.* 113, 4392–4397. doi:10.1073/pnas.1516157113.

Austin, A. T., and Vivanco, L. (2006). Plant litter decomposition in a semi-arid ecosystem controlled by photodegradation. *Nature* 442, 555–558. doi:10.1038/nature05038.

Baker, N. R., and Allison, S. D. (2015). Ultraviolet photodegradation facilitates microbial litter decomposition in a Mediterranean climate. *Ecology* 96, 1994–2003.

Barnes, P. W., Throop, H. L., Archer, S. R., Breshears, D. D., Mcculley, R. L., and Tobler, M. A. (2015). "Sunlight and Soil–Litter Mixing: Drivers of Litter Decomposition in Drylands," in *Progress in Botany*, 273–302. doi:10.1038/1941023a0.

Barnes, P. W., Throop, H. L., Hewins, D. B., Abbene, M. L., and Archer, S. R. (2012). Soil Coverage Reduces Photodegradation and Promotes the Development of Soil-Microbial Films on Dryland Leaf Litter. *Ecosystems* 15, 311–321. doi:10.1007/s10021-011-9511-1.

Bates, D., Mächler, M., Bolker, B., and Walk, S. (2015). Fitting Linear Mixed-Effects Models Using lme4. *J. Stat. Softw.* 67, 1–48. doi:0.18637/jss.v067.i01.

Bear, A. D. A., Jones, T. H., Kandeler, E., and Boddy, L. (2014). Interactive effects of temperature and soil moisture on fungal-mediated wood decomposition and extracellular enzyme activity. *Soil Biol. Biochem.* 70, 151–158. doi:10.1016/j.soilbio.2013.12.017.

Bensch, K., Groenewald, J. Z., Dijksterhuis, J., Starink-Willemse, M., Andersen, B., Summerell, B. A., et al. (2010). Species and ecological diversity within the Cladosporium cladosporioides complex (Davidiellaceae, Capnodiales). *Stud. Mycol.* 67, 1–94. doi:10.3114/sim.2010.67.01.

Berns, A. E., Philipp, H., Narres, H.-D., Burauel, P., Vereecken, H., and Tappe, W. (2008). Effect of gamma-sterilization and autoclaving on soil organic matter structure as studied by solid state NMR, UV and fluorescence spectroscopy. *Eur. J. Soil Sci.* 59, 540–550. doi:10.1111/j.1365-2389.2008.01016.x.

Bilger, W., Johnsen, T., and Schreiber, U. (2014). UV-excited chlorophyll fluorescence as a tool for the assessment of UV-protection by the epidermis of plants. *J. Exp. Bot.* 52, 2007–2014.

Birk, M. A. (2021). respirometry: Tools for Conducting and Analyzing Respirometry Experiments. R package version 1.3.0.

Bolker, B. M., Pacala, S. W., and Parton, W. J. (1998). Linear Analysis of Soil Decomposition: Insights from the CENTURY Model. *Ecol. Appl.* 8, 425–439.

Bonan, G. B., Hartman, M. D., Parton, W. J., and Wieder, W. R. (2013). Evaluating litter decomposition in earth system models with long-term litterbag experiments: an example using the Community Land Model version 4 (CLM4). *Glob. Chang. Biol.* 19, 957–974. doi:10.1111/gcb.12031.

Bradford, M. A., Veen, G. F. (Ciska), Bonis, A., Bradford, E. M., Classen, A. T., Cornelissen, J. H. C., et al. (2017). A test of the hierarchical model of litter decomposition. *Nat. Ecol. Evol.* 1, 1836–1845. doi:10.1038/s41559-017-0367-4.

Brandt, L. A., Bonnet, C., and King, J. Y. (2009). Photochemically induced carbon dioxide production as a mechanism for carbon loss from plant litter in arid ecosystems. *J. Geophys. Res. Biogeosciences* 114, 1–13. doi:10.1029/2008JG000772.

Brokenshire, T., and Cooke, B. M. (1975). The Reaction of Spring Barley Varieties to Selenophoma donacis. *Trans. Br. Mycol. Soc.* 65, 443–449. doi:10.1016/S0007-1536(75)80042-8.

Bruhn, D., Mikkelsen, T. N., Rolsted, M. M. M., Egsgaard, H., and Ambus, P. (2014). Leaf surface wax is a source of plant methane formation under UV radiation and in the presence of oxygen. 16, 512–516. doi:10.1111/plb.12137.

Butler, M. J. (1987). Melanin Production By The Black Yeast Phaeococcomyces Sp.

Byrne, M. P., and Gorman, P. A. O. (2018). Trends in continental temperature and humidity directly linked to ocean warming. *Proc. Natl. Acad. Sci.* 115, 4863–4868. doi:10.1073/pnas.1722312115.

Callahan, B. J., Mcmurdie, P. J., and Holmes, S. P. (2017). Exact sequence variants should replace operational taxonomic units in marker-gene data analysis. 11, 2639–2643. doi:10.1038/ismej.2017.119.

Cavicchioli, R., Bakken, L. R., Baylis, M., Foreman, C. M., Karl, D. M., Koskella, B., et al. (2019). Scientists' warning to humanity: microorganisms and climate change. *Nat. Rev. Microbiol.* 17, 569–586. doi:10.1038/s41579-019-0222-5.

Chen, M., Parton, W. J., Adair, E. C., Asao, S., Hartman, M. D., and Gao, W. (2016). Simulation of the effects of photodecay on long-term litter decay using DayCent. *Ecosphere* 7. doi:10.1002/ecs2.1631.

Chen, S., Tong, X., Woodard, R. W., Du, G., Wu, J., and Chen, J. (2008). Identification and Characterization of Bacterial Cutinase. 283, 25854–25862. doi:10.1074/jbc.M800848200.

Choudoir, M. J., Barberán, A., Menninger, H. L., Dunn, R. R., and Fierer, N. (2018). Variation in range size and dispersal capabilities of microbial taxa. *Ecology* 99, 322–334. doi:10.1002/ecy.2094.

Collins, S. L., Belnap, J., Grimm, N. B., Rudgers, J. a., Dahm, C. N., D'Odorico, P., et al. (2014). A Multiscale, Hierarchical Model of Pulse Dynamics in Arid-Land Ecosystems. *Annu. Rev. Ecol. Evol. Syst.* 45, 397–419. doi:10.1146/annurev-ecolsys-120213-091650.

Collins, S. L., Sinsabaugh, R. L., Crenshaw, C., Green, L., Porras-Alfaro, A., Stursova, M., et al. (2008). Pulse dynamics and microbial processes in aridland ecosystems. *J. Ecol.* 96, 413–420. doi:10.1111/j.1365-2745.2008.01362.x.

Cordero, R. J., and Casadevall, A. (2019). Functions of fungal melanin beyond virulence. *Fungal Biol. Rev.* 31, 99–112. doi:10.1016/j.fbr.2016.12.003.Functions.

Cornwell, W. K., Cornelissen, J. H. C., Amatangelo, K., Dorrepaal, E., Eviner, V. T., Godoy, O., et al. (2008). Plant species traits are the predominant control on litter

decomposition rates within biomes worldwide. *Ecol. Lett.* 11, 1065–1071. doi:10.1111/j.1461-0248.2008.01219.x.

Crous, P. W., and Groenewald, J. Z. (2018). Pseudopithomyces angolensis. *Persoonia* 41, 262–263.

Crous, P. W., Lennox, C. L., and Sutton, B. C. (1995). Selenophoma eucalypti and Stigmina robbenensis spp. nov. from Eucalyptus leaves on Robben Island. *Mycol. Res.* 99, 648–652. doi:10.1016/S0953-7562(09)80521-2.

Dai, A. (2013). Increasing drought under global warming in observations and models. *Nat. Clim. Chang.* 3, 52–58. doi:10.1038/nclimate1633.

Day, T. A., Bliss, M. S., Placek, S. K., Tomes, A. R., and Guénon, R. (2019). Thermal abiotic emission of CO2 and CH4 from leaf litter and its significance in a photodegradation assessment. *Ecosphere* 10. doi:10.1002/ecs2.2745.

de Menezes, G. C. A., Amorim, S. S., Gonçalves, V. N., Godinho, V. M., Simões, J. C., Rosa, C. A., et al. (2019). Diversity, Distribution, and Ecology of Fungi in the Seasonal Snow of Antarctica. *Microorganisms* 7. doi:doi:10.3390/microorganisms7100445.

Dingley, J. M. (1962). Pithomyces chartarum, its occurrence morphology, and taxonomy. *New Zeal. J. Agric. Res.* 5, 49–61. doi:10.1080/00288233.1962.10419976.

Dirks, I., Navon, Y., Kanas, D., Dumbur, R., and Grüenzweig, J. (2010). Atmospheric water vapor as driver of litter decomposition in Mediterranean shrubland and grassland during rainless seasons. *Glob. Chang. Biol.* 16, 2799–2812. doi:10.1111/j.1365-2486.2010.02172.x.

Dix, N. J., and Webster, J. (1995). *Development of fungal communities on herbaceous stems and grasses*.

Ebner, M., Miranda, T., and Roth-Nebelsick, A. (2011). Efficient fog harvesting by Stipagrostis sabulicola (Namib dune bushman grass). *J. Arid Environ.* 75, 524–531. doi:10.1016/j.jaridenv.2011.01.004.

Eckardt, F. D., Soderberg, K., Coop, L. J., Muller, A. A., Vickery, K. J., Grandin, R. D., et al. (2013). The nature of moisture at Gobabeb, in the central Namib Desert. *J. Arid Environ.* 93, 7–19. doi:10.1016/j.jaridenv.2012.01.011.

Edgar, R. C. (2013). UPARSE: highly accurate OTU sequences from microbial amplicon reads. *Nat. Methods* 10, 996–998. doi:10.1038/nmeth.2604.

Edgar, R. C. (2016). UCHIME2: improved chimera prediction for amplicon sequencing. *bioRxiv*, p074252.

Edgar, R. C., and Flyvbjerg, H. (2015). Error filtering, pair assembly and error correction for next-generation sequencing reads. *Bioinformatics* 31, 3476–3482. doi:10.1093/bioinformatics/btv401.

Erdenebileg, E., Wang, C., Ye, X., Cui, Q., Du, J., Huang, Z., et al. (2020). Multiple abiotic and biotic drivers of long-term wood decomposition within and among species in the semi-arid inland dunes: A dual role for stem diameter. *Funct. Ecol.* 34, 1472–1484. doi:10.1111/1365-2435.13559.

Evans, S. E., Dueker, M. E., Logan, J. R., and Weathers, K. C. (2019). The biology of fog: results from coastal Maine and Namib Desert reveal common drivers of fog microbial composition. *Sci. Total Environ.* 647, 1547–1556. doi:10.1016/j.scitotenv.2018.08.045.

Evans, S. E., Todd-brown, K. E. O., Jacobson, K. M., and Jacobson, P. J. (2020). Non-rainfall moisture: A key driver of microbial respiration from standing litter in arid, semiarid, and mesic grasslands. *Ecosystems* 23, 1154–1169. doi:10.1007/s10021-019-00461-y.

Evans, S. E., and Wallenstein, M. D. (2012). Soil microbial community response to drying and rewetting stress: Does historical precipitation regime matter? *Biogeochemistry* 109, 101–116. doi:10.1007/s10533-011-9638-3.

Forthun, G. M., Johnson, M. B., Schmitz, W. G., Blume, J., and Caldwell, R. J. (2006). Trends in fog frequency and duration in the southeast United States. *Phys. Geogr.* 27, 206–222. doi:10.2747/0272-3646.27.3.206.

Fourtouni, A., Manetas, Y., and Christias, C. (1998). Effects of UV-B radiation on growth, pigmentation, and spore production in the phytopathogenic fungus Alternaria solani. *Can. J. Bot.* 76, 2093–2099.

Freitas, M. L. R. (2018). New Species and New Records of Conidial Fungi from Submerged Decayed Leaves in Brazil.

Frossard, A., Ramond, J.-B., Seely, M., and Cowan, D. A. (2015). Water regime history drives responses of soil Namib Desert microbial communities to wetting events. *Sci. Rep.* 5, 12263. doi:10.1038/srep12263.

Gallo, M. E., Porras-Alfaro, A., Odenbach, K. J., and Sinsabaugh, R. L. (2009). Photoacceleration of plant litter decomposition in an arid environment. *Soil Biol. Biochem.* 41, 1433–1441. doi:10.1016/j.soilbio.2009.03.025.

Gehrke, C., Johanson, U., Callaghan, T. V, Chadwick, D., and Robinson, C. H. (1995). The Impact of Enhanced Ultraviolet-B Radiation on Litter Quality and Decomposition Processes in Vaccinium Leaves from the Subarctic. *Oikos* 72, 213–222.

Gilbert, J. A., Jansson, J. K., and Knight, R. (2014). The Earth Microbiome project: successes and aspirations. *BMC Biol.* 12, 1–4.

Glassman, S. I., Weihe, C., Li, J., Albright, M. B. N., Looby, C. I., and Martiny, A. C. (2018). Decomposition responses to climate depend on microbial community composition. *Proc. Natl. Acad. Sci.* 115, 11994–11999. doi:10.1073/pnas.1811269115.

Gliksman, D., Rey, A., Seligmann, R., Dumbur, R., Sperling, O., Navon, Y., et al. (2017). Biotic degradation at night, abiotic degradation at day: positive feedbacks on litter decomposition in drylands. *Glob. Chang. Biol.* 23, 1564–1574. doi:10.1111/gcb.13465.

Gołębiewski, M., Tarasek, A., Sikora, M., Deja-Sikora, E., Tretyn, A., and Niklińska, M. (2019). Rapid microbial community changes during initial stages of pine litter decomposition. *Microb. Ecol.* 77, 56–75.

Gostinčar, C., Grube, M., de Hoog, S., Zalar, P., and Gunde-Cimerman, N. (2010). Extremotolerance in fungi: evolution on the edge. *FEMS Microb. Ecol.* 71, 2–11. doi:10.1111/j.1574-6941.2009.00794.x.

Gostinčar, C., Ohm, R. A., Kogej, T., Sonjak, S., Turk, M., Zajc, J., et al. (2014). Genome sequencing of four Aureobasidium pullulans varieties: biotechnological potential, stress tolerance, and description of new species. *BMC Genomics* 15.

Gunawardhana, L. N., Al-Rawas, G. A., and Kazama, S. (2017). An alternative method for predicting relative humidity for climate change. *Meteorol. Appl.* 24, 551–559.

doi:10.1002/met.1641.

Haelewaters, D., Toome-Heller, M., Albu, S., and Aime, M. C. (2020). Red yeasts from leaf surfaces and other habitats: three new species and a new combination of Symmetrospora (Pucciniomycotina, Cystobasidiomycetes). *Fungal Syst. Evol.* 5, 187–196.

Haensler, A., Cermak, J., Hagemann, S., and Jacob, D. (2011). Will the southern african west coast fog be affected by future climate change? *Erdkunde* 65, 261–275. doi:10.3112/erdkunde.2011.03.04.

Häggblom, P., and Unestam, T. (1979). Blue Light Inhibits Mycotoxin Production and Increases Total Lipids and Pigmentation in Alternaria alternata. *Appl. Environ. Microbiol.* 38, 1074–1077.

Hewins, D. B., Archer, S. R., Okin, G. S., Mcculley, R. L., and Throop, H. L. (2013). Soil–Litter Mixing Accelerates Decomposition in a Chihuahuan Desert Grassland. *Ecosystems* 16, 183–195. doi:10.1007/s10021-012-9604-5.

Hofstetter, V., Buyck, B., Eyssartier, G., Schnee, S., and Gindro, K. (2019). The unbearable lightness of sequenced-based identification. *Fungal Divers.* 3, 243–284. doi:10.1007/s13225-019-00428-3.

Howard, P. J. A., and Frankland, J. C. (1974). Effects of Certain Full and Partial Sterilization Treatments on Leaf Litter. *Soil Biol. Biochem.* 6, 117–123.

Hujslová, M., Kubátová, A., Kostov, M., and Kola, M. (2013). Acidiella bohemica gen. et sp. nov. and Acidomyces spp. (Teratosphaeriaceae), the indigenous inhabitants of extremely acidic soils in Europe. *Fungal Divers.* 58, 33–45. doi:10.1007/s13225-012-0176-7.

Hůnová, I., Brabec, M., Malý, M., and Valeriánová, A. (2020). Science of the Total Environment Long-term trends in fog occurrence in the Czech Republic, Central Europe. *Sci. Total Environ.* 711. doi:10.1016/j.scitotenv.2019.135018.

Huxman, T. E., Snyder, K. A., Tissue, D., Leffler, A. J., Ogle, K., Pockman, W. T., et al. (2004). Precipitation pulses and carbon fluxes in semiarid and arid ecosystems. *Oecologia* 141, 254–268. doi:10.1007/s00442-004-1682-4.

Jacobson, K. M., and Jacobson, P. J. (1998). Rainfall regulates decomposition of buried

cellulose in the Namib Desert. *J. Arid Environ.* 38, 571–583. doi:10.1006/jare.1997.0358.

Jacobson, K. M., van Diepeningen, A., Evans, S. E., Fritts, R., Gemmel, P., Marsho, C., et al. (2015). Non-rainfall moisture activates fungal decomposition of surface litter in the Namib Sand Sea. *PLoS One* 10, e0126977. doi:10.1371/journal.pone.0126977.

Johnstone, J. A., and Dawson, T. E. (2010). Climatic context and ecological implications of summer fog decline in the coast redwood region. *Proc. Natl. Acad. Sci.* 107, 4533–4538. doi:10.1073/pnas.0915062107.

Kattge, J., Bönisch, G., Díaz, S., and Others (2020). TRY plant trait database – enhanced coverage and open access. 26, 119–188. doi:10.1111/gcb.14904.

Kgatle, M. G., Flett, B., Truter, M., Ramusi, M., and Aveling, T. (2019). Distribution of Alternaria leaf blight of sunflowers caused by Alternaria alternata in South Africa. *J. Agric. Rural Dev. Trop. Subtrop.* 120, 71–77. doi:10.17170/kobra-20190613558.

King, J. Y., Brandt, L. A., and Adair, E. C. (2012). Shedding light on plant litter decomposition: advances, implications and new directions in understanding the role of photodegradation. *Biogeochemistry* 111, 57–81. doi:10.1007/s10533-012-9737-9.

Ko, T. W. K., Stephenson, S. L., Bahkali, A. H., and Hyde, K. D. (2011). From morphology to molecular biology: can we use sequence data to identify fungal endophytes? *Fungal Divers.* 50, 113–120. doi:10.1007/s13225-011-0130-0.

Kolb, C. A., Schreiber, U., Gademann, R., and Pundel, E. E. (2005). UV-A screening in plants determined using a new portable fluorimeter. *Photosynthetica* 43, 371–377.

Kõljalg, U., Nilsson, R. H., Abarenkov, K., Tedersoo, L., Taylor, A. F. S., Bahram, M., et al. (2013). Towards a unified paradigm for sequence-based identification of fungi. *Mol. Ecol.* 22, 5271–5277.

Kravchenko, A. N., Toosi, E. R., Guber, A. K., Ostrom, N. E., Yu, J., Azeem, K., et al. (2017). Hotspots of soil N2O emission enhanced through water absoption by plant reside. *Nat. Geosci.* 10, 496–500. doi:10.1038/NGEO2963.

Kutty, S. G., Dimri, A. P., and Gultepe, I. (2019). Climatic trends in fog occurrence

over the Indo-Gangetic plains. *Int. J. Climatol.*, 1–14. doi:10.1002/joc.6317.

Kwon-Chung, K. J. (2011). "Filobasidium Olive (1968)," in *The Yeasts, a Taxonomic Study*, eds. C. P. Kurtzman, J. W. Fell, and T. Boekhout (Elsevier), 1457–1465. doi:10.1016/B978-0-444-52149-1.00115-4.

le Roux, G. J. (1970). The microbiology of sand-dune eco-systems in the Namib Desert.

Lee, H., Fitzgerald, J., Hewins, D. B., McCulley, R. L., Archer, S. R., Rahn, T., et al. (2014). Soil moisture and soil-litter mixing effects on surface litter decomposition: A controlled environment assessment. *Soil Biol. Biochem.* 72, 123–132. doi:10.1016/j.soilbio.2014.01.027.

Lin, Y., Karlen, S. D., Ralph, J., and King, J. Y. (2018). Short-term facilitation of microbial litter decomposition by ultraviolet radiation. *Sci. Total Environ.* 615, 838–848. doi:10.1016/j.scitotenv.2017.09.239.

Lin, Y., and King, J. Y. (2014). Effects of UV Exposure and Litter Position on Decomposition in a California Grassland. *Ecosystems* 17, 158–168. doi:10.1007/s10021-013-9712-x.

Logan, J. R., Barnes, P. W., and Evans, S. E. Photodegradation of plant litter cuticles enhances microbial decomposition by increasing uptake of non-rainfall moisture. *Funct. Ecol.*

Logan, J. R., Jacobson, K. M., Jacobson, P. J., and Evans, S. E. (2021). Fungal Communities on Standing Litter Are Structured by Moisture Type and Constrain Decomposition in a Hyper-Arid Grassland Site Descriptions and Climatic Data. *Front. Microbiol.* 12, 1–15. doi:10.3389/fmicb.2021.596517.

Louw, G. N., and Seely, M. K. (1982). *Ecology of Desert Organisms*. Essex, UK: Longman Group Limited.

Love, M. I., Huber, W., and Anders, S. (2014). Moderated estimation of fold change and dispersion for RNA-seq data with DESeq2. *Genome Biol.* 15, 550. doi:10.1186/s13059-014-0550-8.

Low-Décarie, E., Boatman, T. G., Bennett, N., Passfield, W., Gavalás-olea, A., Siegel, P., et al. (2017). Predictions of response to temperature are contingent on model choice and data quality. *Ecol. Evol.* 7, 10467–10481. doi:10.1002/ece3.3576.

Luo, Y., Ahlström, A., Allison, S. D., Batjes, N. H., Brovkin, V., Carvalhais, N., et al. (2015). Toward more realistic projections of soil carbon dynamics by Earth system models. *Global Biogeochem. Cycles* 30, 40–56. doi:10.1002/2015GB005239.Received.

Lustenhouwer, N., Maynard, D. S., Bradford, M. A., Lindner, D. L., Oberle, B., Zanne, A. E., et al. (2020). A trait-based understanding of wood decomposition by fungi. *Proc. Natl. Acad. Sci.* 117, 11551–11558. doi:10.1073/pnas.1909166117.

Manning, W. J., and Tiedemann, A. (1995). Climate Change: Potential effects of increased atmospheric carbon dioxide (CO2), ozone (O3), and ultraviolet-B (UV-B) radiation on plant diseases. *Environ. Pollut.* 88, 219–245.

Martiny, J. B. H., Martiny, A. C., Weihe, C., Lu, Y., Berlemont, R., Brodie, E. L., et al. (2017). Microbial legacies alter decomposition in response to simulated global change. 490–499. doi:10.1038/ismej.2016.122.

Mattimore, V., and Battista, J. R. (1996). Radioresistance of Deinococcus radiodurans: Functions Necessary To Survive Ionizing Radiation Are Also Necessary To Survive Prolonged Desiccation. *J. Bacteriol.* 178, 633–637.

Matulich, K. L., Weihe, C., Allison, S. D., Amend, A. S., Berlemont, R., Goulden, M. L., et al. (2015). Temporal variation overshadows the response of leaf litter microbial communities to simulated global change. *ISME J.* 9, 2477–2489. doi:10.1038/ismej.2015.58.

McMurdie, P. J., and Holmes, S. (2013). phyloseq : An R Package for Reproducible Interactive Analysis and Graphics of Microbiome Census Data. *PLoS One* 8. doi:10.1371/journal.pone.0061217.

Messenger, D. J., Mcleod, A. R., and Fry, S. C. (2009). The role of ultraviolet radiation , photosensitizers, reactive oxygen species and ester groups in mechanisms of methane formation from pectin. *Plant, Cell Environ.* 32, 1–9. doi:10.1111/j.1365-3040.2008.01892.x.

Moreno-Rico, O., Groenewald, J. Z., and Crous, P. W. (2014). Foliicolous fungi from Arctostaphylos pungens in Mexico. *IMA Fungus* 5, 7–15. doi:10.5598/imafungus.2014.05.01.02.

Necpálová, M., Anex, R. P., Fienen, M. N., Del Grosso, S. J., Castellano, M. J., Sawyer, J. E., et al. (2015). Understanding the DayCent model: Calibration, sensitivity ,

and identifiability through inverse modeling. *Environ. Model. Softw.* 66, 110–130. doi:10.1016/j.envsoft.2014.12.011.

Newsham, K. K., Mcleod, A. R., Roberts, J. D., Greenslade, P. D., and Emmett, B. A. (1997). Direct Effects of Elevated UV-B Radiation on the Decomposition of Quercus robur Leaf Litter. *Oikos* 79, 592–602.

Nilsson, R. H., Kristiansson, E., Ryberg, M., Hallenberg, N., and Larsson, K.-H. (2008). Intraspecific ITS Variability in the Kingdom Fungi as Expressed in the International Sequence Databases and Its Implications for Molecular Species Identification. *Evol. Bioinforma.* 4, 193–201. doi:10.4137/ebo.s653.

Niu, F., Li, Z., Li, C., Lee, K. H., and Wang, M. (2010). Increase of wintertime fog in China : Potential impacts of weakening of the Eastern Asian monsoon circulation and increasing aerosol loading. *J. Geophys. Res.* 115. doi:10.1029/2009JD013484.

Noy-Meir, I. (1973). "Desert Ecosystems: Environment and Producers," in *Annual Review of Ecology and Systematics Vol. 4*, eds. R. Johnston, P. Frank, and C. Michener (Palo Alto.: Annual Reviews Inc.).

Noy-Meir, I. (1974). Desert ecosystems: higher trophic levels. *Annu. Rev. Ecol. Syst.* 5, 195–214.

Oksanen, J., Blanchet, F. G., Friendly, M., Kindt, R., Legendre, P., McGlinn, D., et al. (2019). vegan: Community Ecology Package. R package version 2.5-5.

Oren, A., and Gunde-Cimerman, N. (2007). Mycosporines and mycosporine-like amino acids: UV protectants or multipurpose secondary metabolites? *FEMS Microbiol. Lett.* 269, 1–10. doi:10.1111/j.1574-6968.2007.00650.x.

Palacio-Barrera, A. M., Areiza, D., Zapata, P., Atehortúa, L., Correa, C., and Peñuela-Vásquez, M. (2019). Induction of pigment production through media composition, abiotic and biotic factors in two filamentous fungi. *Biotechnol. Reports* 21, e00308. doi:10.1016/j.btre.2019.e00308.

Pancotto, V. A., Sala, O. E., Cabello, M., López, N. I., Robson, T. M., Ballaré, C. L., et al. (2003). Solar UV-B decreases decomposition in herbaceous plant litter in Tierra del Fuego, Argentina: potential role of an altered decomposer community. *Glob. Chang. Biol.* 9, 1465–1474.

Pancotto, V. A., Sala, O. E., Robson, T. M., Caldwell, M. M., and Scopel, A. L. (2005). Direct and indirect effects of solar ultraviolet-B radiation on long-term decomposition. *Glob. Chang. Biol.* 11, 1982–1989. doi:10.1111/j.1365-2486.2005.1027.x.

Parton, W., Silver, W. L., Burke, I. C., Grassens, L., Harmon, M. E., Currie, W. S., et al. (2007). Global-Scale Similarities in Nitrogen Release Patterns During Long-Term Decomposition. *Science (80-.).* 315, 361–364.

Petraglia, A., Cacciatori, C., Chelli, S., Fenu, G., Calderisi, G., Gargano, D., et al. (2019). Litter decomposition: effects of temperature driven by soil moisture and vegetation type. *Plant Soil* 455, 187–200.

Pieristè, M., Chauvat, M., Kotilainen, T. K., Jones, A. G., Aubert, M., Robson, T. M., et al. (2019). Solar UV-A radiation and blue light enhance tree leaf litter decomposition in a temperate forest. *Oecologia* 191, 191–203. doi:10.1007/s00442-019-04478-x.

Pieristè, M., Forey, E., Sahraoui, A. L., Meglouli, H., Laruelle, F., Delporte, P., et al. (2020). Spectral Composition of Sunlight Affects the Microbial Functional Structure of Beech Leaf Litter During the Initial Phase of Decomposition. *Plant Soil* 451, 515–530.

Pitcairn, C. E. R., Jeffree, C. E., and Grace, J. (1986). Influence of polishing and abrasion on the diffusive conductance of leaf surface of Festuca arundinacea Schreb. *Plant, Cell Environ.* 9, 191–196.

Põlme, S., Abarenkov, K., Nilsson, R. H., Lindahl, B. D., and Clemmensen, K. E. (2021). FungalTraits: a user-friendly traits database of fungi and fungus-like stramenopiles. *Fungal Divers.* 105, 1–16. doi:10.1007/s13225-020-00466-2.

Poulter, B., Frank, D., Ciais, P., Myneni, R. B., Andela, N., Bi, J., et al. (2014). Contribution of semi-arid ecosystems to interannual variability of the global carbon cycle. *Nature* 509, 600–603. doi:10.1038/nature13376.

R Core Team (2020). R: A language and environment for statistical computing. in (Vienna, Austria: R Foundation for Statistical Computing).

Raja, H. A., Miller, A. N., Pearce, C. J., and Oberlies, N. H. (2017). Fungal identification using molecular tools: A primer for the natural products research

community. *J. Nat. Prod.* 80, 756–770. doi:10.1021/acs.jnatprod.6b01085.

Reed, H. E., and Martiny, J. B. H. (2007). Testing the functional significance of microbial composition in natural communities. *FEMS Microb. Ecol.* 62, 161–170. doi:10.1111/j.1574-6941.2007.00386.x.

Ricks, K. D., and Koide, R. T. (2019). The role of inoculum dispersal and plant species identity in the assembly of leaf endophytic fungal communities. *PLoS One* 14, e0219832. doi:https://doi.org/ 10.1371/journal.pone.0219832.

Riederer, M. (2006). "Introduction: biology of the plant cuticle," in *Biology of the Plant Cuticle*, eds. M. Riederer and C. Müller (Blackwell Publishing Ltd), 1–8.

Riederer, M., and Schreiber, L. (2001). Protecting against water loss: analysis of the barrier properties of plant cuticles. *J. Exp. Bot.* 52, 2023–2032. doi:10.1093/jexbot/52.363.2023.

Ritter, F., Berkelhammer, M., and Beysens, D. (2019). Dew frequency across the US from a network of in situ radiometers. *Hydrol. Earth Syst. Sci.* 23, 1179–1197. doi:https://doi.org/10.5194/hess-23-1179-2019.

Roth-Nebelsick, A., Ebner, M., Miranda, T., Gottschalk, V., Voigt, D., Gorb, S., et al. (2012). Leaf surface structures enable the endemic Namib desert grass Stipagrostis sabulicola to irrigate itself with fog water. *J. R. Soc. Interface*, rsif20110847. doi:10.1098/rsif.2011.0847.

Ruibal, C., Gueidan, C., Selbmann, L., Gorbushina, A. A., Crous, P. W., Groenewald, J. Z., et al. (2009). Phylogeny of rock-inhabiting fungi related to Dothideomycetes. *Stud. Mycol.* 64, 123–133. doi:10.3114/sim.2009.64.06.

Salah, Y. M. S., and Scholes, M. C. (2011). Effect of temperature and litter quality on decomposition rate of Pinus patula needle litter. *Procedia Environ. Sci.* 6, 180–193. doi:10.1016/j.proenv.2011.05.019.

Schimel, D. S. (2010). Drylands in the Earth System. *Science (80-.).* 327, 418–420.

Schimel, J., Balser, T. C., and Wallenstein, M. (2007). Microbial stress-response physiology and its implications for ecosystem function. *Ecology* 88, 1386–1394.

Seely, M. K., and Louw, G. N. (1980). First approximation of the effects of rainfall on

the ecology of a Namib Desert dune ecosystem. *J. Arid Environ.* 3, 25–54.

Sentelhas, P. C., Marta, A. D., Orlandini, S., Santos, E. A., Gillespie, T. J., and Gleason, M. L. (2008). Suitability of relative humidity as an estimator of leaf wetness duration. *Agric. For. Meteorol.* 148, 392–400. doi:DOI 10.1016/j.agrformet.2007.09.011.

Shepherd, T., and Griffiths, D. W. (2006). The effects of stress on plant cuticular waxes. *New Phytol.* 171, 469–499. doi:10.1111/j.1469-8137.2006.01826.x.

Sierra, C. A. (2012). Temperature sensitivity of organic matter decomposition in the Arrhenius equation : some theoretical considerations. 1–15. doi:10.1007/s10533-011-9596-9.

Sierra, C. A., Trumbore, S. E., Davidson, E. A., Vicca, S., and Janssens, I. (2015). Sensitivity of decomposition rates of soil organic matter with respect to simultaneous changes in temperature and moisture. *J. Adv. Model. Earth Syst.*, 335–356. doi:10.1002/2014MS000358.Received.

Sokolov, A., Kicklighter, D., Schlosser, A., Wang, C., Monier, E., Brown-Steiner, B., et al. (2018). Description and Evaluation of the MIT Earth System Model (MESM). *J. Adv. Model. Earth Syst.* 10, 1759–1789. doi:10.1029/2018MS001277.

Song, Z., Vail, A., Sadowsky, M. J., Schilling, J. S., and Baldrian, P. (2014). Quantitative PCR for measuring biomass of decomposer fungi in planta. *Fungal Ecol.* 7, 39–46. doi:10.1016/j.funeco.2013.12.004.

Sutton, B. C., and Sankaran, K. V (1995). A new species of Selenophoma on Elaeocarpus from India. *Mycol. Res.* 99, 1199–1200. doi:10.1016/S0953-7562(09)80278-5.

Tedersoo, L., Bahram, M., Põlme, S., Kõljalg, U., Yorou, N. S., Wijesundera, R., et al. (2014). Global diversity and geography of soil fungi. *Science (80-.).* 346. doi:10.1126/science.aaa1185.

Throop, H., and Archer, S. (2009). Resolving the dryland decomposition conundrum: some new perspectives on potential drivers. *Prog. Bot.* 70, 171–194.

Treseder, K. K., and Lennon, J. T. (2015). Fungal traits that drive ecosystem dynamics on land. *Microbiol. Mol. Biol. Rev.* 79, 243–262. doi:10.1128/MMBR.00001-15.

Tschinkel, W. R. (1973). The sorption of water vapor by windborne plant debris in the Namib Desert. *Madoqua* 2, 21–24.

Vanterpool, T. C. (1947). Selenophoma linicola sp . nov . on Flax in Saskatchewan. *Mycologia* 39, 341–348.

Voříšková, J., and Baldrian, P. (2013). Fungal community on decomposing leaf litter undergoes rapid successional changes. *ISME J.* 7, 477–486. doi:10.1038/ismej.2012.116.

Wang, J., Liu, L., Wang, X., and Chen, Y. (2015). The interaction between abiotic photodegradation and microbial decomposition under ultraviolet radiation. *Glob. Chang. Biol.* 21, 2095–2104. doi:10.1111/gcb.12812.

Wang, J., Liu, L., Wang, X., Yang, S., Zhang, B., Li, P., et al. (2017a). High night-time humidity and dissolved organic carbon content support rapid decomposition of standing litter in a semi-arid landscape. *Funct. Ecol.* 31, 1659–1668. doi:10.1111/1365-2435.12854.

Wang, J., Yang, S., Zhang, B., Liu, W., Deng, M., Chen, S., et al. (2017b). Temporal dynamics of ultraviolet radiation impacts on litter decomposition in a semi-arid ecosystem. *Plant Soil* 419, 71–81. doi:10.1007/s11104-017-3290-1.

Wenndt, A. J., Evans, S. E., Diepeningen, A. D. van, Logan, J. R., Jacobson, P. J., Seely, M. K., et al. Why plants harbor complex endophytic fungal communities: Insights from perennial bunchgrass Stipagrostis sabulicola in the Namib Sand Sea. *Front. Microbiol.*

Whitford, W. G., Meentemeyer, V., Seastedt, T. R., Cromack Jr., K., Crossley Jr., D. A., Santos, P., et al. (1981). Exceptions to the AET Model: Deserts and Clear-Cut Forest. *Ecology* 62, 275–277.

Xie, Y. (2020). A meta-analysis of critique of litterbag method used in examining decomposition of leaf litters. *J. Soils Sediments* 20, 1881–1886. doi:https://doi.org/10.1007/s11368-020-02572-9.

Yeaton, R. I. (1988). Structure and function of the Namib dune grasslands: Characteristics of the environmental gradients and species distributions. *J. Ecol.* 76, 744–758.

Yu, S., Mo, Q., Li, Y., Li, Y., Zou, B., Xia, H., et al. (2019). Changes in seasonal precipitation distribution but not annual amount affect litter decomposition in a secondary tropical forest. *Ecol. Evol.* 9, 11344–11352. doi:10.1002/ece3.5635.

Zhang, D., Hui, D., Luo, Y., and Zhou, G. (2008). Rates of litter decomposition in terrestrial ecosystems: global patterns and controlling factors. *J. Plant Ecol.* 1, 85–93. doi:10.1093/jpe/rtn002.

Zhang, Y., Xiao, X., Guanter, L., Zhou, S., Ciais, P., Joiner, J., et al. (2016). Precipitation and carbon-water coupling jointly control the interannual variability of global land gross primary production. *Nat. Publ. Gr.*, 1–9. doi:10.1038/srep39748.

Zhou, X., Talley, M., and Luo, Y. (2009). Biomass, litter, and soil respiration along a precipitation gradient in southern Great Plains, USA. *Ecosystems* 12, 1369–1380. doi:10.1007/s10021-009-9296-7.

Zukswert, J. M., and Prescott, C. E. (2017). Relationships among leaf functional traits, litter traits, and mass loss during early phases of leaf litter decomposition in 12 woody plant species. *Oecologia* 185, 305–316. doi:10.1007/s00442-017-3951-z.